US Army Corps of Engineers®

Technical Assessment of the Old, Mississippi, Atchafalaya, and Red (OMAR) Rivers: HEC-RAS Model

MRG&P Report No. 41; Volume 8 • August 2022

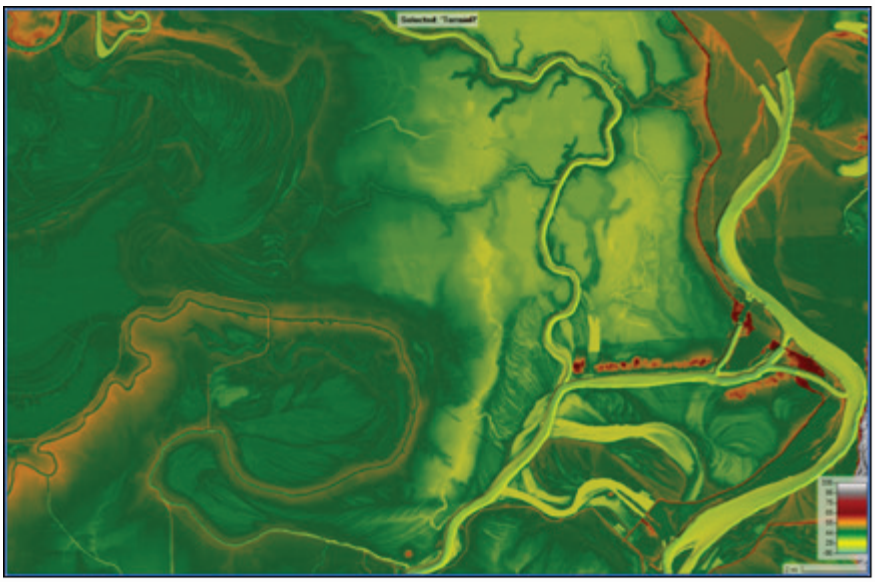

MRG&P
Mississippi River Geomorphology & Potamology Program

Mississippi River Geomorphology and
Potamology Program

MRG&P Report No. 41; Vol. 8
August 2022

Technical Assessment of the Old, Mississippi, Atchafalaya, and Red (OMAR) Rivers

HEC-RAS Model

David A. Fertitta and Maxwell E. Agnew

Hydrology, Hydraulics, and Coastal Branch
7400 Leake Ave
New Orleans, Louisiana 70118

David A. Ramirez

River Engineering Branch
7400 Leake Ave
New Orleans, Louisiana 70118

Report 8 of a series

Approved for public release; distribution is unlimited.

Prepared for US Army Corps of Engineers, Mississippi Valley Division
1400 Walnut Street
Vicksburg, MS 39180-6199

Under Project No. 478534

Abstract

Upstream of the confluence of the Red River, Atchafalaya River, and ORCC Outflow Channel are vast low-lying flat areas on both sides of the Lower Red River. During times of high water on the Lower Red—whether from upstream water in the Red or from the ORCC Outflow Channel—enormous amounts of water flow over the natural riverbanks and flood this land. The loss of this water from the river into storage affects the operation of the ORCC, which in turn affects the stages and flows down the Atchafalaya and Mississippi Rivers. An improved understanding of this area and how water is stored during flood events is required to inform ORCC water management operations.

Hydraulic analyses provide a basis to assess the changes in water levels, current directions and velocities, and flow rates for the assessment area. The hydraulic model HEC-RAS is used to expand on existing models of the area and to help overcome gaps in data. Understanding the processes of how water leaves the Red River channel, the volume and timing of the water moving into storage, and when the storage area begins to drain, will greatly inform the water managers and operators of the ORCC.

DISCLAIMER: The contents of this report are not to be used for advertising, publication, or promotional purposes. Citation of trade names does not constitute an official endorsement or approval of the use of such commercial products. All product names and trademarks cited are the property of their respective owners. The findings of this report are not to be construed as an official Department of the Army position unless so designated by other authorized documents.

DESTROY THIS REPORT WHEN NO LONGER NEEDED. DO NOT RETURN IT TO THE ORIGINATOR.

Contents

Abstract ii

Figures and Tables v

Preface x

1 Introduction 1

1.1 Background 2
1.2 Objective 2
1.3 Approach 3

2 Methodology 4

3 Model Calibration and Alternative Assessments 5

3.1 Model calibration and alternative assessments setup 5
3.2 Calibration run: 2011 Hindcast setup (High Mississippi, Low Red) 5
3.3 Black River boundary condition 7
3.4 2011 Hindcast results and comparison to observations 9
3.5 Observed versus modeled outputs 11

4 Alternative Assessments Setup and Results 12

4.1 High Red River, Low Mississippi River (motivated by 2015) 12
4.2 Old River 60/40 split 13
4.3 Old River 80/20 split 14
4.4 Modeled extreme flows 15

5 Discussion 17

5.1 West bank of Red River—Bayou Natchitoches basin 19
5.2 West bank of Red River—Alligator Bayou basin 23

6 Conclusions and Recommendations 32

References 33

Appendix A : Supplemental Figures 34

A.1 High Red River, Low Mississippi River Scenario (motivated by 2015 Floods) 34
A.2 West bank of Red River—Bayou Natchitoches basin 36
A.3 East bank of Red River—Alligator Bayou basin 38
A.4 Old River 60/40 split 41
A.5 West bank of Red River—Bayou Natchitoches basin 44
A.6 East bank of Red River—Alligator Bayou basin 46
A.7 Old River 80/20 Split 49
A.8 West bank of Red River—Bayou Natchitoches basin 51
A.9 East bank of Red River—Alligator Bayou basin 53
A.10 Extreme flows simulation 56

A.11 West bank of Red River—Bayou Natchitoches basin 58
A.12 East bank of Red River—Alligator Bayou basin 60

Appendix B : Supplemental Tables 63

Report Documentation Page (SF 298) 65

Figures and Tables

Figures

Figure 1. RAS terrain showing the spatial extent of the 2D flow areas and the cross sections for the 1D reaches. 1

Figure 2. River Analysis System (RAS) terrain showing the spatial extent of the 2D flow areas and the cross sections for the 1D reaches. 4

Figure 3. Flow rates in cubic feet per second for Mississippi River, Red River, and combined flows at ORCS. 6

Figure 4. Modeled output of flow in the Black River at Jonesville from the 2011 hindcast simulation. 8

Figure 5. Modeled output of flow in the Black River at Jonesville from the flowline model. 8

Figure 6. Max depth plotted for 2011 simulation. 9

Figure 7. Locations of modeled outputs shown. Blue indicates location of modeled output only; red indicates modeled and observed data available..... 9

Figure 8. Modeled flow in the Red River upstream of the confluence with the Black River from the 2011 simulation..... 10

Figure 9. Modeled flow at the site of the new stream gage at Madam Lee (downstream from the confluence with the Black River) from the 2011 simulation. 10

Figure 10. Modeled flow for Wax Lake Outlet (outlet to the west of the main Atchafalaya River outlet) from the 2011 simulation. 10

Figure 11. Observed versus modeled flow at Simmesport along the Atchafalaya River south of the ORCC. .. 11

Figure 12. Observed versus modeled stages in the Whiskey Bay Pilot Channel. 11

Figure 13. Observed versus modeled flow in the Gulf Intracoastal Waterway (GIWW) south of Morgan City. 11

Figure 14. Max depth plotted for high Red River simulation..... 13

Figure 15. Max depth plotted for ORCC diversion split altered to be 60% Mississippi River, 40% Atchafalaya River. 14

Figure 16. Max depth plotted for ORCC diversion split altered to be 80% Mississippi River, 20% Atchafalaya River. 15

Figure 17. Maximum depth plotted for extreme flows scenario. 16

Figure 18. Map showing levees (both federal and local) in region. Image from National Levee Database website (https.//levees.sec.usace.army.mil/#/). 17

Figure 19. RAS terrain near the 2D flow areas of interest on the west and east banks of the Red River just upstream of ORCS. 17

Figure 20. Location of points where output time series of water surface elevation was extracted. 18

Figure 21. Volume-elevation curve for the Bayou Natchitoches basin on the west bank of the Red River..... 19

Figure 22. Time series of modeled water surface elevation for the west bank of the Red River from a point located at 91.7071193°W 31.182803°N (1337547.3503, 2985581.611 in the RAS model) for each simulation. 20

Figure 23. Time series of interpolated volume for the 2D flow area on the west bank of the Red River for each simulation. 20

Figure 24. Time series of flow in cfs at Simmesport (*blue line*) overlaid with a time series of computed volume of water in the area on the west bank of the Red River (*red line*) for the 2011 simulation. 21

Figure 25. Plot of flow in cfs at Simmesport versus computed volume of water in the area on the west

bank of the Red River. *Line color* changes by simulation date for the 2011 simulation. 21

Figure 26. Time series of stage at Simmesport (*blue line*) overlaid with a time series of computed volume of water in the area on the west bank of the Red River (*red line*) for the 2011 simulation. 22

Figure 27. Plot of stage at Simmesport versus computed volume of water in the area on the west bank of the Red River. *Line color* changes by simulation date for the 2011 simulation..... 22

Figure 28. Volume-elevation curve for the Alligator Bayou basin on the east bank of the Red River north of ORCC..... 24

Figure 29. Time series of modeled water surface elevation for the east bank of the Red River from a point located at 91.677312°W 31.1309638°N (1347685.0014, 2967106.4525 in the RAS model) for each simulation. 24

Figure 30. Time series of interpolated volume for the 2D flow area on the east bank of the Red River for each simulation..... 25

Figure 31. Time series of flow in cfs at Simmesport (*blue line*) overlaid with a time series of computed volume of water in the area on the east bank of the Red River (*red line*) for the 2011 simulation. 25

Figure 32. Plot of flow in cfs at Simmesport versus computed volume of water in the area on the east bank of the Red River. *Line color* changes by simulation date for the 2011 simulation. 26

Figure 33. Time series of stage at Simmesport (*blue line*) overlaid with a time series of computed volume of water in the area on the east bank of the Red River (*red line*) for the 2011 simulation..... 26

Figure 34. Plot of stage at Simmesport versus computed volume of water in the area on the east bank of the Red River. *Line color* changes by simulation date for the 2011 simulation..... 27

Figure 35. Flow into storage (*blue* is western storage area, *orange* is eastern storage area) versus flow at Simmesport (cfs). 28

Figure 36. Percentage of ORCC flows going into storage (*blue*, western area; *orange*, eastern area) versus flow at Simmesport (cfs)..... 28

Figure 37. Flow into the western storage area versus flow at Simmesport (cfs) for each simulation. 29

Figure 38. Flow into the eastern storage area versus flow at Simmesport (cfs) for each simulation..... 30

Figure 39. Snapshot of velocity from 2011 run on simulation day May 6. Particle tracing overlaid on *top* of the velocity surface. Arrows added to show direction of flow into 2D flow areas..... 31

Figure 40. Snapshot of velocity from 2011 run on simulation day May 26 when water is starting to leave the 2D flow area. Particle tracing overlaid on *top* of the velocity surface. Arrows overlaid to show the direction of flow into or out of the 2D flow areas. 31

Figure A-1. Modeled flow in the Red River upstream of the confluence with the Black River from the High Red River simulation. 34

Figure A-2. Modeled flow at the site of the new stream gage at Madam Lee (downstream from the confluence with the Black River) from the High Red River simulation. 34

Figure A-3. Modeled flow for Wax Lake Outlet (outlet to the west of the main Atchafalaya River outlet) from the High Red River simulation..... 35

Figure A-4. Modeled flow at Simmesport along the Atchafalaya River south of the Old River Control Complex from the High Red River simulation. 35

Figure A-5. Modeled stages in the Whiskey Bay Pilot Channel from the High Red River simulation..... 35

Figure A-6. Modeled stages in the GIWW south of Morgan City from the High Red River simulation..... 36

Figure A-7. Time series of flow in cfs at Simmesport (*blue line*) overlaid with a time series of computed volume of water in the area on the west bank of the Red River (*red line*) for the High Red River simulation..... 36

Figure A-8. Plot of flow in cfs at Simmesport versus computed volume of water in the area on the west bank of the Red River. *Line color* changes by simulation date for the High Red River simulation. 37

Figure A-9. Time series of stage at Simmesport (*blue line*) overlaid with a time series of computed volume of water in the area on the west bank of the Red River (*red line*) for the High Red River simulation. 37

Figure A-10. Plot of stage at Simmesport versus computed volume of water in the area on the west bank of the Red River. *Line color* changes by simulation date for the High Red River simulation. 38

Figure A-11. Time series of flow in cfs at Simmesport (*blue line*) overlaid with a time series of computed volume of water in the area on the east bank of the Red River (*red line*) for the High Red River simulation. 38

Figure A-12. Plot of flow in cfs at Simmesport versus computed volume of water in the area on the east bank of the Red River. *Line color* changes by simulation date for the High Red River simulation. 39

Figure A-13. Time series of stage at Simmesport (*blue line*) overlaid with a time series of computed volume of water in the area on the east bank of the Red River (*red line*) for the High Red River simulation. 39

Figure A-14. Plot of stage at Simmesport versus computed volume of water in the area on the east bank of the Red River. *Line color* changes by simulation date for the High Red River simulation. 40

Figure A-15. Flow into storage (*blue* is western storage area, *orange* is eastern storage area) versus flow at Simmesport (cfs) for the High Red River simulation. 40

Figure A-16. Percentage of ORCC flows going into storage (*blue*, western area; *orange*, eastern area) versus flow at Simmesport (cfs) for the High Red River simulation. 41

Figure A-17. Modeled flow in the Red River upstream of the confluence with the Black River from the 60/40 simulation. 41

Figure A-18. Modeled flow at the site of the new stream gage at Madam Lee (downstream from the confluence with the Black River) from the 60/40 simulation. 42

Figure A-19. Modeled flow for Wax Lake Outlet (outlet to the west of the main Atchafalaya River outlet) from the 60/40 simulation. 42

Figure A-20. Modeled flow at Simmesport along the Atchafalaya River south of the Old River Control Complex from the 60/40 simulation. 42

Figure A-21. Modeled stages in the Whiskey Bay Pilot Channel from the 60/40 simulation. 43

Figure A-22. Modeled stages in the Gulf Intracoastal Waterway (GIWW) south of Morgan City from the 60/40 simulation. 43

Figure A-23. Time series of flow in cfs at Simmesport (*blue line*) overlaid with a time series of computed volume of water in the area on the west bank of the Red River (*red line*) for the 60/40 simulation. 44

Figure A-24. Plot of flow in cfs at Simmesport versus computed volume of water in the area on the west bank of the Red River. *Line color* changes by simulation date for the 60/40 simulation. 44

Figure A-25. Time series of stage at Simmesport (*blue line*) overlaid with a time series of computed volume of water in the area on the west bank of the Red River (*red line*) for the 60/40 simulation. 45

Figure A-26. Plot of stage at Simmesport versus computed volume of water in the area on the west bank of the Red River. *Line color* changes by simulation date for the 60/40 simulation. 45

Figure A-27. Time series of flow in cfs at Simmesport (*blue line*) overlaid with a time series of computed volume of water in the area on the east bank of the Red River (*red line*) for the 60/40 simulation. 46

Figure A-28. Plot of flow in cfs at Simmesport versus computed volume of water in the area on the east bank of the Red River. *Line color* changes by simulation date for the 60/40 simulation. 46

Figure A-29. Time series of stage at Simmesport (*blue line*) overlaid with a time series of computed volume of water in the area on the east bank of the Red River (*red line*) for the 60/40 simulation. 47

Figure A-30. Plot of stage at Simmesport versus computed volume of water in the area on the east bank of the Red River. *Line color* changes by simulation date for the 60/40 simulation. 47

Figure A-31. Flow into storage (*blue* is western storage area, *orange* is eastern storage area) versus flow at Simmesport (cfs) for the 60/40 simulation. 48

Figure A-32. Percentage of ORCC flows going into storage (*blue*, western area; *orange*, eastern area) versus flow at Simmesport (cfs) for the 60/40 simulation. 48

Figure A-33. Modeled flow in the Red River upstream of the confluence with the Black River from the 80/20 simulation. 49

Figure A-34. Modeled flow at the site of the new stream gage at Madam Lee (downstream from the confluence with the Black River) from the 80/20 simulation. 49

Figure A-35. Modeled flow for Wax Lake Outlet (outlet to the west of the main Atchafalaya River outlet) from the 80/20 simulation. 49

Figure A-36. Modeled flow at Simmesport along the Atchafalaya River south of the Old River Control Complex from the 80/20 simulation. 50

Figure A-37. Modeled stages in the Whiskey Bay Pilot Channel from the 80/20 simulation. 50

Figure A-38. Modeled stages in the GIWW south of Morgan City from the 80/20 simulation. 50

Figure A-39. Time series of flow in cfs at Simmesport (*blue line*) overlaid with a time series of computed volume of water in the area on the west bank of the Red River (*red line*) for the 80/20 simulation. 51

Figure A-40. Plot of flow in cfs at Simmesport versus computed volume of water in the area on the west bank of the Red River. *Line color* changes by simulation date for the 80/20 simulation. 51

Figure A-41. Time series of stage at Simmesport (*blue line*) overlaid with a time series of computed volume of water in the area on the west bank of the Red River (*red line*) for the 80/20 simulation. 52

Figure A-42. Plot of stage at Simmesport versus computed volume of water in the area on the west bank of the Red River. *Line color* changes by simulation date for the 80/20 simulation. 52

Figure A-43. Time series of flow in cfs at Simmesport (*blue line*) overlaid with a time series of computed volume of water in the area on the east bank of the Red River (*red line*) for the 80/20 simulation. 53

Figure A-44. Plot of flow in cfs at Simmesport versus computed volume of water in the area on the east bank of the Red River. *Line color* changes by simulation date for the 80/20 simulation. 53

Figure A-45. Time series of stage at Simmesport (*blue line*) overlaid with a time series of computed volume of water in the area on the east bank of the Red River (*red line*) for the 80/20 simulation. 54

Figure A-46. Plot of stage at Simmesport versus computed volume of water in the area on the east bank of the Red River. *Line color* changes by simulation date for the 80/20 simulation. 54

Figure A-47. Flow into storage (*blue* is western storage area, *orange* is eastern storage area) versus flow at Simmesport (cfs) for the 80/20 simulation. 55

Figure A-48. Percentage of ORCC flows going into storage (*blue*, western area; *orange*, eastern area) versus flow at Simmesport (cfs) for the 80/20 simulation. 55

Figure A-49. Modeled flow in the Red River upstream of the confluence with the Black River from the extreme flows simulation. 56

Figure A-50. Modeled flow at the site of the new stream gage at Madam Lee (downstream from the confluence with the Black River) from the extreme flows simulation. 56

Figure A-51. Modeled flow for Wax Lake Outlet (outlet to the west of the main Atchafalaya River outlet) from the extreme flows simulation. 56

Figure A-52. Modeled flow at Simmesport along the Atchafalaya River south of the Old River Control Complex from the extreme flows simulation. 57

Figure A-53. Modeled stages in the Whiskey Bay Pilot Channel from the extreme flows simulation. 57

Figure A-54. Modeled stages in the GIWW south of Morgan City from the extreme flows simulation. 57

Figure A-55. Time series of flow in cfs at Simmesport (*blue line*) overlaid with a time series of computed volume of water in the area on the west bank of the Red River (*red line*) for the extreme flows

simulation.....58
Figure A-56. Plot of flow in cfs at Simmesport versus computed volume of water in the area on the west bank of the Red River. *Line color* changes by simulation date for the extreme flows simulation.....58
Figure A-57. Time series of stage at Simmesport (*blue line*) overlaid with a time series of computed volume of water in the area on the west bank of the Red River (*red line*) for the extreme flows simulation.....59
Figure A-58. Plot of stage at Simmesport versus computed volume of water in the area on the west bank of the Red River. *Line color* changes by simulation date for the extreme flows simulation.....59
Figure A-59. Time series of flow in cfs at Simmesport (*blue line*) overlaid with a time series of computed volume of water in the area on the east bank of the Red River (*red line*) for the extreme flows simulation.....60
Figure A-60. Plot of flow in cfs at Simmesport versus computed volume of water in the area on the east bank of the Red River. *Line color* changes by simulation date for the extreme flows simulation.....60
Figure A-61. Time series of stage at Simmesport (*blue line*) overlaid with a time series of computed volume of water in the area on the east bank of the Red River (*red line*) for the extreme flows simulation.....61
Figure A-62. Plot of stage at Simmesport versus computed volume of water in the area on the east bank of the Red River. *Line color* changes by simulation date for the extreme flows simulation.....61
Figure A-63. Flow into storage (*blue* is western storage area, *orange* is eastern storage area) versus flow at Simmesport (cfs) for the extreme flows simulation. 62
Figure A-64. Percentage of ORCC flows going into storage (*blue*, western area; *orange*, eastern area) versus flow at Simmesport (cfs) for the extreme flows simulation. 62

Tables

Table 1. List of reports included in the overall project. 3
Table 2. Peak flows for 2011 calibration used at the upstream boundaries for the Mississippi River, Red River, and Old River Control Structure (ORCS). 6
Table 3. Showing the peak flows in cfs for each scenario at the upstream boundaries for the Mississippi River, Red River, and ORCC.....12
Table 4. Peak flows and associated flow multipliers for 2015 (high Red, low Mississippi) scenario used at the upstream boundaries for the Mississippi River, Red River, and ORCS. 13
Table 5. Peak flows and associated flow multipliers for 60/40 split (60% flow to the Mississippi; 40% flow to the Atchafalaya) scenario used at the upstream boundaries for the Mississippi River, Red River, and ORCS.....14
Table 6. Peak flows and associated flow multipliers for 80/20 split (80% flow to the Mississippi; 20% flow to the Atchafalaya) scenario used at the upstream boundaries for the Mississippi River, Red River, and ORCC. 15
Table 7. Peak flows and associated flow multipliers for extreme flows scenario used at the upstream boundaries for the Mississippi River, Red River, and ORCC for the time period when the Mississippi River was at its peak. 16
Table B-1. Outlet rating curve for how the Morganza spillway is operated as specified in RAS. 63
Table B-2. Outlet rating curve for how the Bonnet Carré spillway is operated as specified in RAS. 63

Preface

The investigation documented in this report was conducted for the US Army Corps of Engineers, Mississippi Valley Division (MVD), as part of the Mississippi River and Tributaries Project, under Project No. 478534, and published through the Mississippi River Geomorphology and Potamology (MRG&P) Program. At the time of publication of this report, the MRG&P Program director was Dr. James W. Lewis. The MVD commander was MG Diana M. Holland, and the MVD director of programs was Mr. Edward E. Belk.

The work was performed by the Coastal Engineering and Environmental Section of the Hydraulics, Hydrology, and Coastal Branch and the Lower Mississippi River and Tributary Branch of the Engineering and Construction Division, New Orleans District. At the time of publication of this report, Ms. Stacey U. Frost was chief of the Coastal Engineering and Environmental Section, Ms. Amena M. Henville was chief of the Hydraulics, Hydrology and Coastal Branch, Mr. David A. Ramirez, Jr., was chief of the Lower Mississippi River and Tributary Branch, and Mr. Christopher L. Dunn was chief of the Engineering and Construction Division. COL Stephen F. Murphy was commander of the New Orleans District.

1 Introduction

There are two primary sources of flooding in the floodplain areas along the Lower Red River above the Old River Control Complex (ORCC) Outflow Channel confluence. The first source of flooding is a riverine flood event on the Red River, with its source being a large precipitation event upstream in its watershed. A flood event of this type happened in 2015. The second flooding source is backwater flooding from high flows out of the ORCC Outflow Channel, which occurs due to high water or flooding occurring in the Mississippi River Valley. In this situation, the flows in the Red River are typically average to low, and the flows and stages in the Mississippi River are above normal or considered high, which results in the total outflow from the entire ORCC, including Sidney A. Murray Hydropower Plant, to be high. These flows can be up to 620,000 cfs[1,2]. Water levels anywhere near this range would cause extensive backwater flooding in the Lower Red River watershed.

Figure 1. RAS terrain showing the spatial extent of the 2D flow areas and the cross sections for the 1D reaches.

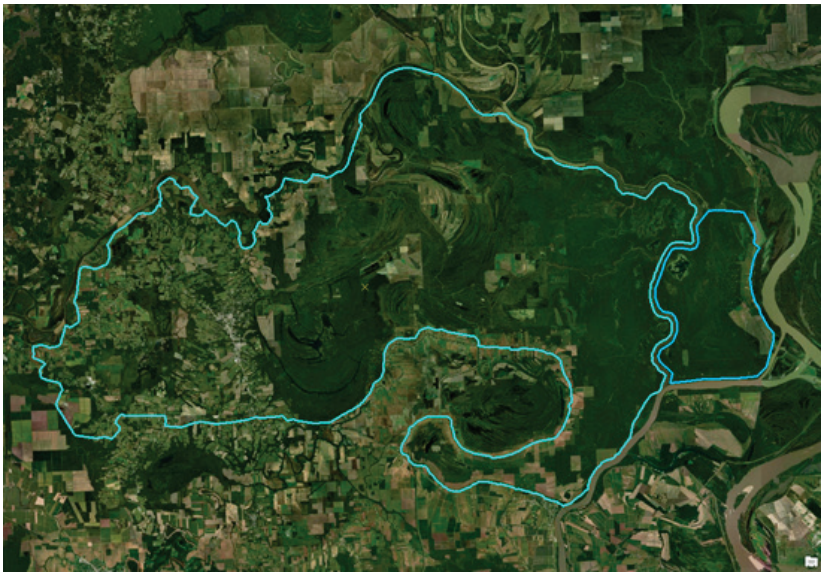

[1] For a full list of the spelled-out forms of the units of measure used in this document, please refer to *US Government Publishing Office Style Manual*, 31st ed. (Washington, DC: US Government Publishing Office 2016), 248-52, https://www.govinfo.gov/content/pkg/GPO-STYLEMANUAL-2016/pdf/GPO-STYLEMANUAL-2016.pdf.

[2] For a full list of the unit conversions used in this document, please refer to *US Government Publishing Office Style Manual*, 31st ed. (Washington, DC: US Government Publishing Office 2016), 345-7, https://www.govinfo.gov/content/pkg/GPO-STYLEMANUAL-2016/pdf/GPO-STYLEMANUAL-2016.pdf.

There are specifically two areas just upriver of ORCC on both the east (Alligator Bayou basin—an area containing Three Rivers Wildlife Management Area) and west (Bayou Natchitoches basin—an area containing Glassy Lake State Wildlife Management Area, Lake Ophelia National Wildlife Refuge, and Spring Bayou State Wildlife Management Area) sides of the Lower Red River (Figure 1) that frequently flood during high water events, as these sections along the Red River feature only natural levees and river banks.

1.1 Background

Under normal river conditions and using the current ORCC operating criteria, there is still much to learn about the volume and timing of the water that is stored in the Red River floodplain areas described above. In a fast-rising Mississippi River condition, the water managers calculate how much water to divert at ORCC based on upstream conditions of both the Mississippi and Red Rivers. Once the proper flow distribution is determined, gate change orders are sent to the ORCC structures, and the structure gates are adjusted as specified in accordance with the Water Control Manual. To check that the diversion flows are correct, there are gages located downstream on both the Mississippi and Atchafalaya Rivers at Red River Landing and Simmesport, respectively. In times when the Mississippi River flows are high and the Red River flows are low, the Simmesport gage downstream on the Atchafalaya River can sometimes indicate a lower flow than what is expected by the Water Manager computing the gate setting at the ORCC. The difference in the flow allocation at ORCC and the increase in flows at Simmesport are being stored on the Red River floodplain.

1.2 Objective

The goal of this task in the OMAR Assessment is to investigate how water during flood events is stored in the Lower Red River floodplain just above the confluence of the ORCC Outflow Channel. Understanding the processes and differences of how water leaves the Red River channel during both high Red River Flows and high flows from the ORCC will greatly inform the water managers and operators of the ORCC and could help to optimize operation decisions that could potentially benefit downstream river conditions on the Atchafalaya and Mississippi Rivers.

This effort is a part of the overall Old, Mississippi, Atchafalaya, and Red (OMAR) Rivers Assessment. Table 1 lists the series of reports associated with the overall project, with this report listed in bold font.

Table 1. List of reports included in the overall project.

Vol.	Report name	Description
1	Main Report	Summarizes the entire project assessment
2	Geomorphic Assessment	Analyzes the historic trends in hydrology, sedimentation, and channel geometry of the river reaches of interest
3	Channel Geometry Analysis	Analyzes the hydrographic surveys over the past 6 to 7 decades
4	Mississippi River HEC-6T Model	Evaluate the long-term and system-wide sedimentation effects on the Mississippi River
5	Atchafalaya River HEC-6T Model	Evaluate the long-term and system-wide sedimentation effects on the Old, Atchafalaya, and Red Rivers
6	Mississippi River Multi-Dimensional Model	Evaluate the short-term effects on the Mississippi River
7	Red and Atchafalaya Rivers Adaptive Hydraulics (AdH) Model	Evaluate the short-term effects on the Old, Atchafalaya and Red Rivers
8	**HEC-RAS Model**	Investigate how water is stored in the Lower Red River floodplain
9	HEC-RAS BSTEM Analysis of the Atchafalaya River	Compare the relative impact of various scenarios on bank retreat in the upper portion of the Atchafalaya River

1.3 Approach

This analysis intends to quantify the volume of the water moving into the Lower Red River floodplain as well as the timing of when this begins to occur, when the areas fill up, and when the floodplain areas begin to drain. All these processes inform the operation decisions that occur at ORCC.

2 Methodology

The model used in this study combined two existing Hydrologic Engineering Center River Analysis System (HEC-RAS) models—one for the Lower Mississippi River and Atchafalaya River and one for the Lower Red and Black Rivers. The setup is a combined 1D/2D model (Figure 2) with 1D reaches in the main channels and features 2D flow areas for the spatial extent outside the riverbanks. The model for the Lower Mississippi and Atchafalaya Rivers is a 1D/2D flowline model for both rivers and was derived from the New Orleans District-developed South Louisiana Master Model (SLaMM) model as of Summer 2020. This model was updated to be run in HEC-RAS 6.2 on the release of that update. The model of the Red River area was obtained from the Vicksburg District. The modeling setup has a terrain resolution of 20 ft obtained from the US Geological Survey (USGS) for the Northern Gulf of Mexico (NGOM) (USGS NGOM data) and uses 2016 National Land Cover Database (NLCD) land cover data (https://www.mrlc.gov/data/nlcd-2016-land-cover-conus). Tables showing the values for the outlet rating curves for the Morganza and Bonnet Carré Spillways are shown in Appendix B. This model was tested with observed inputs from the 2011 flood and used proportional scaling on the 2011 hydrographs to compute other scenarios.

Figure 2. River Analysis System (RAS) terrain showing the spatial extent of the 2D flow areas and the cross sections for the 1D reaches.

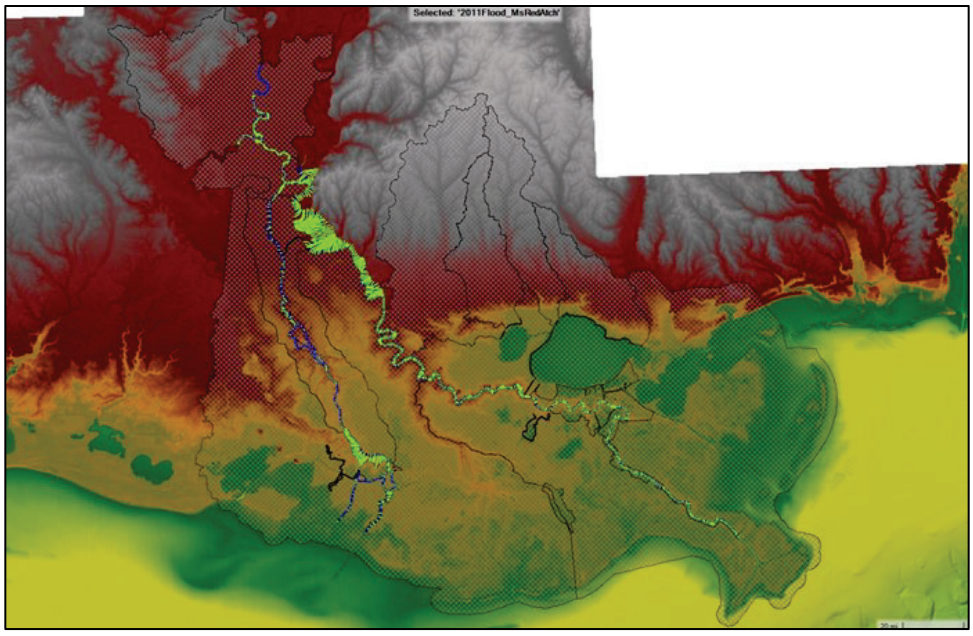

3 Model Calibration and Alternative Assessments

3.1 Model calibration and alternative assessments setup

To fully understand the hydrodynamics that occur in the Lower Red River floodplain, it is necessary to investigate the different flooding sources of the area. The two prominent flooding sources are a Red River flood such as was observed in 2015, and a Mississippi River flood, along with a low Red River, which was observed in 2011. Modeling these two flood events and observing the filling and draining of the Red River floodplain will illustrate the hydrodynamics of this area and its impacts on the operation of the ORCC.

In addition to these two flood events, the hydraulic model was set up to run two different ORCC operations scenarios to investigate and to illustrate the impacts on the Lower Red River floodplain area. Finally, the full Mississippi River and Tributaries (MR&T) Project Design Flood event was run in the hydraulic models.

Using the 2011 flood event, the hydraulic model was calibrated to match observed data in many gage locations around ORCC. Below is a detailed description of the model calibration process.

3.2 Calibration run: 2011 Hindcast setup (High Mississippi, Low Red)

The 2011 Flood Event was historic in terms of flows on the Mississippi River where both the Bonnet Carré and Morganza Spillways were opened to alleviate flooding pressure in the Lower Mississippi River. The high stages and flows in the Lower Mississippi River and the opening of these spillway structures in 2011 provided a suitable event to calibrate the hydraulic model that had been developed to historical data. This is the first time in history that the Morganza Floodway was operated based on exceeding the flow trigger. Note that while the flows on the Mississippi River were high, the flows in the Red River were extremely low.

The simulation run is from 24 February 2011 to 30 June 2011, using observations from the same period as the boundary conditions. Flow hydrograph (Figure 3) boundary conditions were implemented using

observed flows from the Mississippi River at Red River Landing, ORCS Low Sill Structure, ORCS Auxiliary Structure, the Sidney Murray hydropower structure, and Red River at Alexandria, LA. These observations were available at Alexandria but not Lock and Dam #1, and engineers at US Army Corps of Engineers (USACE) Vicksburg District noted that this approach of applying Alexandria flows rather than Lock and Dam #1 flows at this location has been done previously, as the flows tend to be similar. Peak flows for each flow boundary condition are shown in Table 2. Stage hydrograph boundary conditions were implemented using river stage observations from the Black River at Jonesville Lock and Dam (flow observations were not available at this location) and tidal levels at the downstream boundary for the Atchafalaya and Wax Lake Outlets. Initial conditions of 1.2 ft were added at the coastal boundaries.

Figure 3. Flow rates in cubic feet per second for Mississippi River, Red River, and combined flows at ORCS.

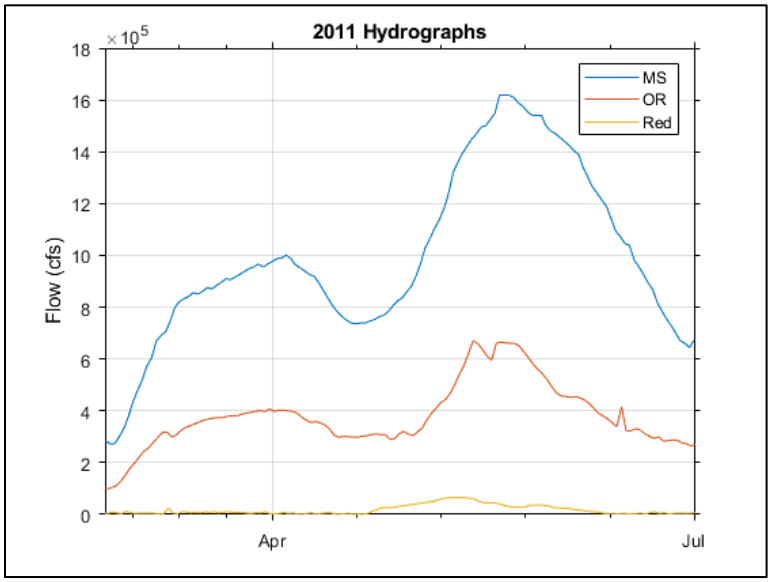

Table 2. Peak flows for 2011 calibration used at the upstream boundaries for the Mississippi River, Red River, and Old River Control Structure (ORCS).

River	Peak Flow (cfs)
Mississippi	1,619,000
Red	65,013
ORCC (Low Sill)	316,000
ORCC (Auxiliary)	233,000
ORCC (Hydropower)	162,000

All subsequent simulations use proportional adjustments to the 2011 hydrographs shown in Figure 3. These proportional adjustments were made by using the multiplier in the flow hydrograph that is defined in the unsteady flow data editor in HEC-RAS. For using implementing model scenarios, hydraulic scaling factors of 1 were used for the Mississippi River flows, Red River flows, and flows for each of the Old River sites (i.e., Low Sill, Hydropower/Sidney Murray, and Auxiliary) in the 2011 simulation. Therefore, a multiplier between 0 and 1 would decrease flows for a given boundary condition, and values greater than 1 would increase flows for that reach in any subsequent simulations.

3.3 Black River boundary condition

Since observations of river stage were available on the Black River at Jonesville but not observations of flow, a stage boundary condition was used in the RAS model for the 2011 hindcast simulation. However, to ensure proper river stages in the Black River for subsequent simulations, a flow boundary condition was needed. The time series of the outputs of flow from the 2011 hindcast simulation (Figure 4) was used for the High Red, 60/40 Split, and 80/20 Split simulations. For the High Red simulation, these flows were scaled down using a flow multiplier of 0.77 (to account for the increase in flows in the Red River and to maintain the 70/30 split of flow for the Mississippi and Atchafalaya Rivers, respectively) to prevent the model from crashing due to the rapid change in the flow time series. For the 80/20 Split scenario, all flows <1,000 cfs (and all negative flows) were changed to a flow of 1,000 cfs to maintain a minimum flow at the boundary for the model to remain stable. A separate time series (Figure 5) was used as flow input for the Extreme Flows scenario using model outputs from Lewis et al. (2018). That model covered a shorter time period than these simulation runs, so the flows were held constant at the beginning and end of the time series to complete the input record.

Figure 4. Modeled output of flow in the Black River at Jonesville from the 2011 hindcast simulation.

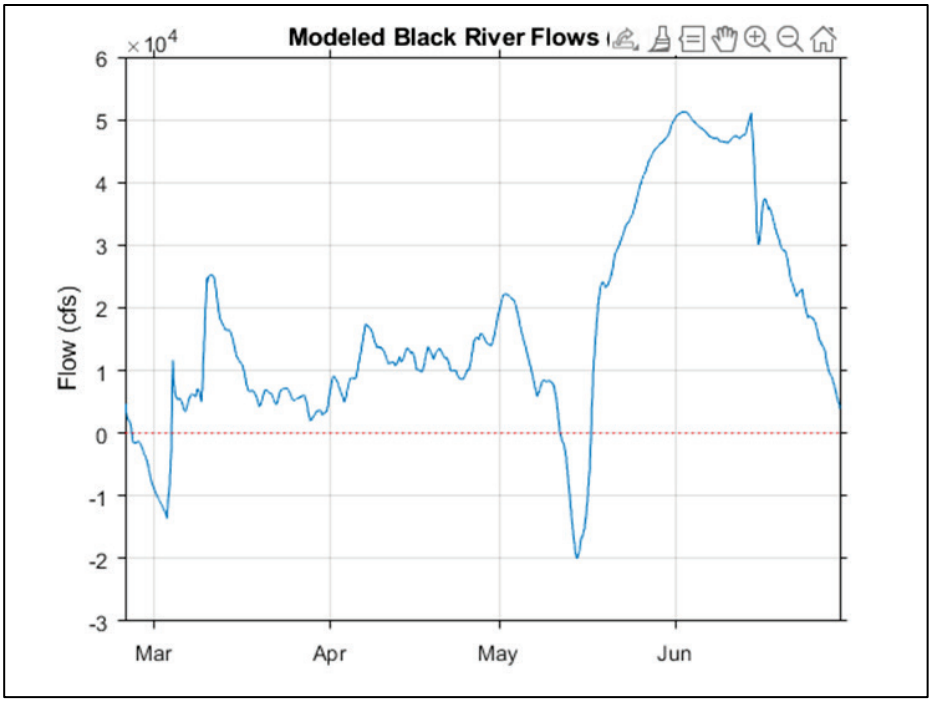

Figure 5. Modeled output of flow in the Black River at Jonesville from the flowline model.

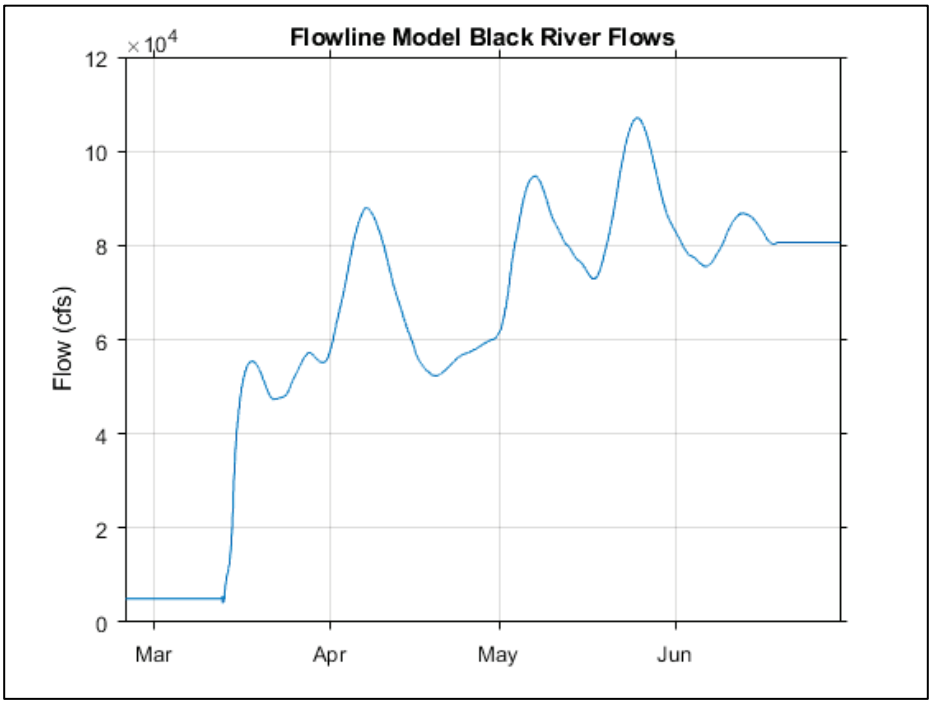

3.4 2011 Hindcast results and comparison to observations

Output of maximum water depth for the 2011 hindcast is shown in Figure 6. The openings of the Morganza and Bonnet Carré Spillways are evident in the spatial extent of the flooding. Sample outputs of flow from various cross sections are shown in Figure 7, Figure 8, Figure 9, and Figure 10. Comparisons of the time series of observed versus modeled outputs of flow (Figure 11) and stages (Figure 12 and Figure 13) are also shown, and the model performs well compared with these historical observations from 2011. Locations of modeled output shown in Figure 7.

Figure 6. Max depth plotted for 2011 simulation.

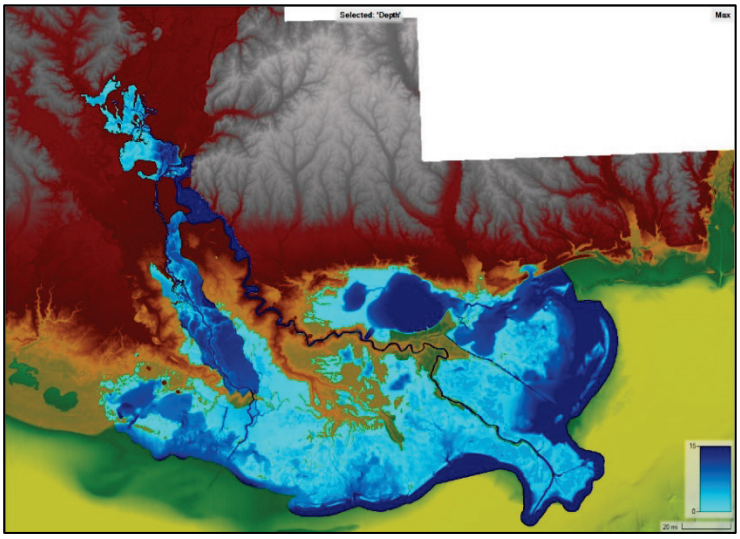

Figure 7. Locations of modeled outputs shown. Blue indicates location of modeled output only; red indicates modeled and observed data available.

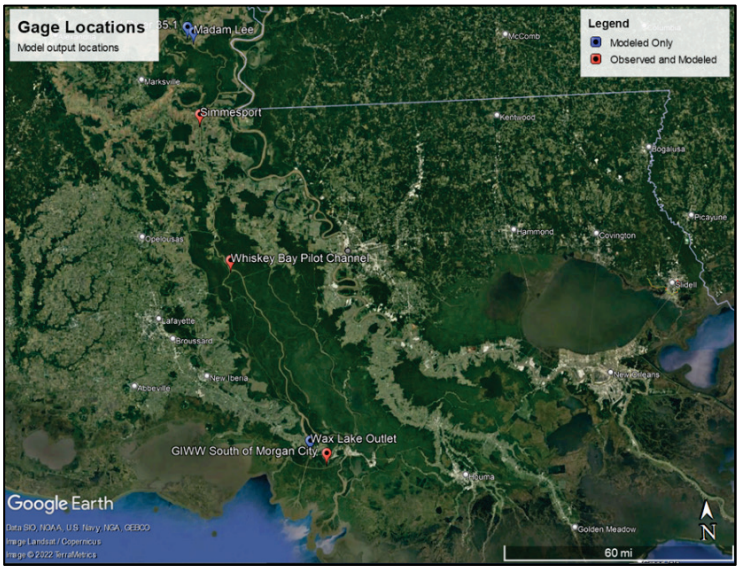

Figure 8. Modeled flow in the Red River upstream of the confluence with the Black River from the 2011 simulation.

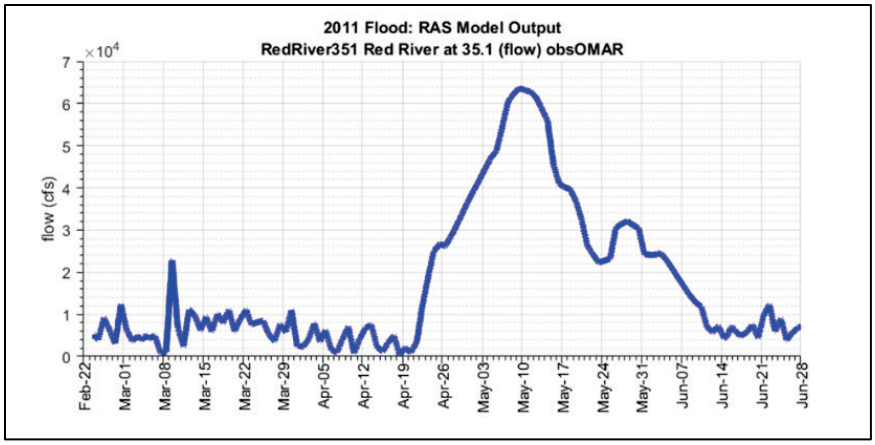

Figure 9. Modeled flow at the site of the new stream gage at Madam Lee (downstream from the confluence with the Black River) from the 2011 simulation.

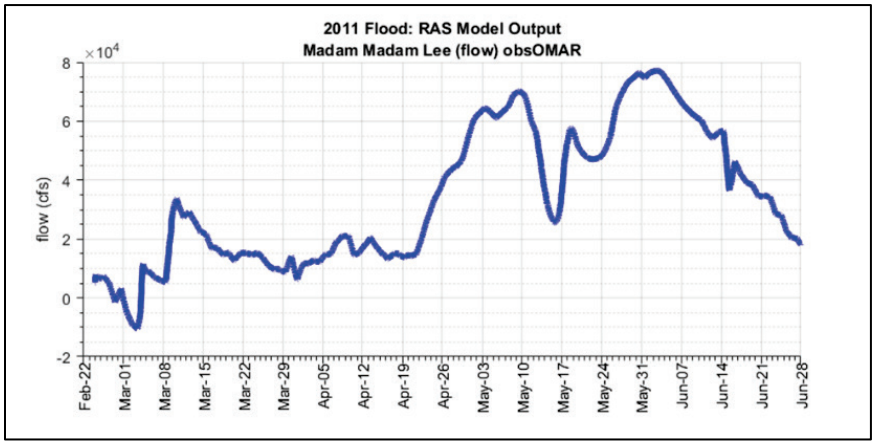

Figure 10. Modeled flow for Wax Lake Outlet (outlet to the west of the main Atchafalaya River outlet) from the 2011 simulation.

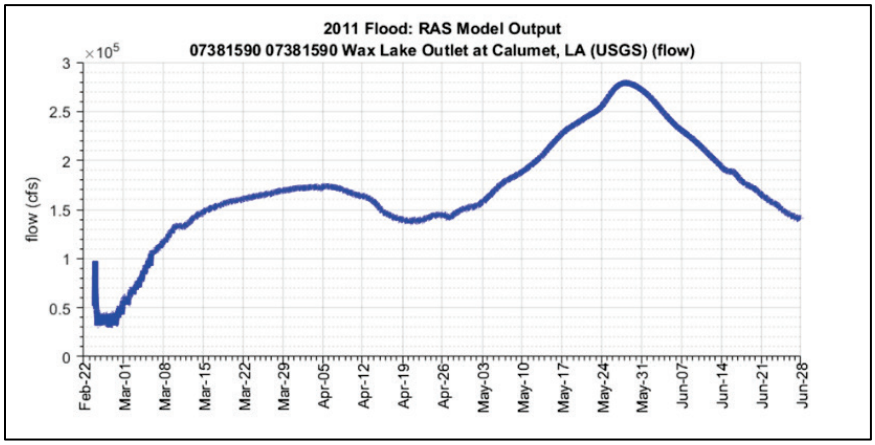

3.5 Observed versus modeled outputs

Figure 11. Observed versus modeled flow at Simmesport along the Atchafalaya River south of the ORCC.

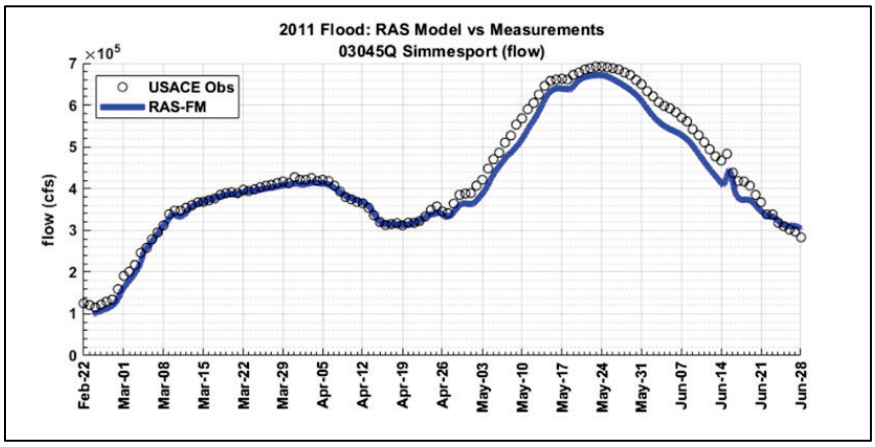

Figure 12. Observed versus modeled stages in the Whiskey Bay Pilot Channel.

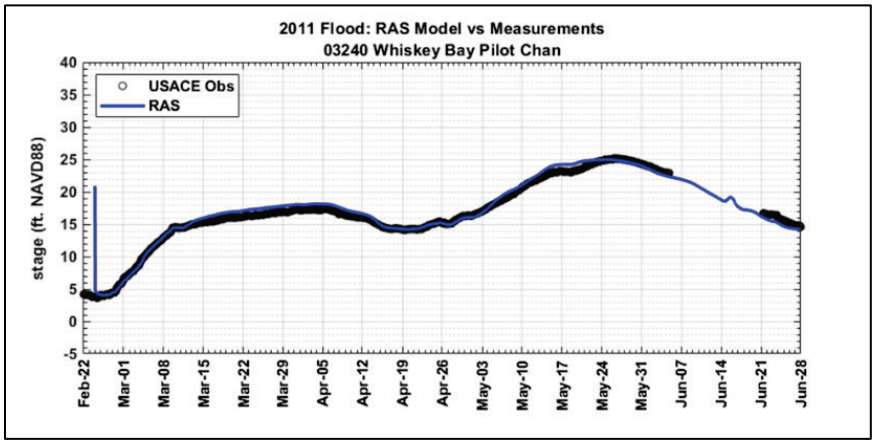

Figure 13. Observed versus modeled flow in the Gulf Intracoastal Waterway (GIWW) south of Morgan City.

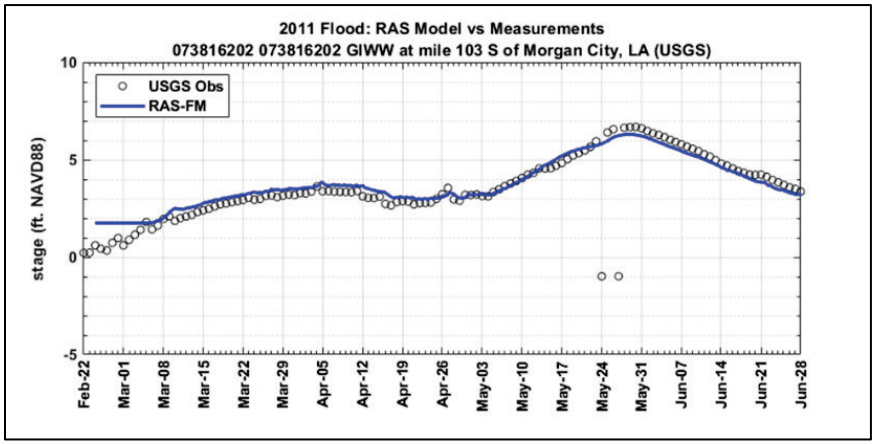

4 Alternative Assessments Setup and Results

The hydraulic model was calibrated using a 2011 as a test case. Below is a detailed description of additional simulations conducted using the calibrated RAS model. A summary table of the simulations is shown in Table 3.

Table 3. Showing the peak flows in cfs for each scenario at the upstream boundaries for the Mississippi River, Red River, and ORCC.

River	2011	High Red	60/40	80/20	Extreme Flows
Mississippi	1,619,000	971,000	1,619,000	1,619,000	2,881,820
Red	65,013	250,300	65,013	65,013	300,000
ORCC (total)	671,000	426,600	1,244,250	1,011,150	711,000

4.1 High Red River, Low Mississippi River (motivated by 2015)

This scenario simulates high flows in the Red River and relatively low flows in the Mississippi River—which is the opposite dynamic as was seen in 2011—and is motivated by the flooding events along the Red River seen in 2015. The flooding events in 2015 were not directly modeled but were simulated using proportional adjustments (Figure 14 and Table 4) to the 2011 flows to create the effect of a high Red River and relatively low Mississippi River. The maximum water depths from the simulation are shown in Figure 14. Additional outputs can be found in Appendix A.

Figure 14. Max depth plotted for high Red River simulation.

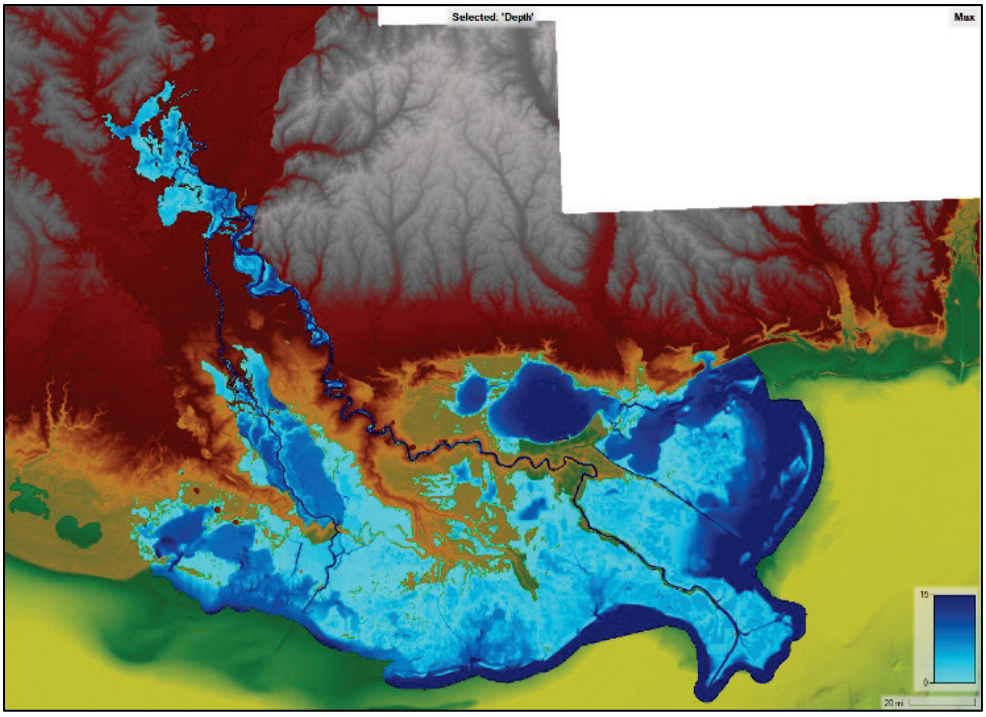

Table 4. Peak flows and associated flow multipliers for 2015 (high Red, low Mississippi) scenario used at the upstream boundaries for the Mississippi River, Red River, and ORCS.

River	Peak Flow (cfs)	Flow Multiplier
Mississippi	971,400	0.6
Red	250,300	3.85
ORCC (Low Sill)	189,600	0.6
ORCC (Auxiliary)	139,800	0.6
ORCC (Hydropower)	97,200	0.6

4.2 Old River 60/40 split

The ORCS regulates the amount of flow from the Mississippi River to the Atchafalaya River keeping the average percentages of the combined latitudinal flow to be 70% in the Mississippi River and 30% down the Atchafalaya River (70/30). This scenario alters the 70/30 split of the proportional latitude flow to be 60% in the Mississippi River and 40% in the Atchafalaya River but keeping the 2011 flows in the Mississippi. Table 5 shows the flow multiplier values used for each flow boundary condition. Maximum water depth output from the simulation is shown in Figure 15. Additional outputs can be found in Appendix A.

Figure 15. Max depth plotted for ORCC diversion split altered to be 60% Mississippi River, 40% Atchafalaya River.

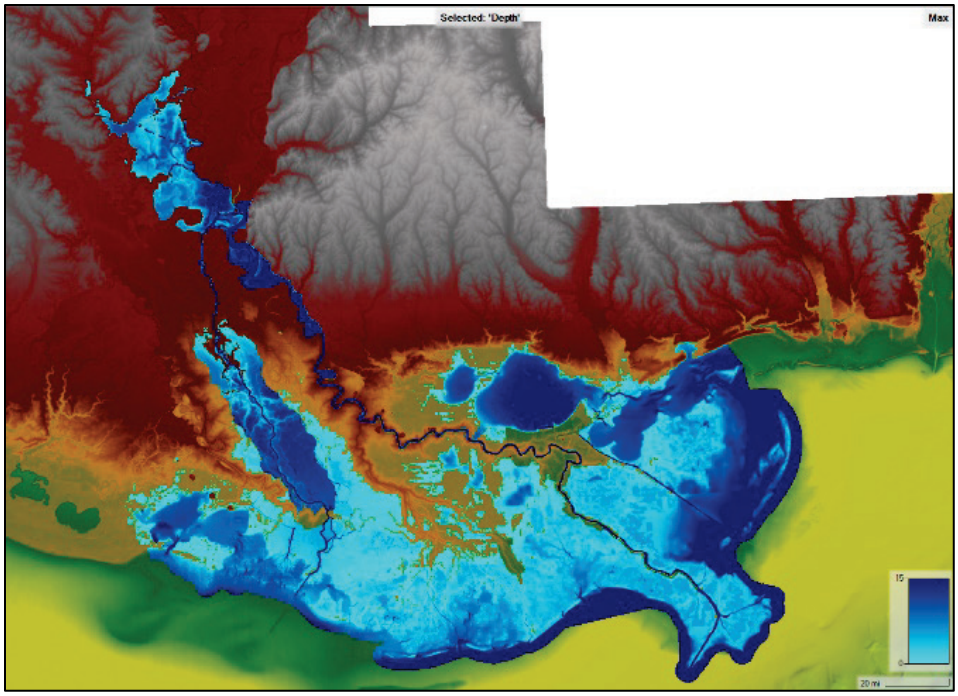

Table 5. Peak flows and associated flow multipliers for 60/40 split (60% flow to the Mississippi; 40% flow to the Atchafalaya) scenario used at the upstream boundaries for the Mississippi River, Red River, and ORCS.

River	Peak Flow (cfs)	Flow Multiplier
Mississippi	1,343,770	0.83
Red	65,013	1
ORCC (Low Sill)	391,840	1.24
ORCC (Auxiliary)	288,920	1.24
ORCC (Hydropower)	200,880	1.24

4.3 Old River 80/20 split

The ORCC regulates the amount of flow from the Mississippi River to the Atchafalaya River keeping the average annual percentages of the combined latitudinal flow to be 70% in the Mississippi River and 30% down the Atchafalaya River. This scenario alters the 70/30 split of latitudinal flow at ORCS to be 80% in the Mississippi River and 20% in the Atchafalaya River but keeping the 2011 flows in the Mississippi. Table 6 shows the flow multiplier values used for each flow boundary condition. Maximum water depth output from the simulation is shown in Figure 16. Additional outputs can be found in Appendix A.

Figure 16. Max depth plotted for ORCC diversion split altered to be 80% Mississippi River, 20% Atchafalaya River.

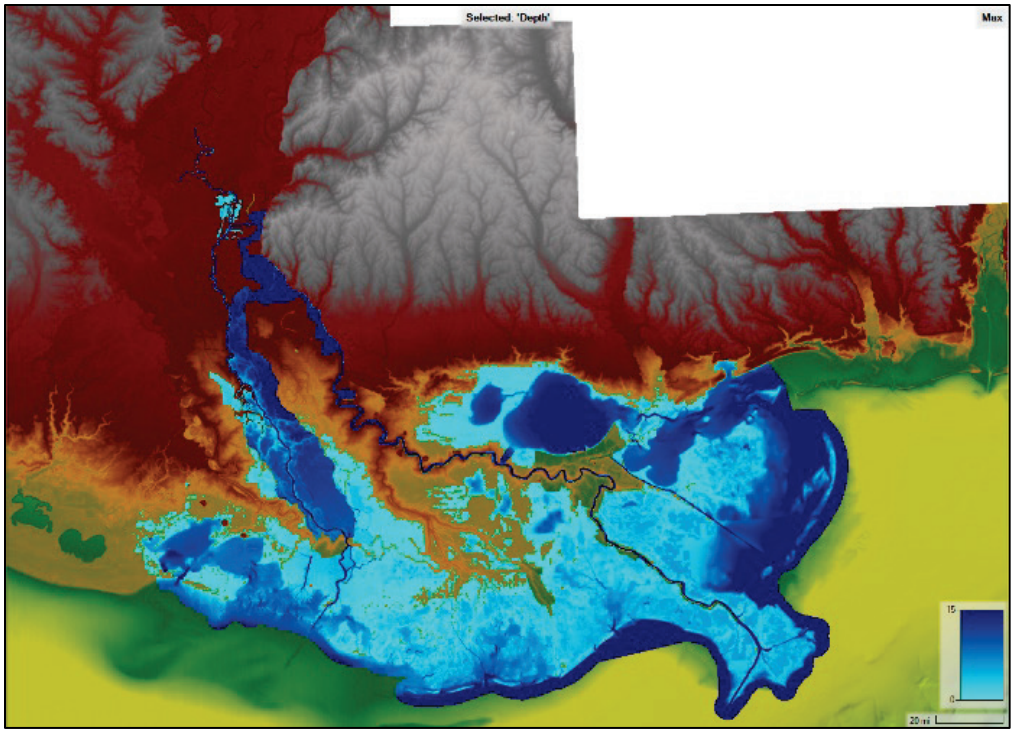

Table 6. Peak flows and associated flow multipliers for 80/20 split (80% flow to the Mississippi; 20% flow to the Atchafalaya) scenario used at the upstream boundaries for the Mississippi River, Red River, and ORCC.

River	Peak Flow (cfs)	Flow Multiplier
Mississippi	1,797,090	1.11
Red	65,013	1
ORCC (Low Sill)	180,120	0.57
ORCC (Auxiliary)	132,810	0.57
ORCC (Hydropower)	92,340	0.57

4.4 Modeled extreme flows

This scenario simulates the flow inputs of the extreme flows scenario for the Mississippi River, Red River, ORCS, Bonnet Carré Spillway, and Morganza Spillway. This scenario is motivated by Project Design but flows are adapted for use in a nonsteady state model. The flow multipliers (Table 7) were chosen based on the flow during the time of the highest flows for the Mississippi River to obtain the appropriate flows for the extreme flows

scenario occurring at the same time. The output maximum water depth is shown in Figure 17. Additional outputs can be found in Appendix A.

Figure 17. Maximum depth plotted for extreme flows scenario.

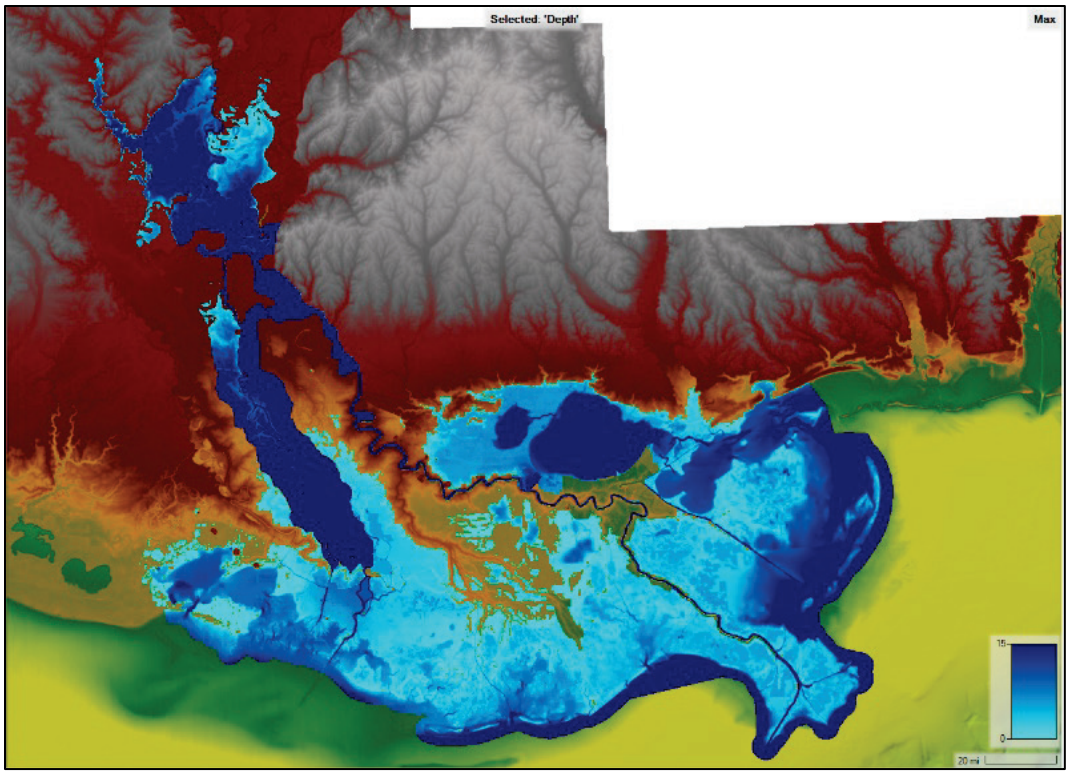

Table 7. Peak flows and associated flow multipliers for extreme flows scenario used at the upstream boundaries for the Mississippi River, Red River, and ORCC for the time period when the Mississippi River was at its peak.

River	Peak Flow (cfs)	Flow Multiplier
Mississippi	2,881,820	1.78
Red	300,000	10.06
ORCC (Low Sill)	316,000	1
ORCC (Auxiliary)	233,000	1
ORCC (Hydropower)	162,000	1

5 Discussion

During high flows, the two 2D flow areas on either side of the Red River fill with water. This region is characterized by the presence of only natural levees along the Red River (Figure 18) and has relatively flat topography (Figure 19). Determining how much water floods these areas is therefore crucial for improving operations by water managers during periods of high flows on the Red, Mississippi, and Atchafalaya Rivers.

Figure 18. Map showing levees (both federal and local) in region. Image from National Levee Database website (https://levees.sec.usace.army.mil/#/).

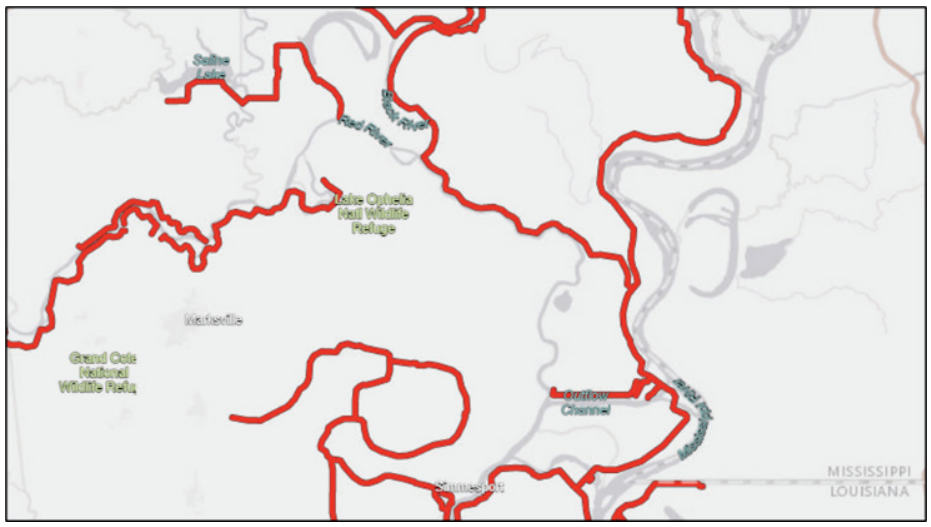

Figure 19. RAS terrain near the 2D flow areas of interest on the west and east banks of the Red River just upstream of ORCS.

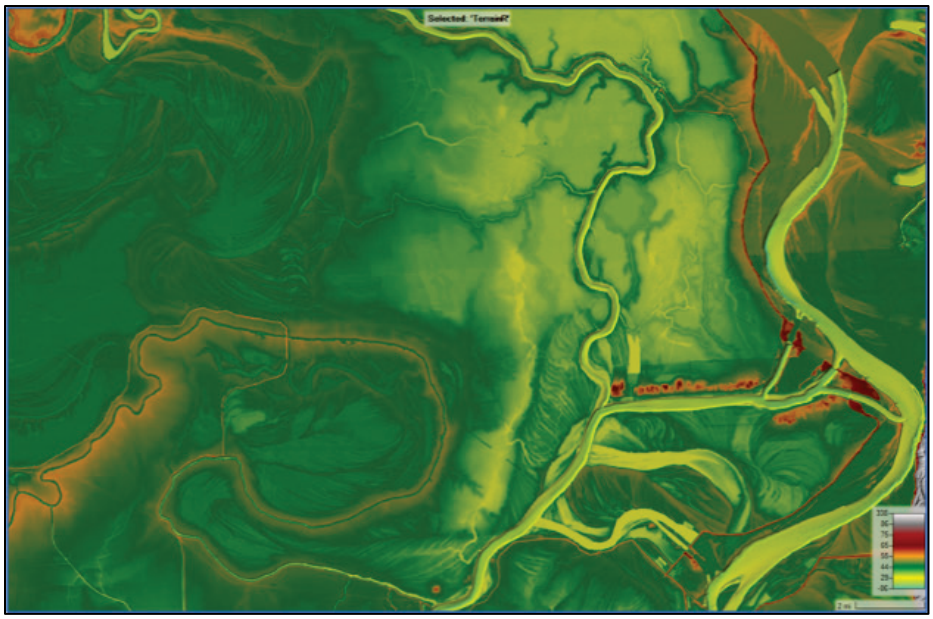

Using the bathymetry in the 2D flow areas defined in RAS, a volume-elevation was created by converting the 2D flow area after simulations were complete to a RAS storage area in RAS Mapper and exporting the volume-elevation curve provided for each region on the west (Figure 21) and east (Figure 28) sides of the Red River. At locations chosen to represent low-elevation sites within the respective storage areas (Figure 20), time series of water surface elevation outputs from each modeled scenario were extracted to better understand the timing of flooding within the areas on both the west (Figure 22) and east (Figure 29) banks of the Red River. Using the volume-elevation curve computed from the topography in RAS, time series of computed stage elevations for each simulation could be interpolated to create a time series of the volume of the water inundated in each area on either side of the Red River (Figure 23 and Figure 30). The time series of volume provide more insight into how much water is in each storage area as a function of time. The understanding of the relationship between the stage and volume of water in each of these areas will be crucial for helping improve operations at the ORCC.

Figure 20. Location of points where output time series of water surface elevation was extracted.

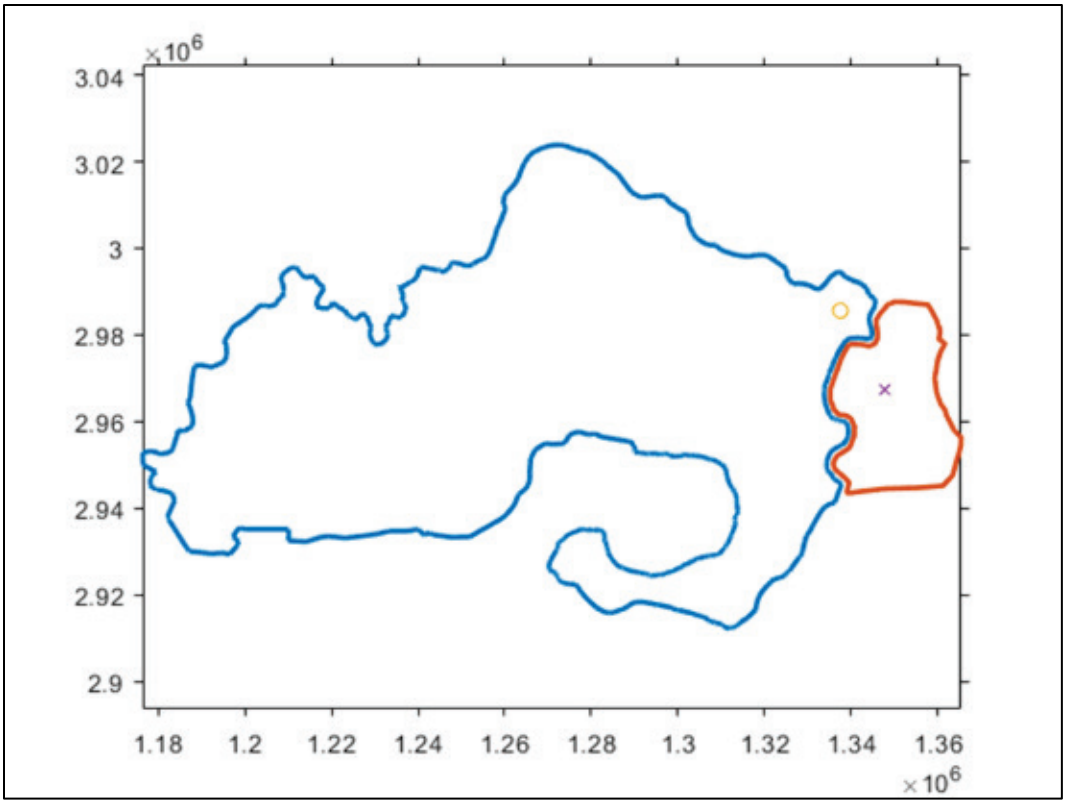

5.1 West bank of Red River—Bayou Natchitoches basin

Figure 21. Volume-elevation curve for the Bayou Natchitoches basin on the west bank of the Red River.

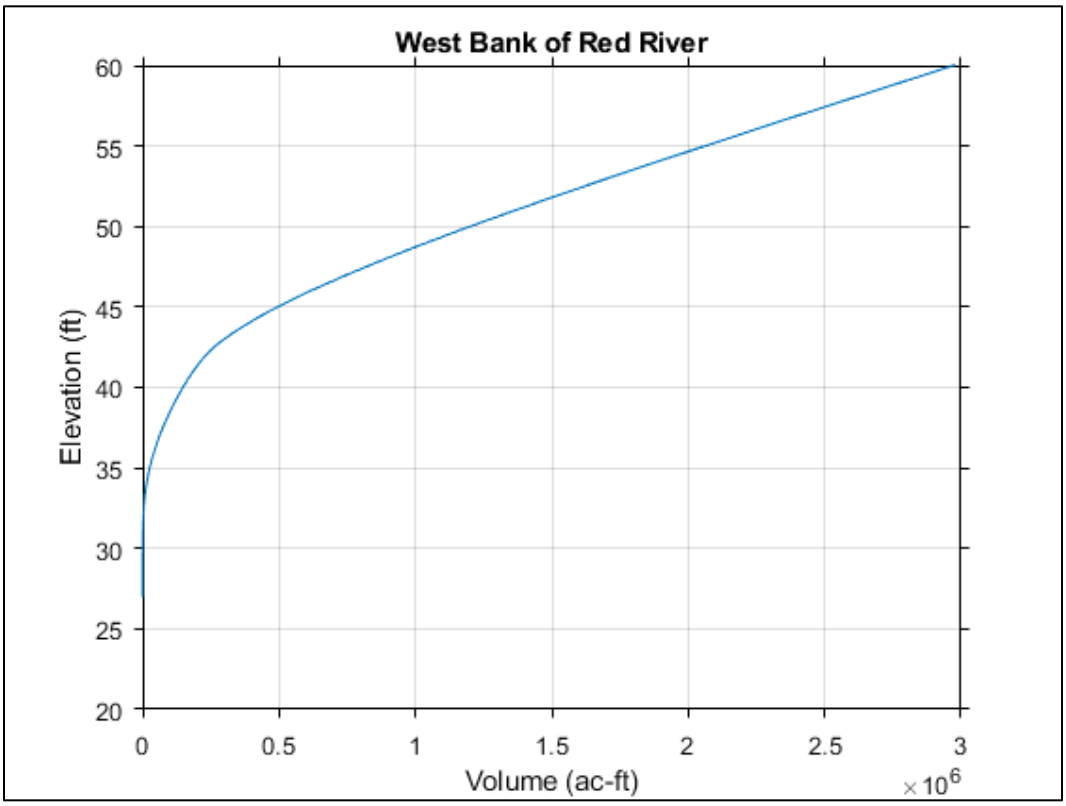

Using the volume-elevation curve from the bathymetry (Figure 21), the modeled output time series of stage (Figure 22) for a specified location in the watershed was interpolated for each simulation to create a time series of the volume contained within the RAS 2D flow area (Figure 23). The modeled stages and calculated volumes from each simulation are plotted together to show the relative difference in the amount of water and the timing of the onset of flooding in the areas. Results show that the amount of water in the 2011 is greater than the amount of water for the high Red River simulation motivated by the 2015 flood events as well as the 80/20 scenario. However, flooding is less than in the 60/40 split scenario—where extra water is diverted through ORCC—and in the extreme flows scenario. Additionally, it can be seen how the draining of the floodwaters after the peak compares between the scenarios. This information can help show approximately how much water is stored depending on the type of flood event and can be useful for water managers.

Figure 22. Time series of modeled water surface elevation for the west bank of the Red River from a point located at 91.7071193°W 31.182803°N (1337547.3503, 2985581.611 in the RAS model) for each simulation.

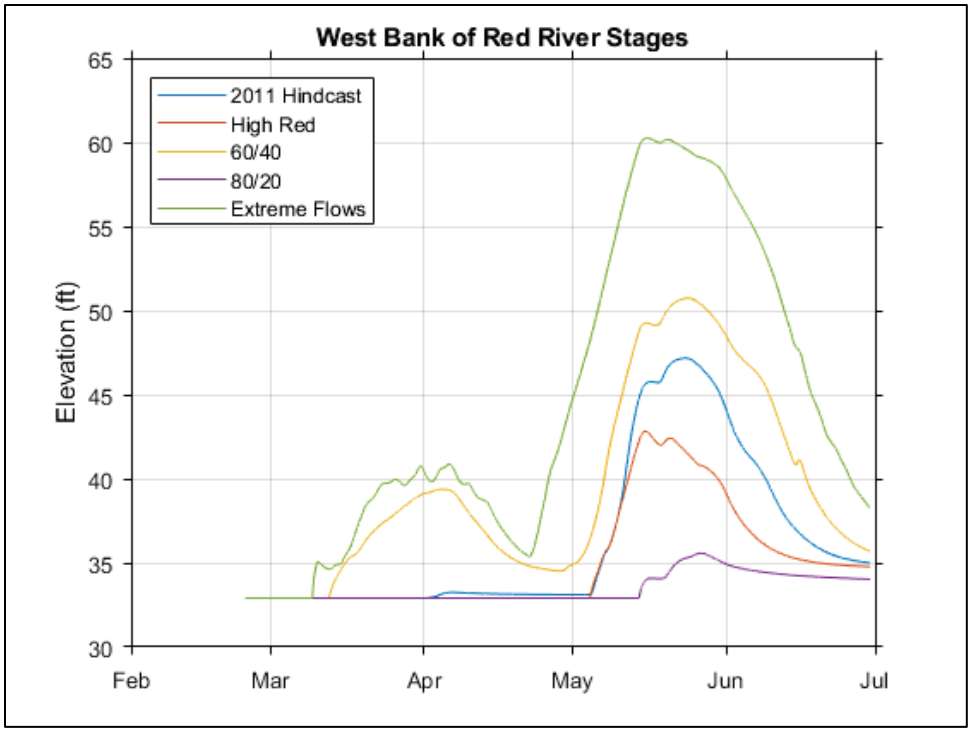

Figure 23. Time series of interpolated volume for the 2D flow area on the west bank of the Red River for each simulation.

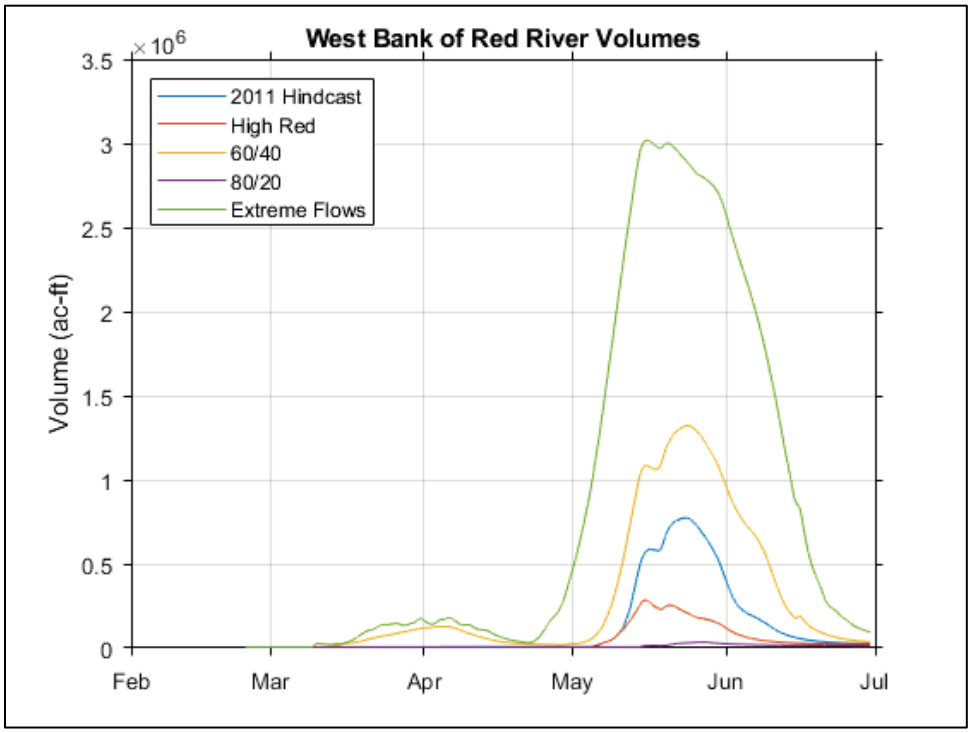

Figure 24. Time series of flow in cfs at Simmesport (*blue line*) overlaid with a time series of computed volume of water in the area on the west bank of the Red River (*red line*) for the 2011 simulation.

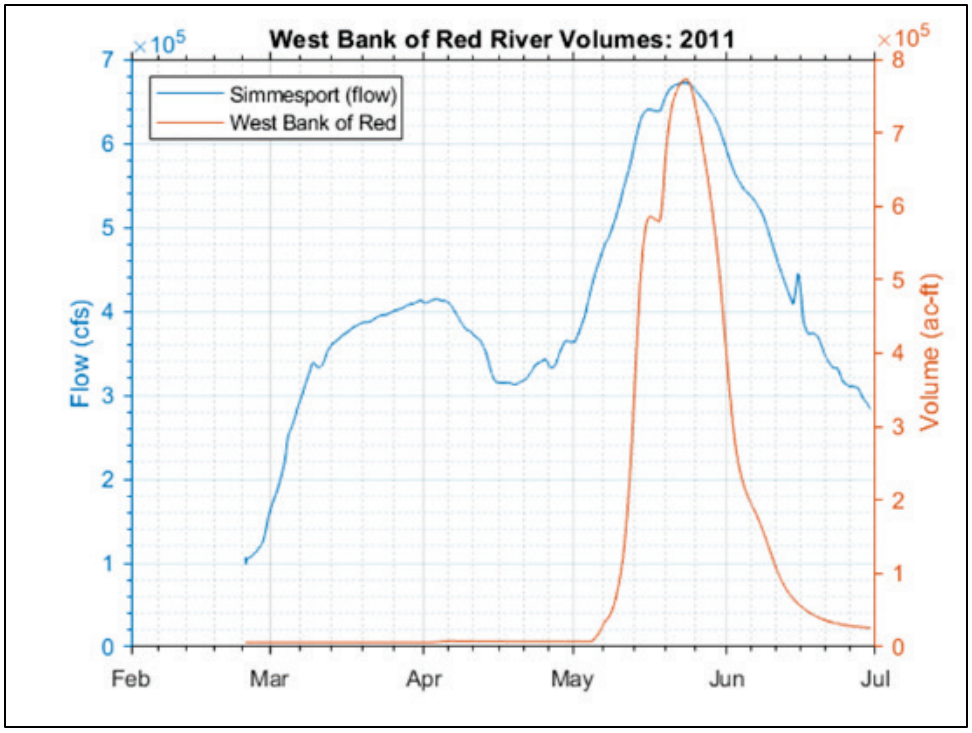

Figure 25. Plot of flow in cfs at Simmesport versus computed volume of water in the area on the west bank of the Red River. *Line color* changes by simulation date for the 2011 simulation.

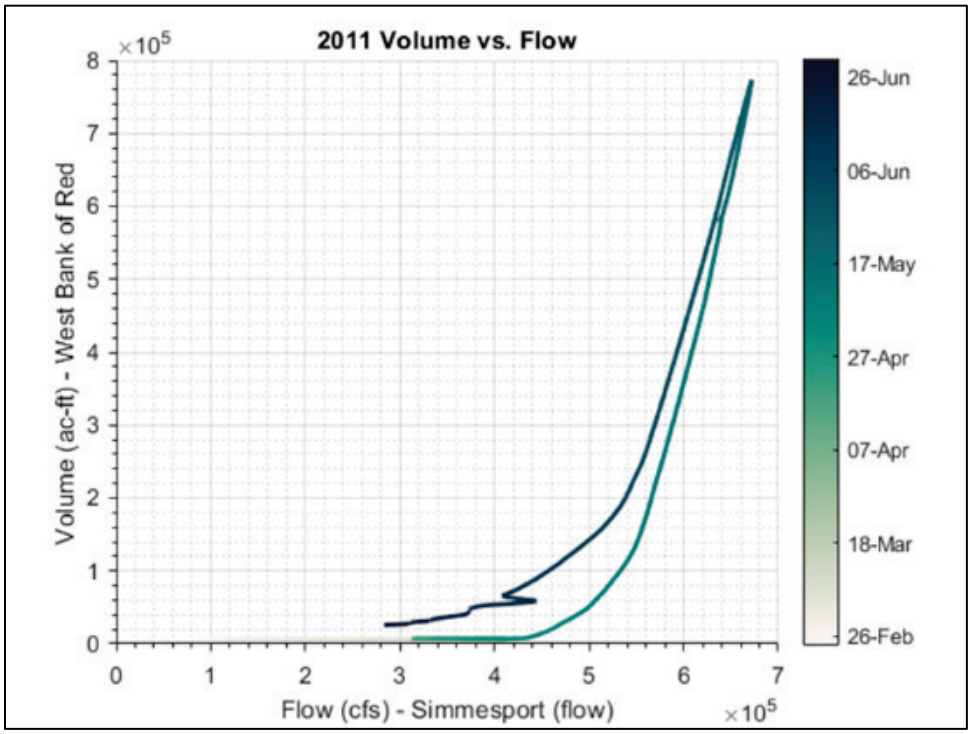

Figure 26. Time series of stage at Simmesport (*blue line*) overlaid with a time series of computed volume of water in the area on the west bank of the Red River (*red line*) for the 2011 simulation.

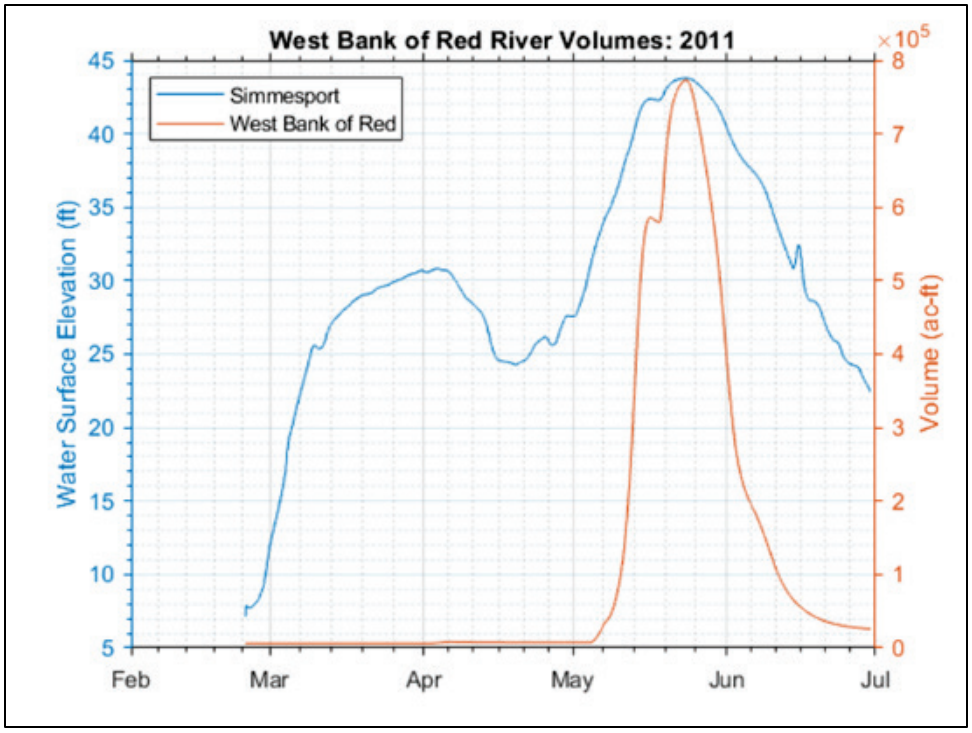

Figure 27. Plot of stage at Simmesport versus computed volume of water in the area on the west bank of the Red River. *Line color* changes by simulation date for the 2011 simulation.

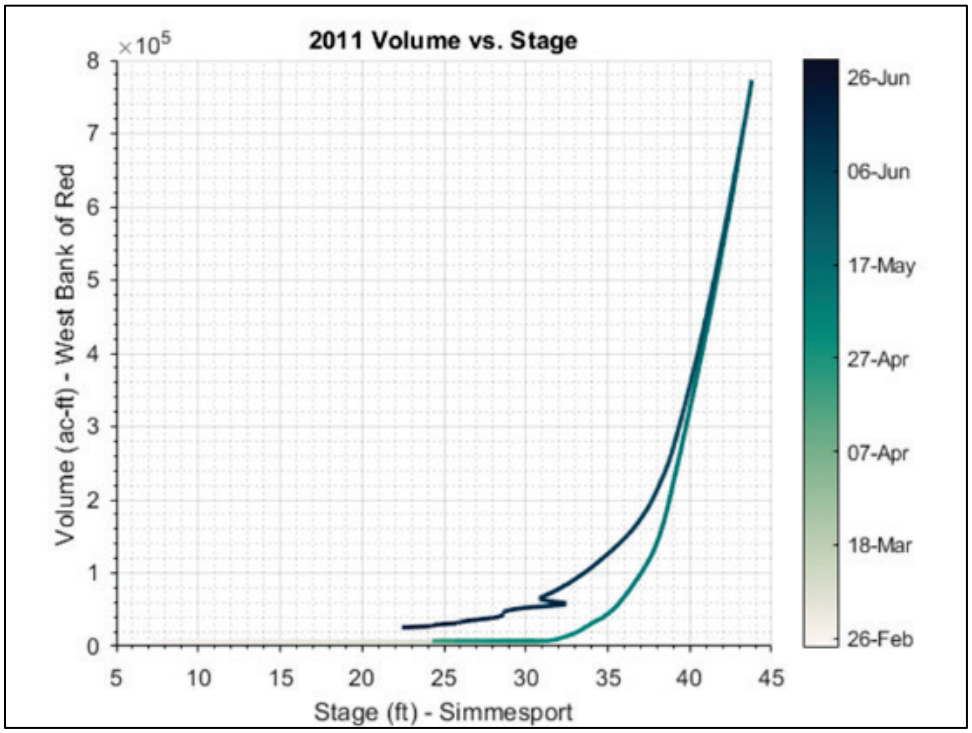

Understanding the timing of the flow of water into the two floodplains to the north of ORCC is helpful for operations. While these modeled outputs of stage and the associated calculated volumes can foster a better understanding of the flooding in these regions, a relationship between these outputs and observational data would still be useful. To better relate the calculated volumes of the flooded areas to flow observations, a time series of flow at Simmesport is overlaid with the time series of the volume of flooded water for the West Bank of the Red River in Figure 24. Looking further at this relationship is Figure 25, which shows flooded volume versus Simmesport flow with the line colored by simulation date to better represent the inflow versus outflow of water in the region on the west bank of the Red River. The plots of time series of stage and volume as well as volume versus stage are shown in Figure 26 and Figure 27.

5.2 West bank of Red River—Alligator Bayou basin

The preceding analyses computed for the west bank of the river are now shown for the east bank of the river. Using the volume-elevation curve from the bathymetry (Figure 28), the modeled output time series of stage (Figure 29) for a specified location in the watershed was interpolated for each simulation to create a time series of the volume contained within the RAS 2D flow area (Figure 30). This allows for a comparison between each simulation of the relative amounts of flooding in the region. While there is less water being stored in the eastern region than in the western region, the overall trends of flooding remain the same with flooding greater than 2011 in the 60/40 and extreme flows scenarios and less than in high Red River and 80/20 scenarios. To gain a better sense of the relationship between waters in the Atchafalaya and waters in the flooded region, a time series of flow at Simmesport is overlaid with the time series of the volume of flooded water for the East Bank of the Red River in Figure 31. Figure 32 shows flooded volume versus Simmesport flow with the line colored by simulation date. The plots of time series of stage and volume as well as volume versus stage are shown in Figure 33 and Figure 34. The region on the east side of the Red River contains much less water than the area on the west of the Red River which is expected since the area of the region is also much smaller. The timing of the flooding on either side of the Red River is similar.

Figure 28. Volume-elevation curve for the Alligator Bayou basin on the east bank of the Red River north of ORCC.

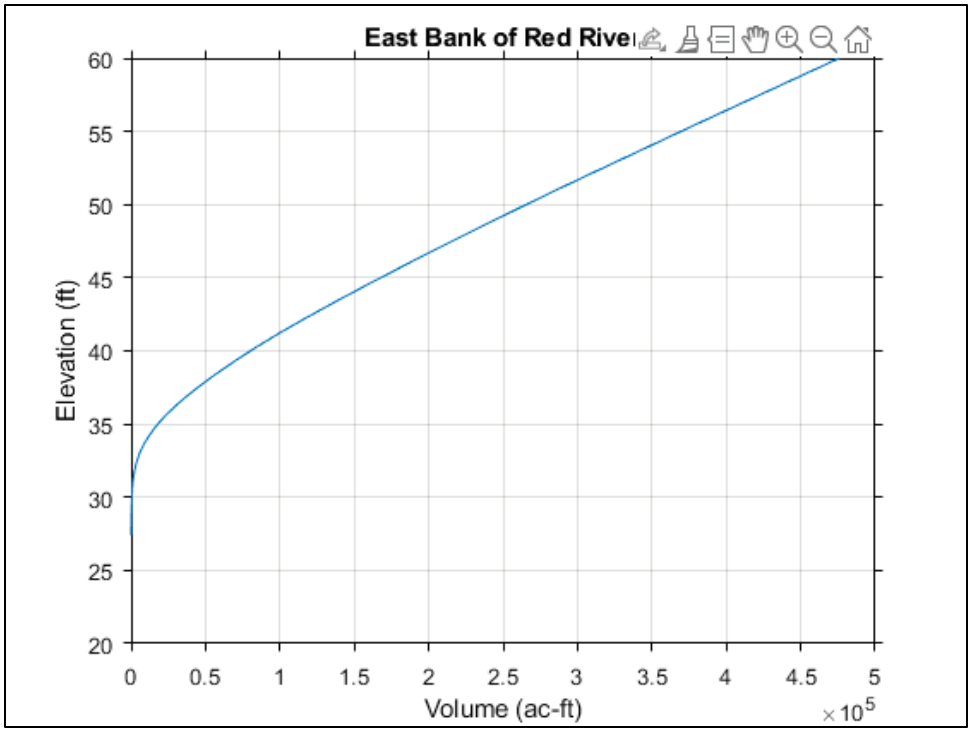

Figure 29. Time series of modeled water surface elevation for the east bank of the Red River from a point located at 91.677312°W 31.1309638°N (1347685.0014, 2967106.4525 in the RAS model) for each simulation.

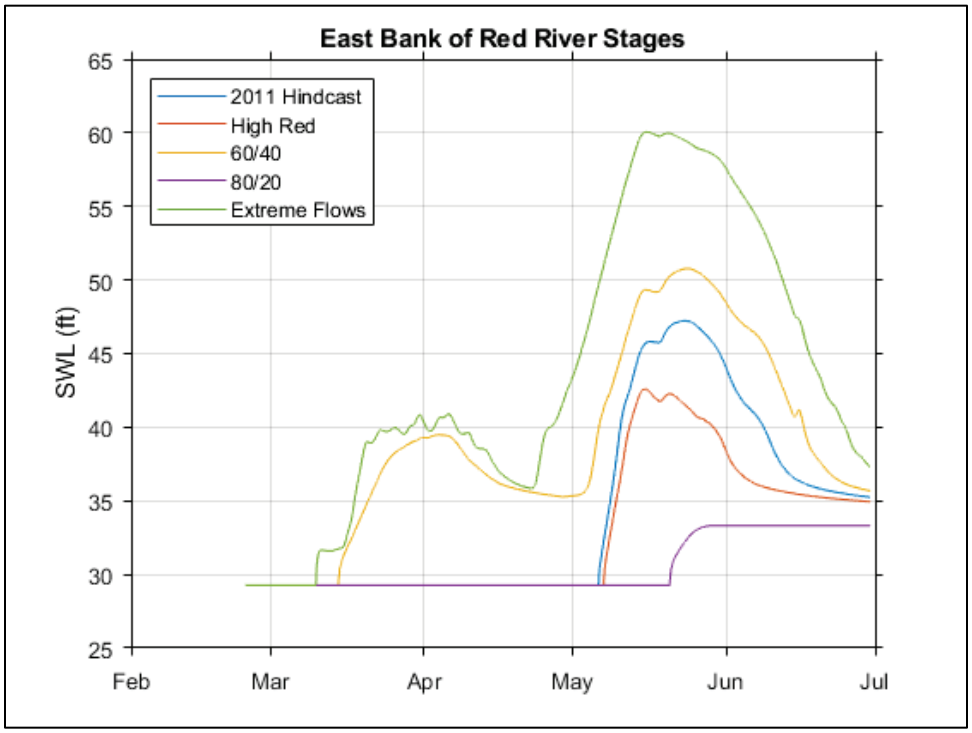

Figure 30. Time series of interpolated volume for the 2D flow area on the east bank of the Red River for each simulation.

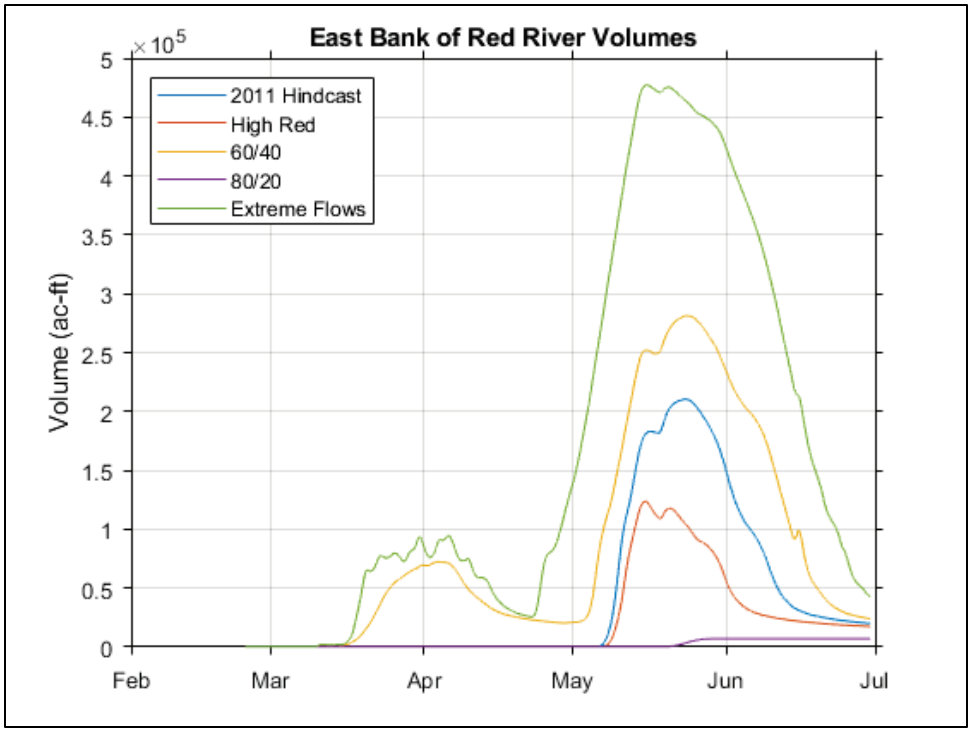

Figure 31. Time series of flow in cfs at Simmesport (*blue line*) overlaid with a time series of computed volume of water in the area on the east bank of the Red River (*red line*) for the 2011 simulation.

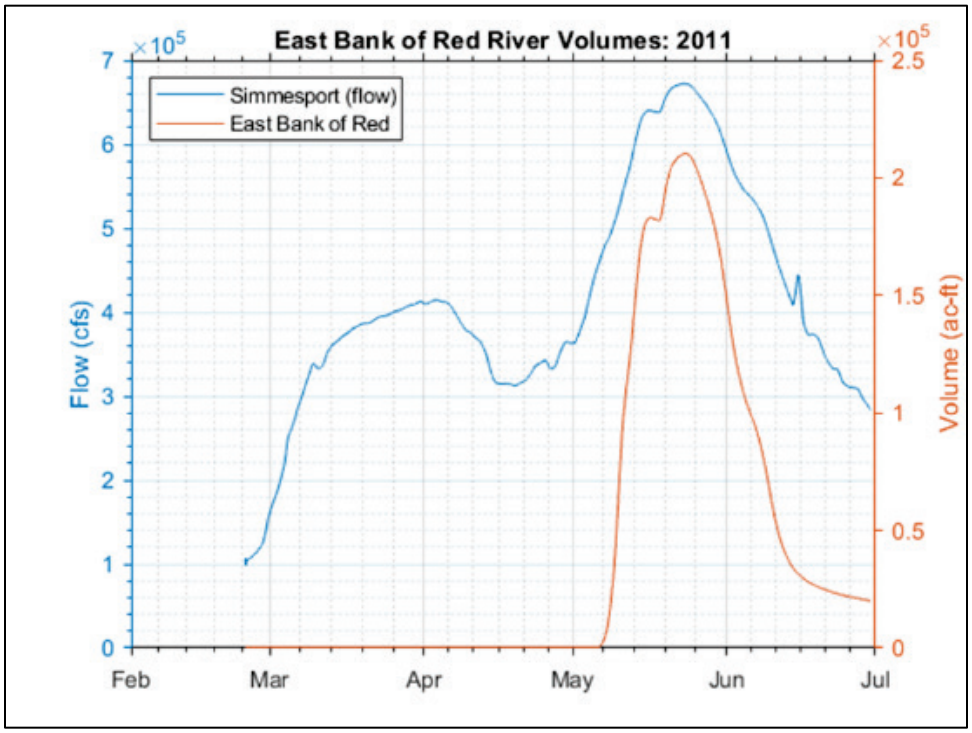

Figure 32. Plot of flow in cfs at Simmesport versus computed volume of water in the area on the east bank of the Red River. *Line color* changes by simulation date for the 2011 simulation.

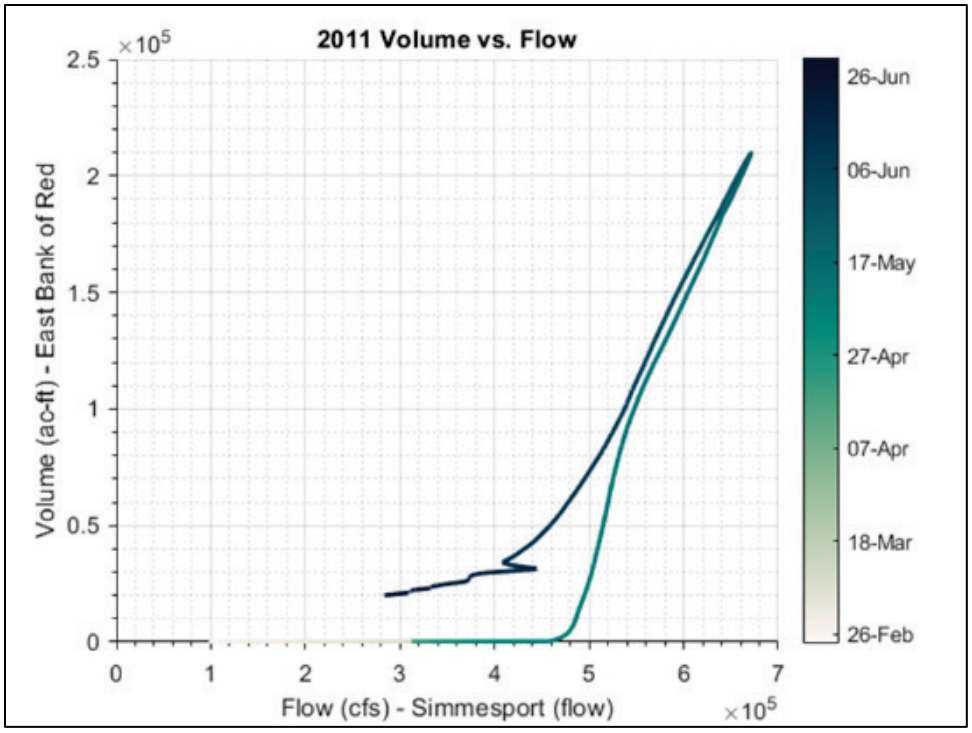

Figure 33. Time series of stage at Simmesport (*blue line*) overlaid with a time series of computed volume of water in the area on the east bank of the Red River (*red line*) for the 2011 simulation.

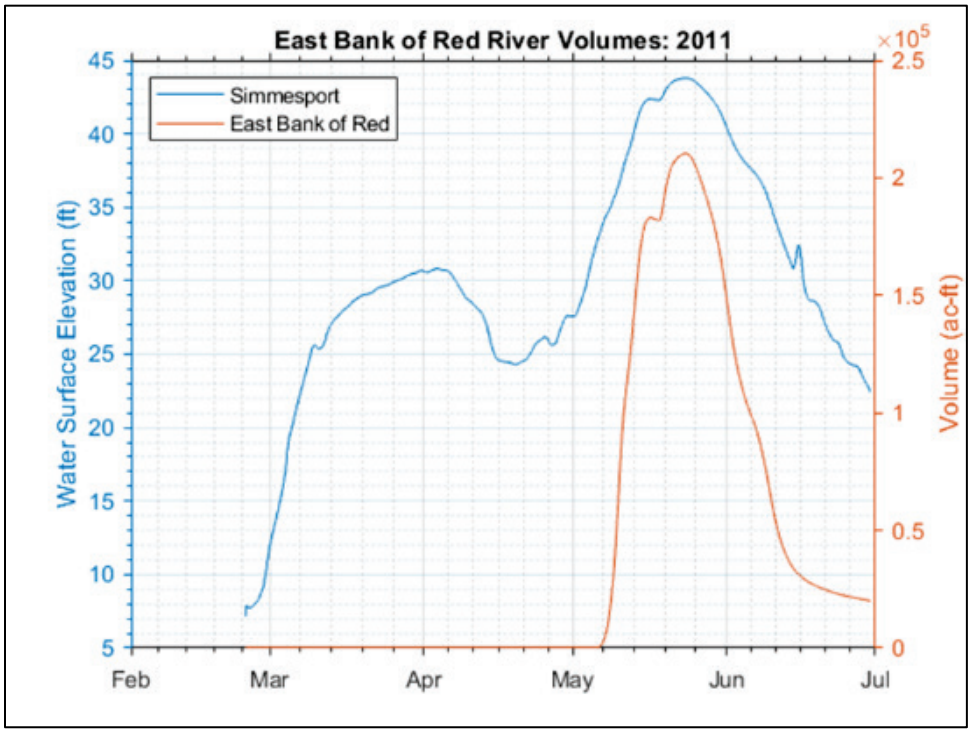

Figure 34. Plot of stage at Simmesport versus computed volume of water in the area on the east bank of the Red River. *Line color* changes by simulation date for the 2011 simulation.

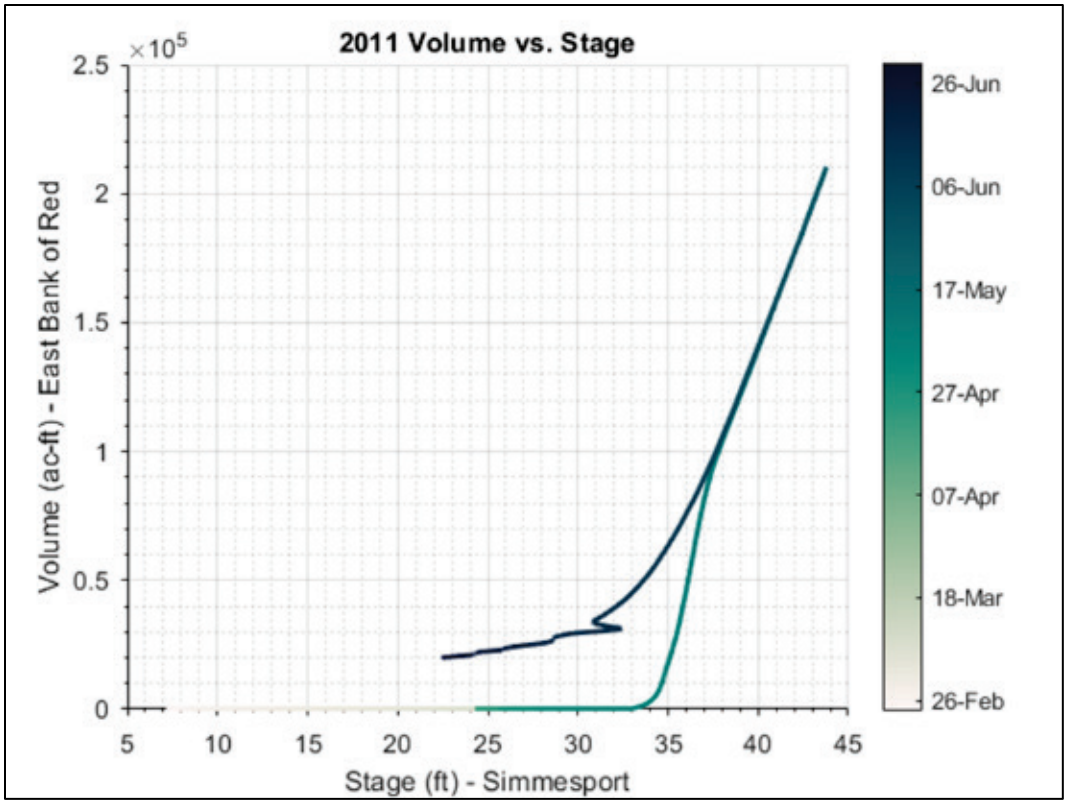

Of further interest to water managers are new data regarding the flow of water into the storage areas on either side of the Red River (Figure 35 shown for 2011). This was calculated by taking the daily average of the hourly RAS output and converting the change in volume to a flow into each storage area for each day with negative values indicating water leaving the storage areas. Similarly, the relative proportions of flow from ORCC winding up in storage (Figure 36, shown for 2011) would be useful for water managers and were computed with the previously computed discharges into storage divided by the flow of water diverted through ORCC for that day. The result help to show the much larger flows in and out of the storage area on the western side of the Red River as compares to the storage area on the eastern side. For the 2011 simulation, the amount of flow of water diverted through ORCC going into storage on the western side of the Red River was upwards of 10% with peak flows being approximately 65,000 cfs.

Figure 35. Flow into storage (*blue* is western storage area, *orange* is eastern storage area) versus flow at Simmesport (cfs).

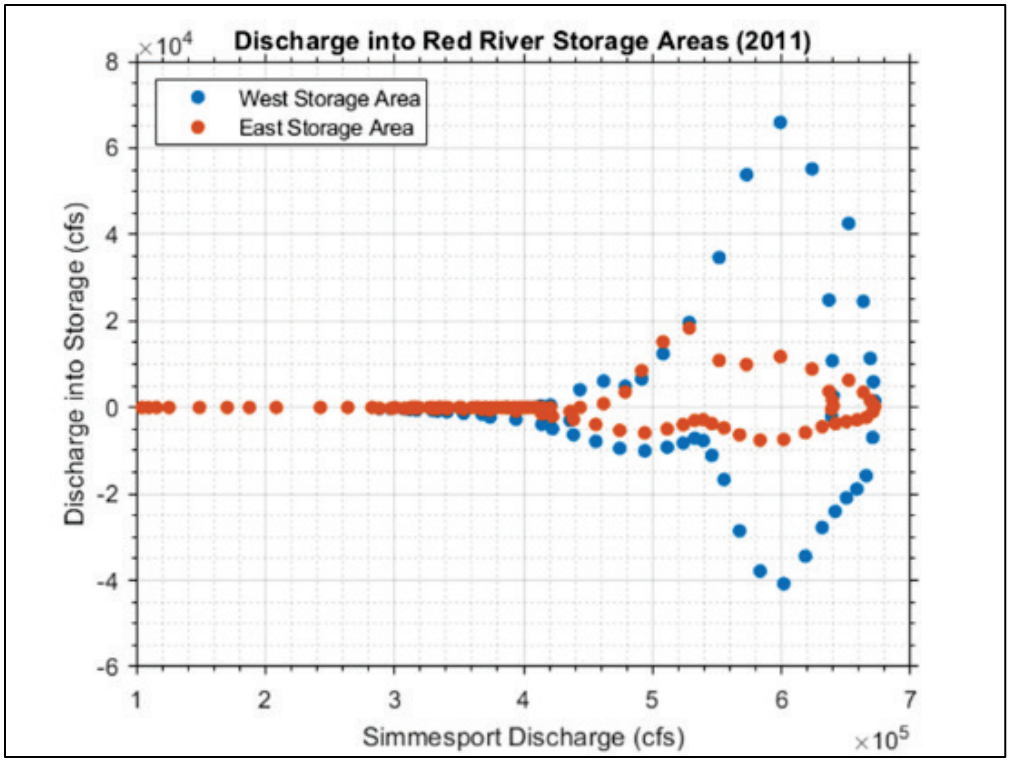

Figure 36. Percentage of ORCC flows going into storage (*blue*, western area; *orange*, eastern area) versus flow at Simmesport (cfs).

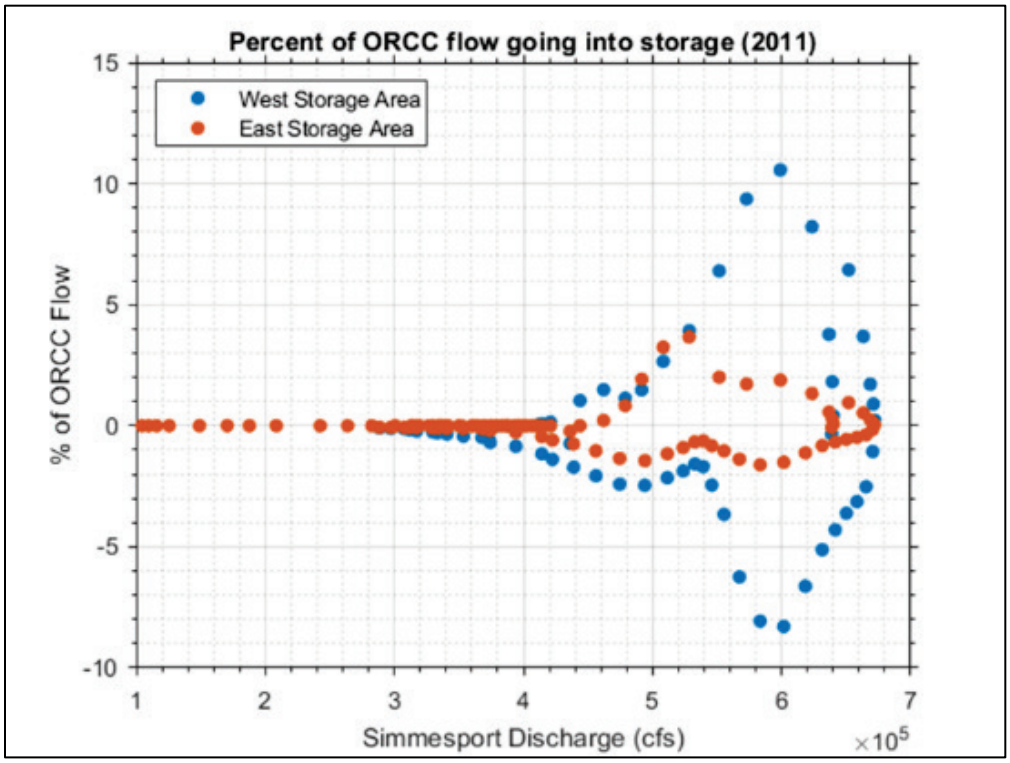

The relationship between discharge into the western storage area versus flows at Simmesport for each simulation is shown in Figure 37, and the relationship between discharge into the eastern storage area versus flows at Simmesport for each simulation is shown in Figure 38. Comparing between the simulations, a strong dependence on flows coming through ORCC can be seen. Results show that when flows at Simmesport are rising and reach approximately 500kcfs, approximately 10kcfs of water is going into the western storage area (although this is slightly higher for the extreme flows scenario). When flows at Simmesport approach 600kcfs, approximately 70kcfs of water going into the west storage area. For the eastern storage area, the flow is smaller but with a faster rate of increase in the amount of water flowing in. When flows at Simmesport approach 500kcfs, approximately 1–1.5kcfs is flowing into the eastern storage area.

Figure 37. Flow into the western storage area versus flow at Simmesport (cfs) for each simulation.

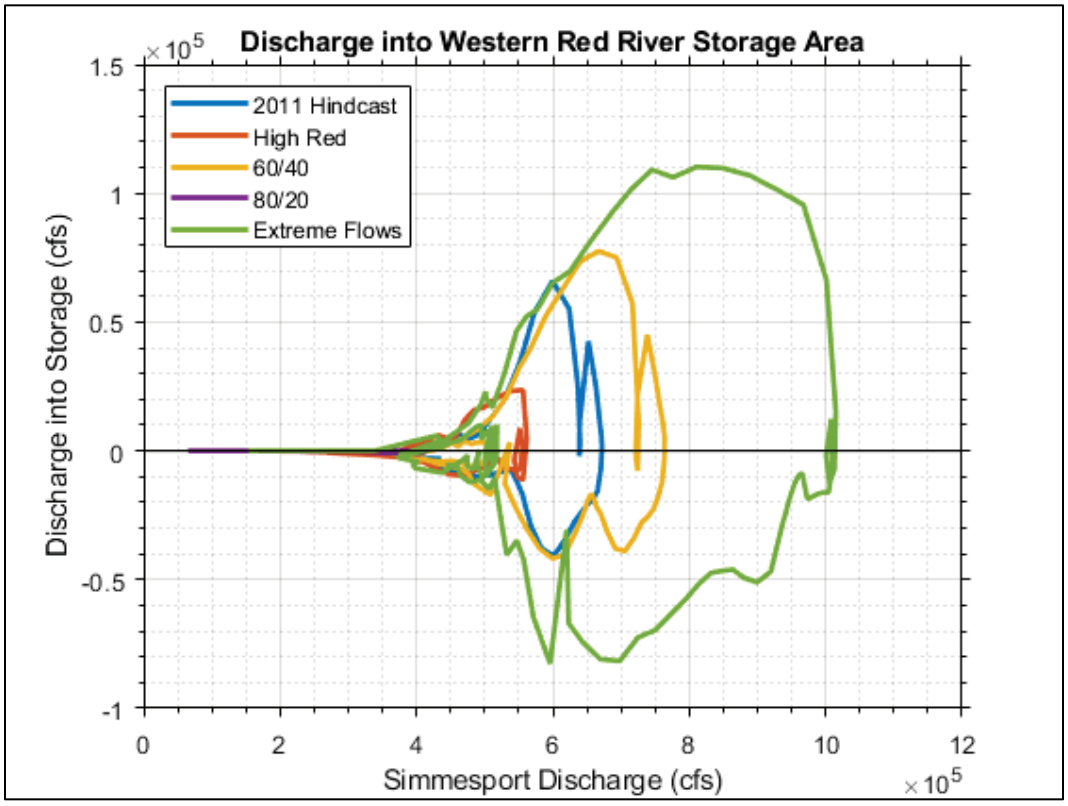

Figure 38. Flow into the eastern storage area versus flow at Simmesport (cfs) for each simulation.

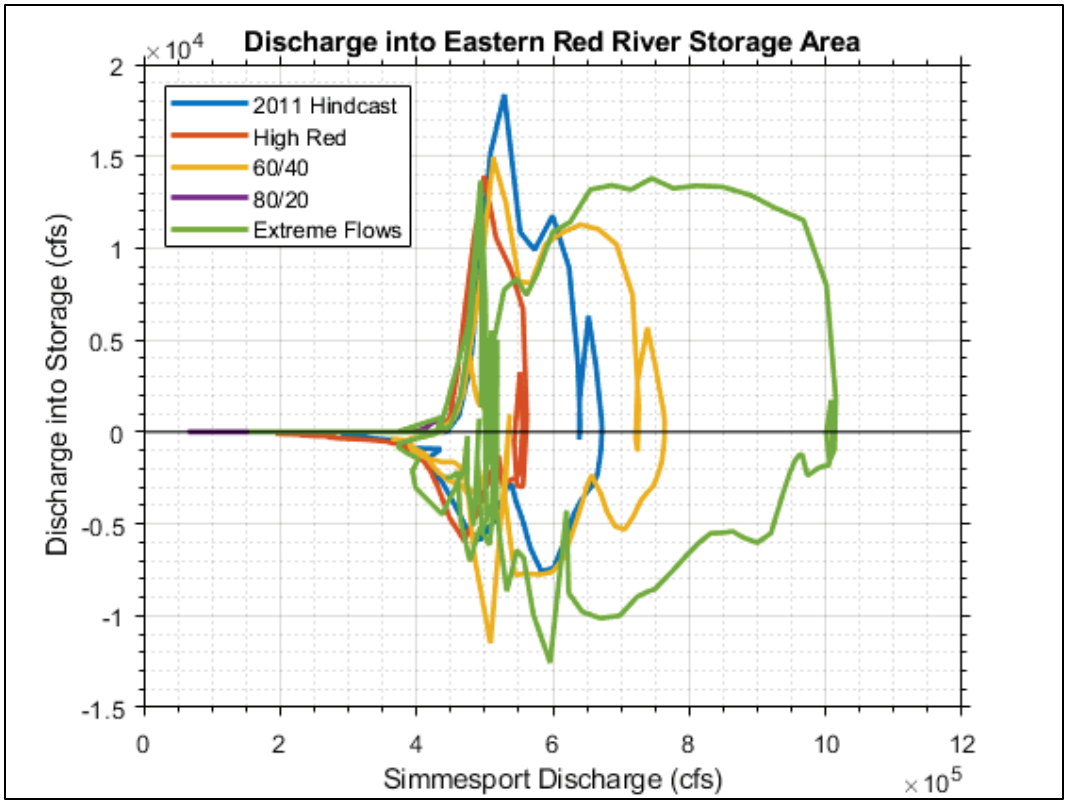

The previous section detailed the relationship between stage and volume but did not determine how and where waters leave the Red River and enter these areas. Flooding in these areas happens easily as much of the Red River upstream of ORCC is not leveed (Figure 18). Animations of depth and velocity suggest that the water first enters these 2D areas via the bayous that branch off from the Red River and then fill in from the bayous and water coming over the main riverbank (Figure 39). Most notably, it appears water can enter the area on the west bank of the Red River via both Bayou Natchitoches to the north of ORCS and via Bayou Courville to the south of ORCS, which then becomes an outlet of water when the 2D area drains (Figure 40).

Figure 39. Snapshot of velocity from 2011 run on simulation day May 6. Particle tracing overlaid on *top* of the velocity surface. Arrows added to show direction of flow into 2D flow areas.

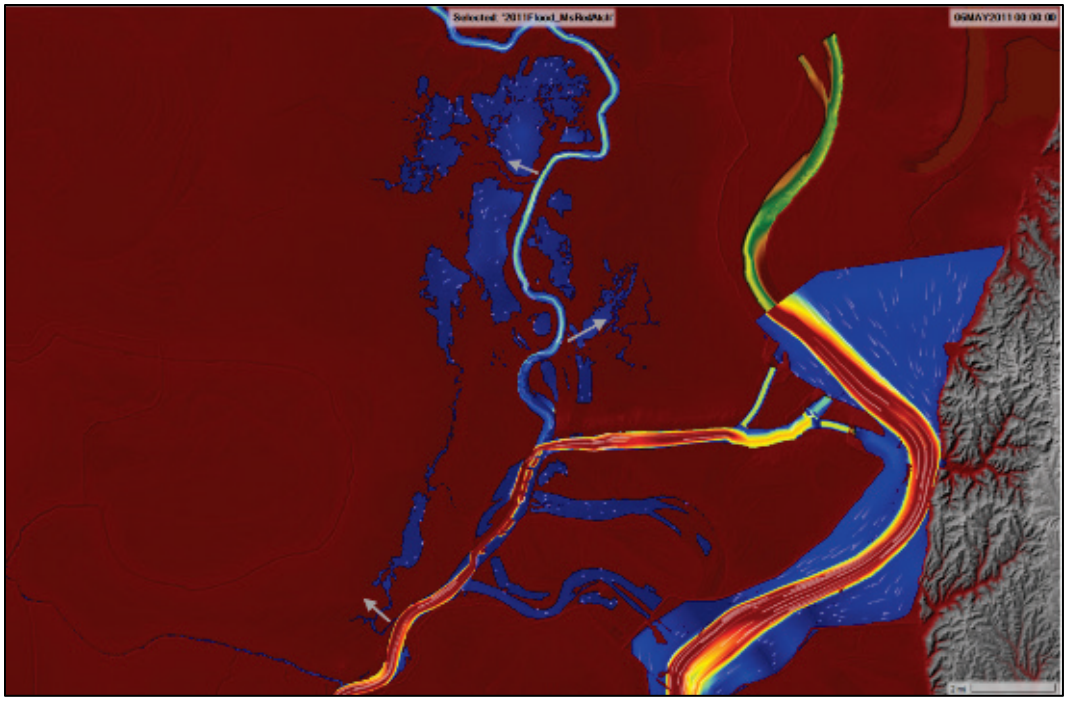

Figure 40. Snapshot of velocity from 2011 run on simulation day May 26 when water is starting to leave the 2D flow area. Particle tracing overlaid on *top* of the velocity surface. Arrows overlaid to show the direction of flow into or out of the 2D flow areas.

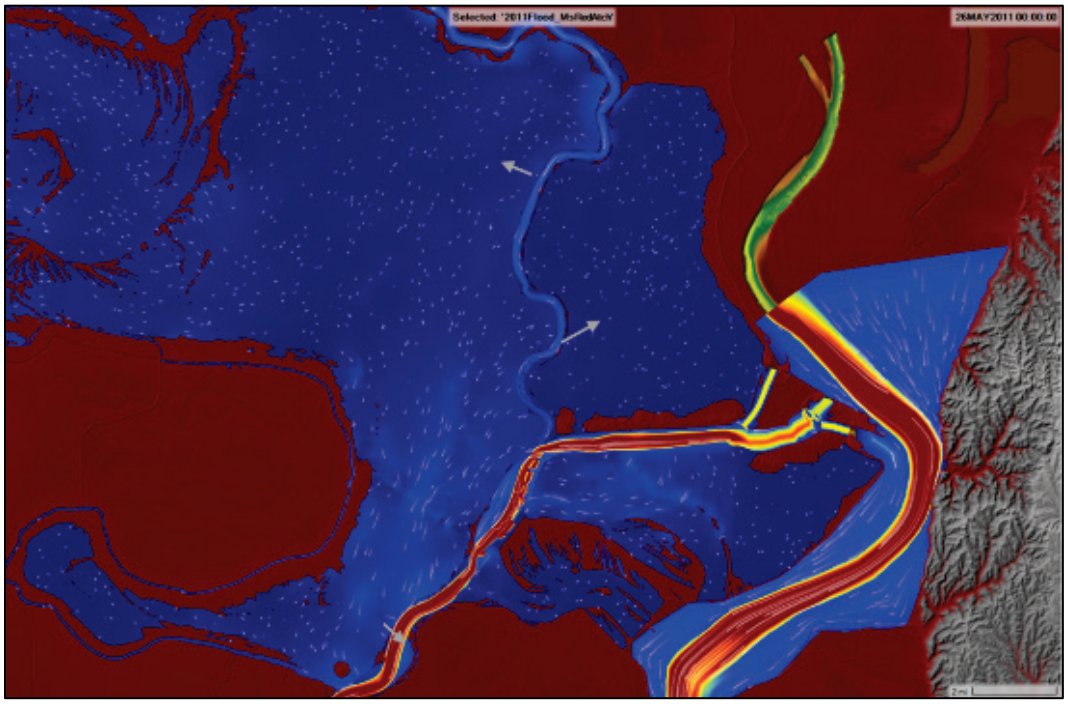

6 Conclusions and Recommendations

The results of this analysis illustrate the role of the Lower Red River floodplain in the storage of floodwaters from the ORCC as well as from the upper Red River Watershed. These areas benefit the Mississippi River Below ORCC on a rising hydrograph because floodwaters are stored until the peak river flows have crested. On a falling hydrograph the opposite effects are being observed. Floodwaters that were stored in the Lower Red River floodplain begin to drain back into the river channel. This causes higher flows in the Atchafalaya River than is normally computed at ORCC. This effectively causes the ORCC to cut back on diverted flow to meet the annual flow distribution of 30% at Simmesport.

The analysis provides useful data to the water managers, who operate the ORCC, concerning the timing and volumes of the water being stored in the Lower Red River and how it interacts with the gage readings at Simmesport and governs the operational decisions at ORCC to ensure that authorized flows are met. A review of operations at Old River, with any resulting beneficial adjustments, may help to ensure the amount of flooded water stored in the areas just upstream of ORCC on the Lower Red River is understood.

References

Lewis, J., E. Howe, C. A. Cruz, M. L. Dove, W. A. Crosby, R. J. Taylor, D. A. Ramirez, M. S. Dircksen, and R. Gambill. 2018. *Mississippi River and Tributaries Flowline Assessment Hydraulics Report*. MRG&P Report No. 24; Vol. 3. Vicksburg, MS: US Army Engineer Research and Development Center.

Appendix A: Supplemental Figures

This appendix contains figures from the simulations conducted after the 2011 model validation scenario was compared with observations (Figures A-1 through A-64) . This allows for further comparison between the different simulations. Comparisons to observations not available for these simulated events since the input flows are artificially created. Note that for comparisons between scenarios, the limits of the *y*-axis change for each simulation to better see the variation within that scenario.

A.1 High Red River, Low Mississippi River Scenario (motivated by 2015 Floods)

Figure A-1. Modeled flow in the Red River upstream of the confluence with the Black River from the High Red River simulation.

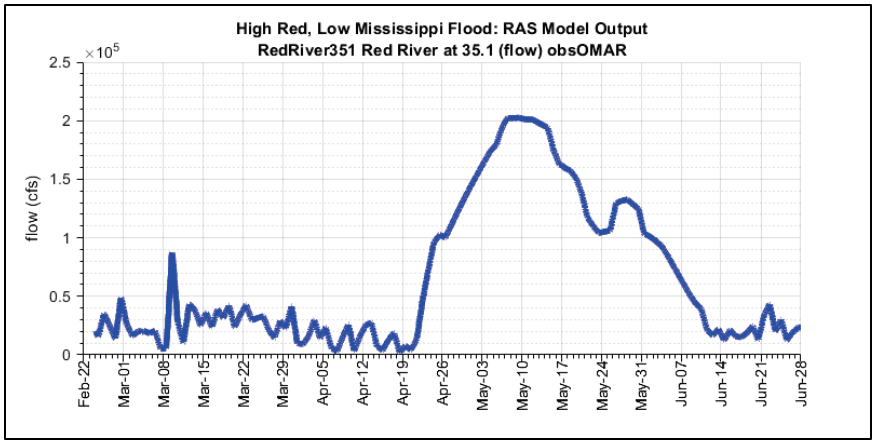

Figure A-2. Modeled flow at the site of the new stream gage at Madam Lee (downstream from the confluence with the Black River) from the High Red River simulation.

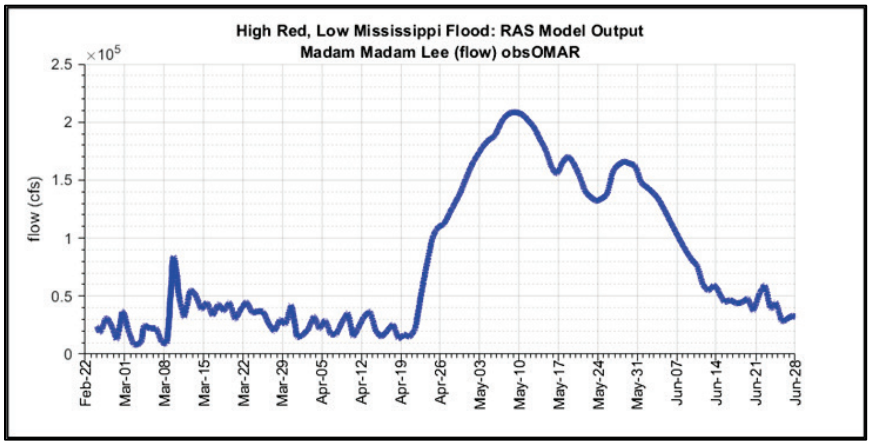

Figure A-3. Modeled flow for Wax Lake Outlet (outlet to the west of the main Atchafalaya River outlet) from the High Red River simulation.

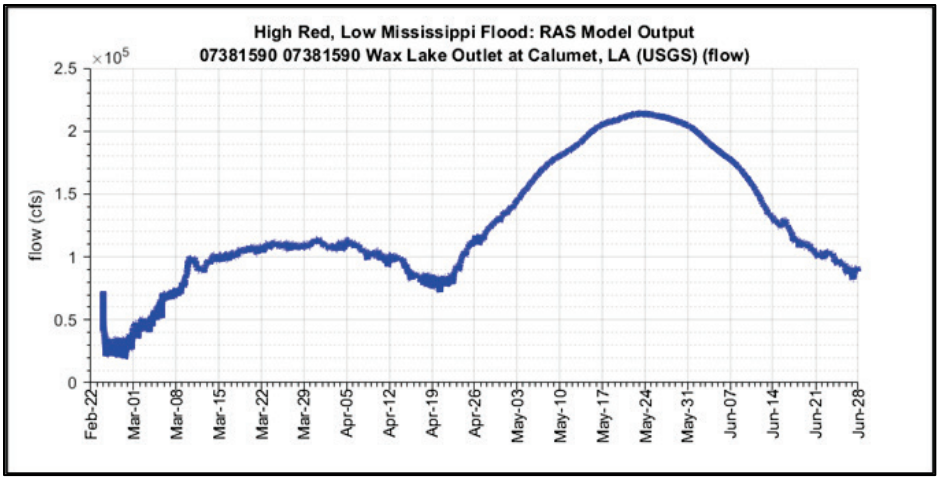

Figure A-4. Modeled flow at Simmesport along the Atchafalaya River south of the Old River Control Complex from the High Red River simulation.

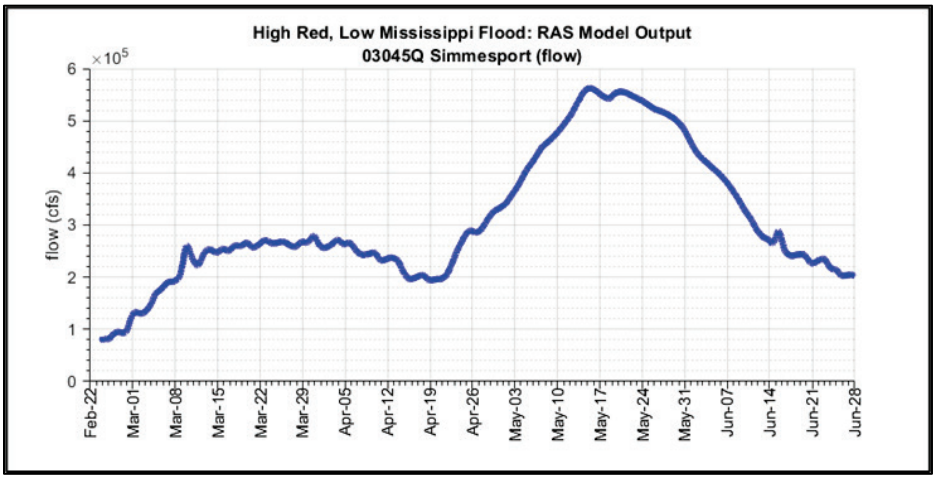

Figure A-5. Modeled stages in the Whiskey Bay Pilot Channel from the High Red River simulation.

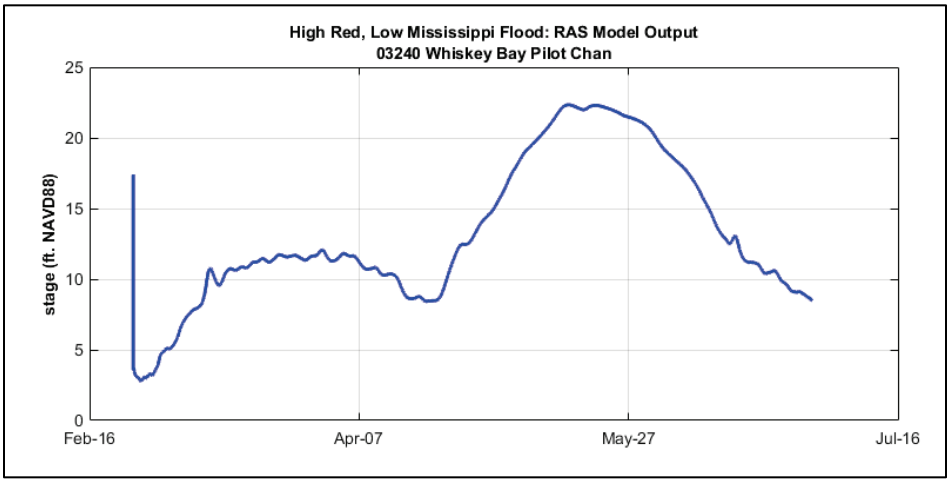

Figure A-6. Modeled stages in the GIWW south of Morgan City from the High Red River simulation.

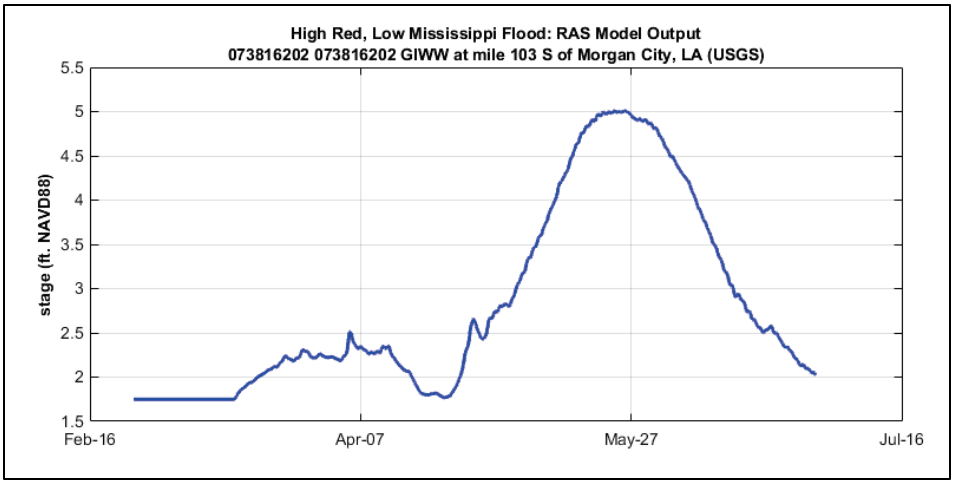

A.2 West bank of Red River—Bayou Natchitoches basin

Figure A-7. Time series of flow in cfs at Simmesport (*blue line*) overlaid with a time series of computed volume of water in the area on the west bank of the Red River (*red line*) for the High Red River simulation.

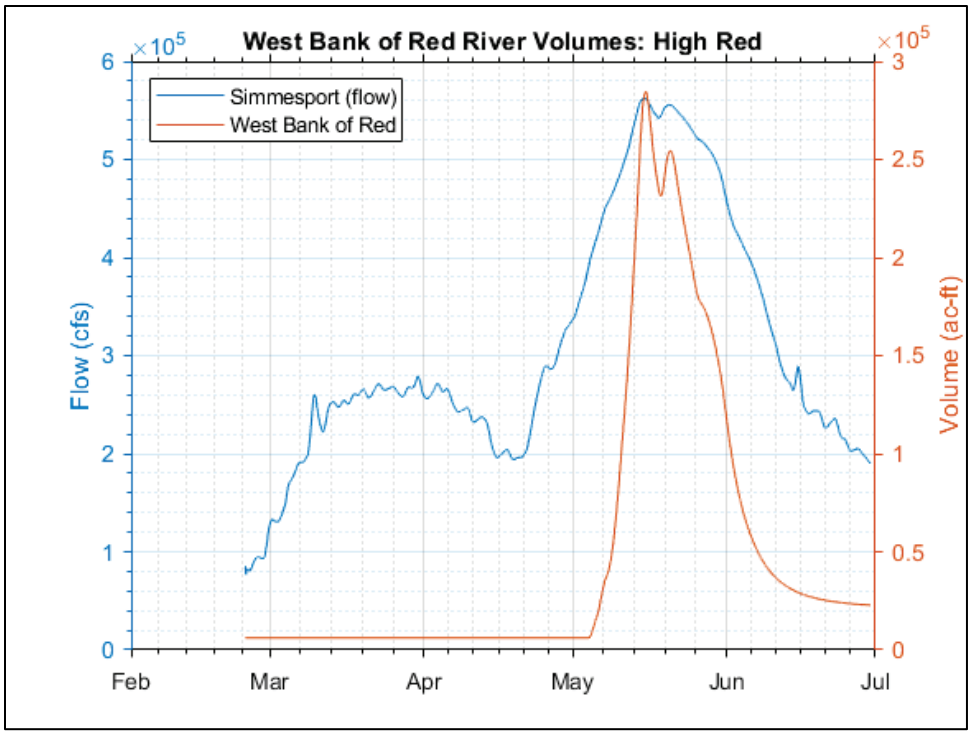

Figure A-8. Plot of flow in cfs at Simmesport versus computed volume of water in the area on the west bank of the Red River. *Line color* changes by simulation date for the High Red River simulation.

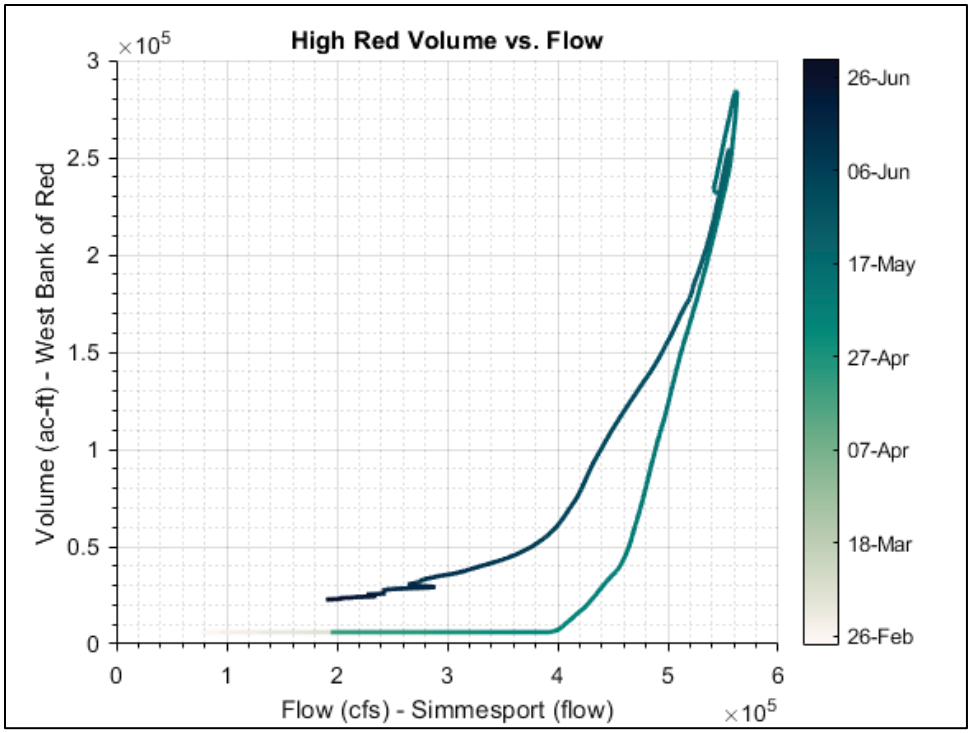

Figure A-9. Time series of stage at Simmesport (*blue line*) overlaid with a time series of computed volume of water in the area on the west bank of the Red River (*red line*) for the High Red River simulation.

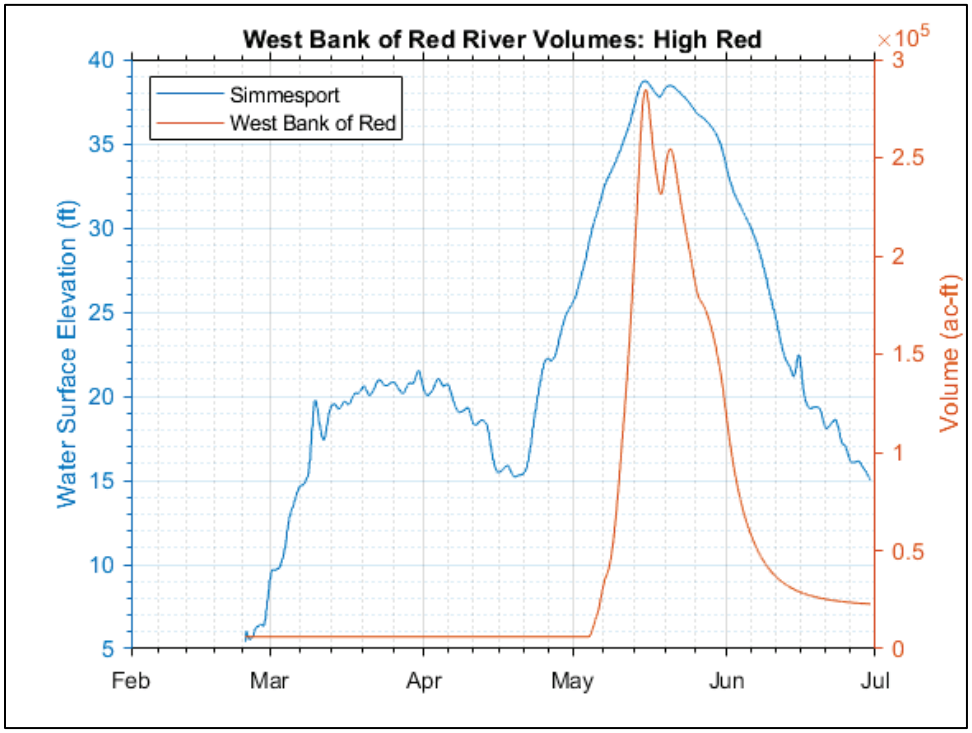

Figure A-10. Plot of stage at Simmesport versus computed volume of water in the area on the west bank of the Red River. *Line color* changes by simulation date for the High Red River simulation.

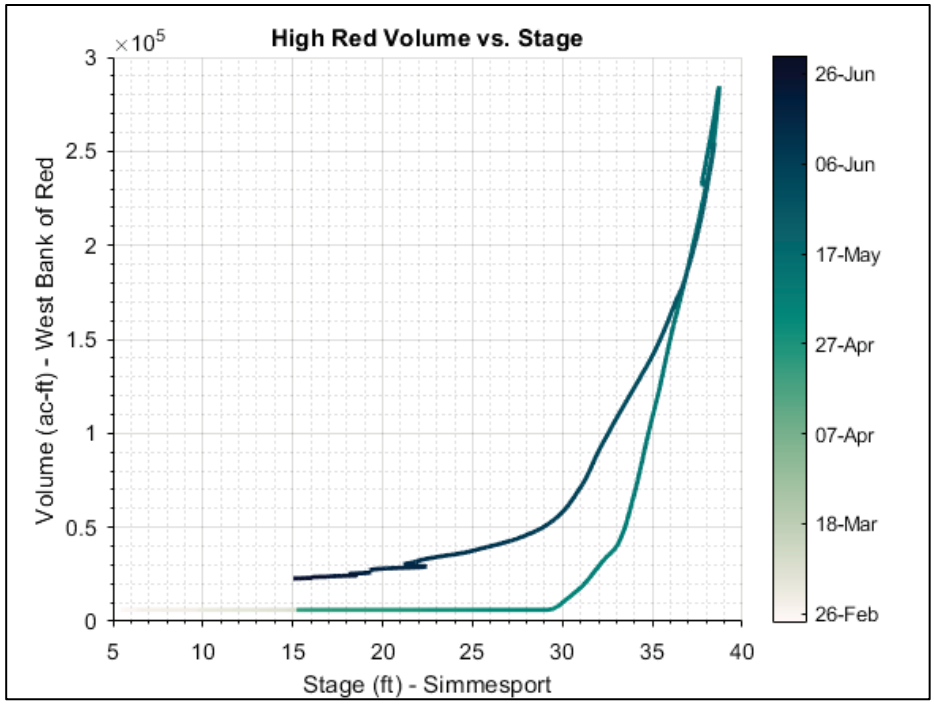

A.3 East bank of Red River—Alligator Bayou basin

Figure A-11. Time series of flow in cfs at Simmesport (*blue line*) overlaid with a time series of computed volume of water in the area on the east bank of the Red River (*red line*) for the High Red River simulation.

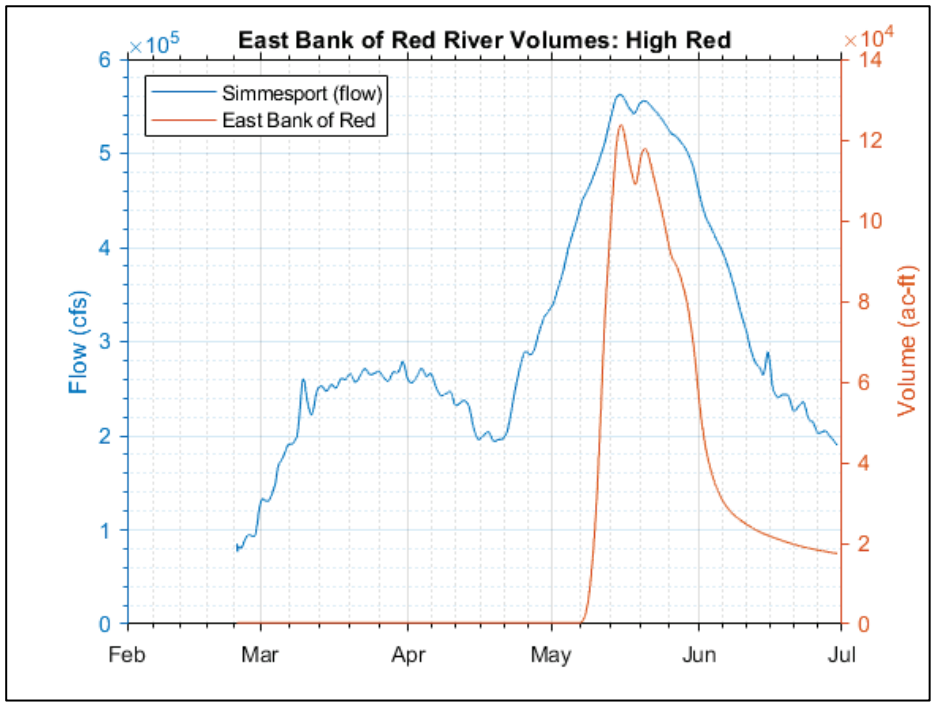

Figure A-12. Plot of flow in cfs at Simmesport versus computed volume of water in the area on the east bank of the Red River. *Line color* changes by simulation date for the High Red River simulation.

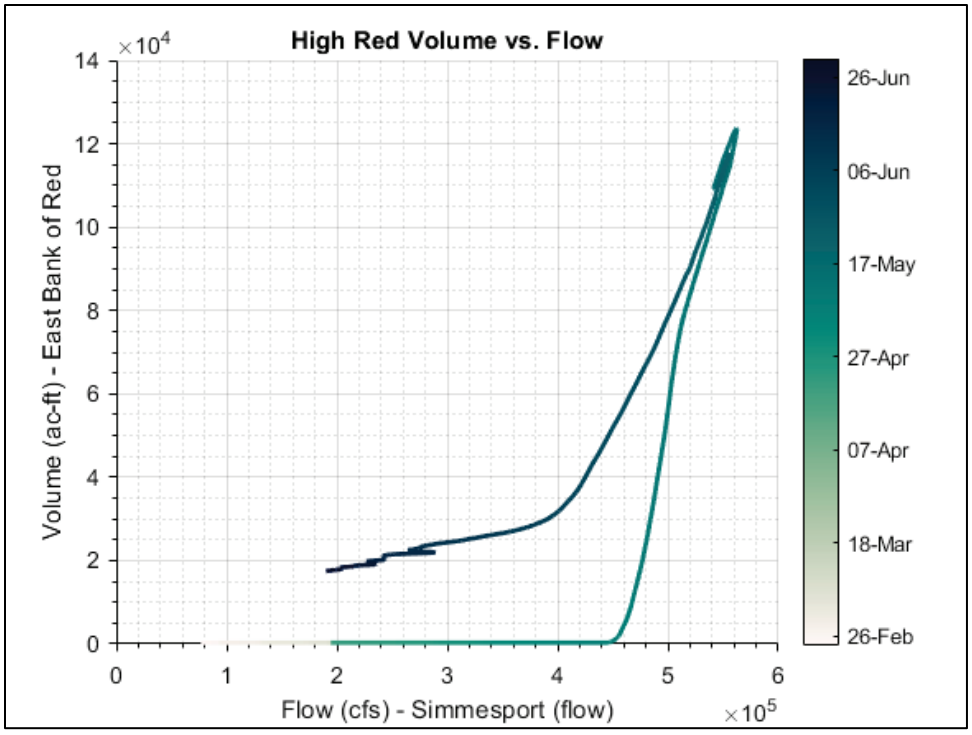

Figure A-13. Time series of stage at Simmesport (*blue line*) overlaid with a time series of computed volume of water in the area on the east bank of the Red River (*red line*) for the High Red River simulation.

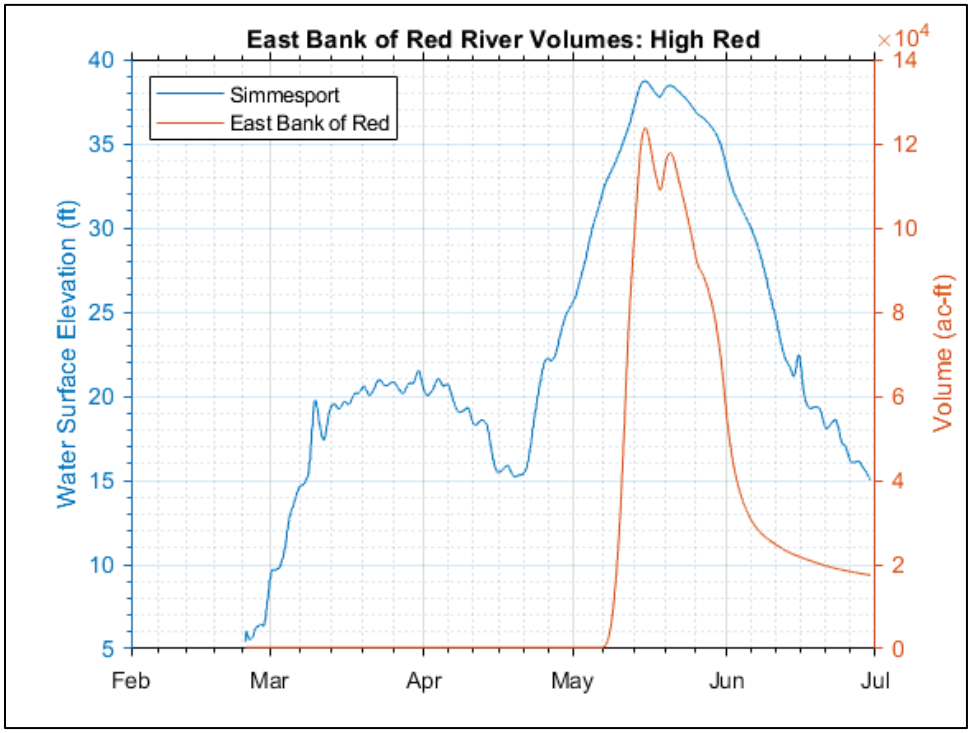

Figure A-14. Plot of stage at Simmesport versus computed volume of water in the area on the east bank of the Red River. *Line color* changes by simulation date for the High Red River simulation.

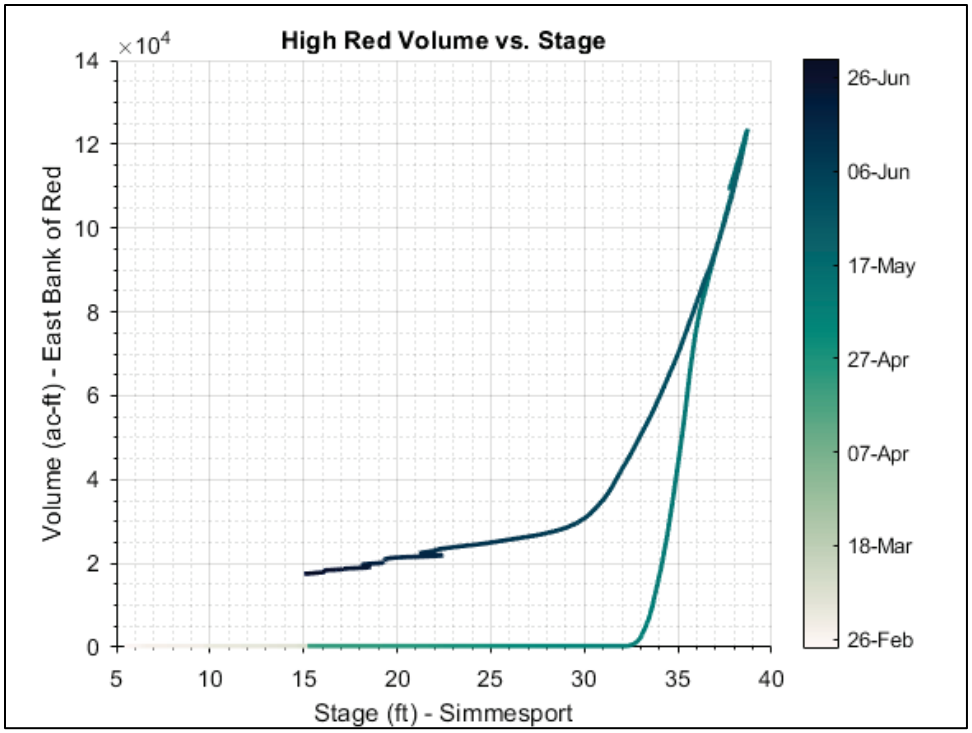

Figure A-15. Flow into storage (*blue* is western storage area, *orange* is eastern storage area) versus flow at Simmesport (cfs) for the High Red River simulation.

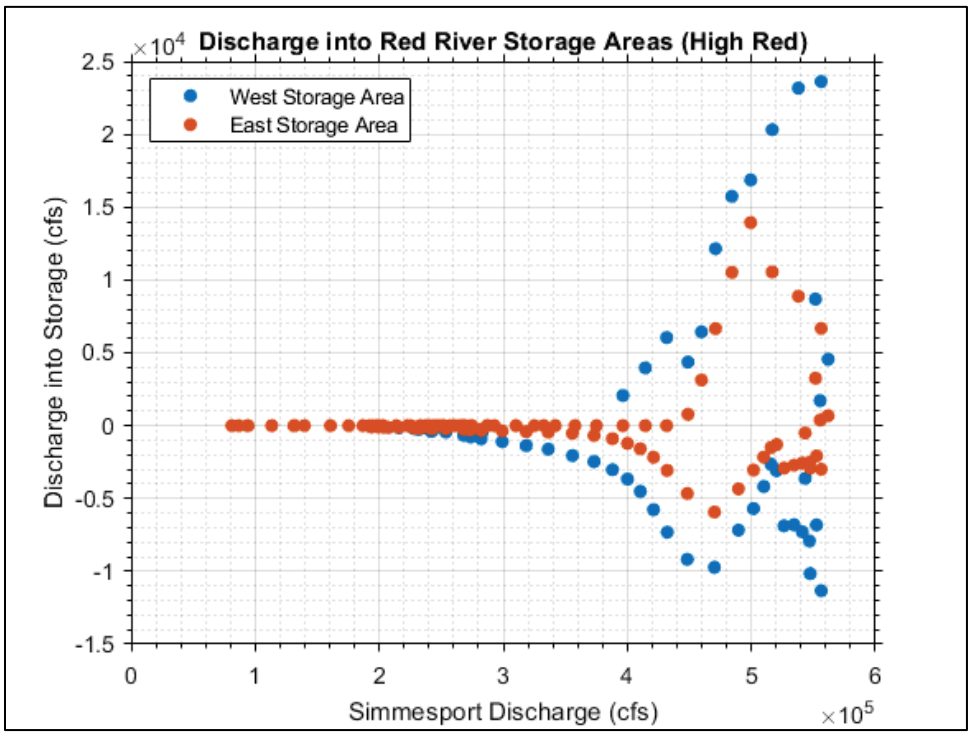

Figure A-16. Percentage of ORCC flows going into storage (*blue*, western area; *orange*, eastern area) versus flow at Simmesport (cfs) for the High Red River simulation.

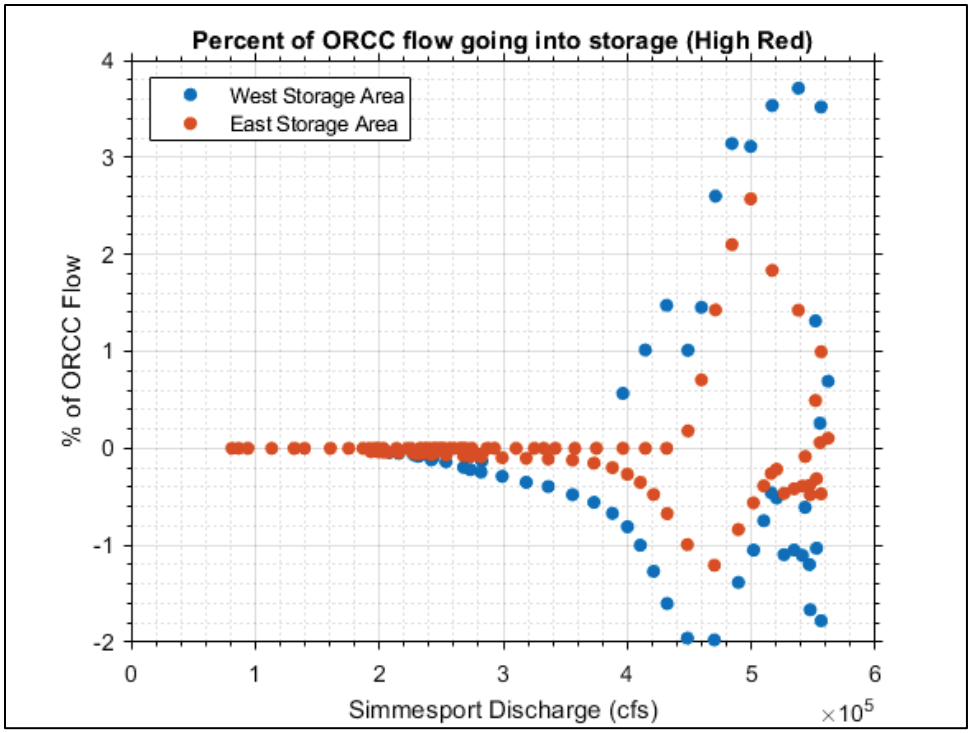

A.4 Old River 60/40 split

Figure A-17. Modeled flow in the Red River upstream of the confluence with the Black River from the 60/40 simulation.

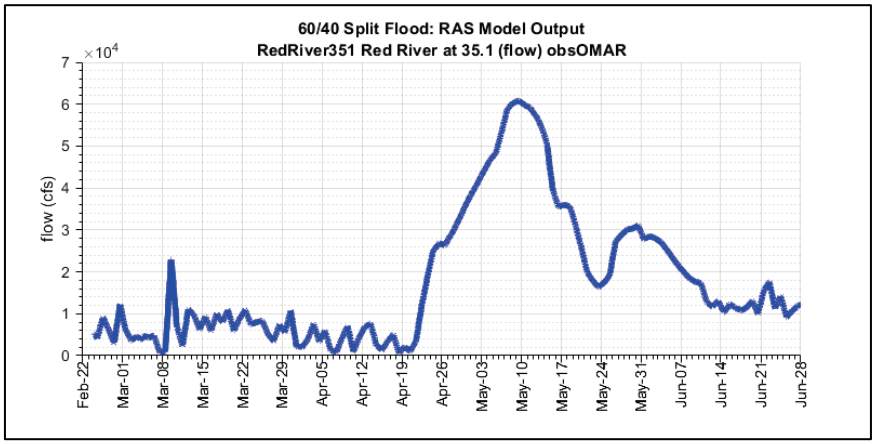

Figure A-18. Modeled flow at the site of the new stream gage at Madam Lee (downstream from the confluence with the Black River) from the 60/40 simulation.

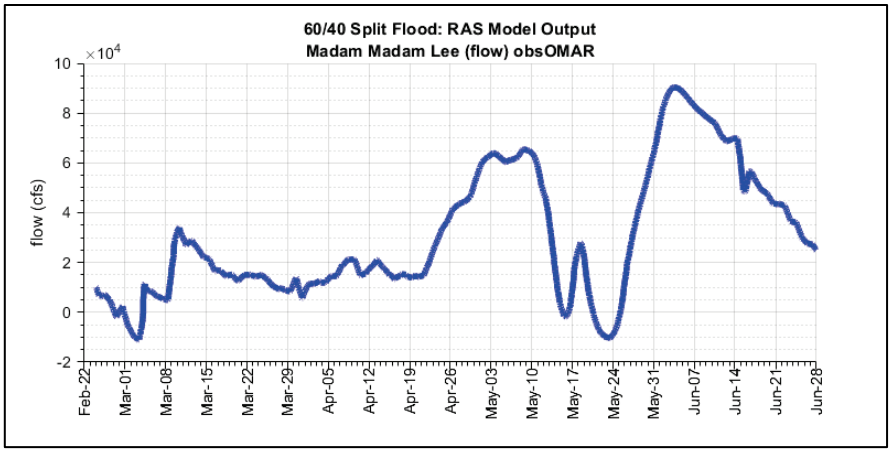

Figure A-19. Modeled flow for Wax Lake Outlet (outlet to the west of the main Atchafalaya River outlet) from the 60/40 simulation.

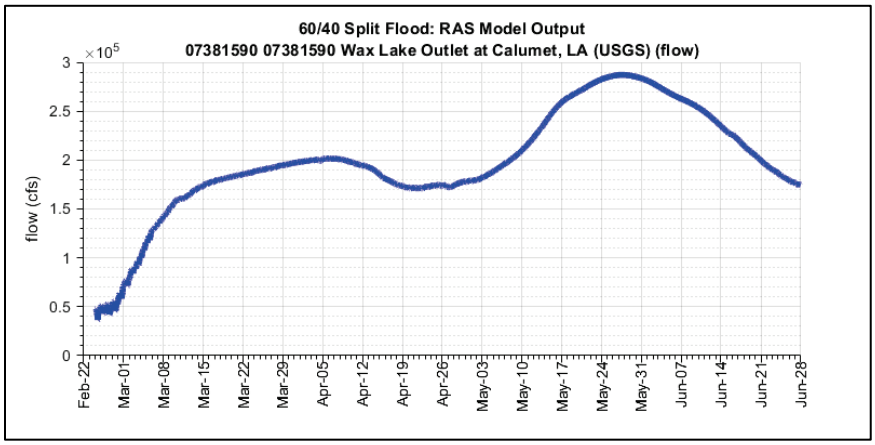

Figure A-20. Modeled flow at Simmesport along the Atchafalaya River south of the Old River Control Complex from the 60/40 simulation.

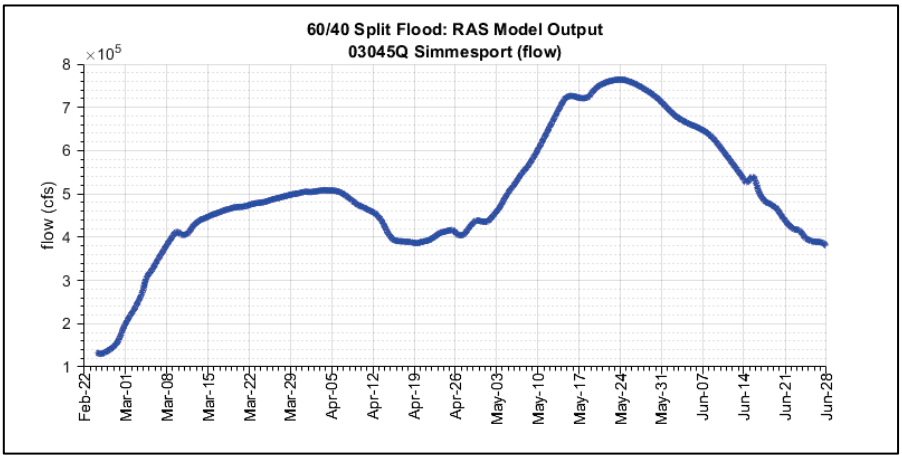

Figure A-21. Modeled stages in the Whiskey Bay Pilot Channel from the 60/40 simulation.

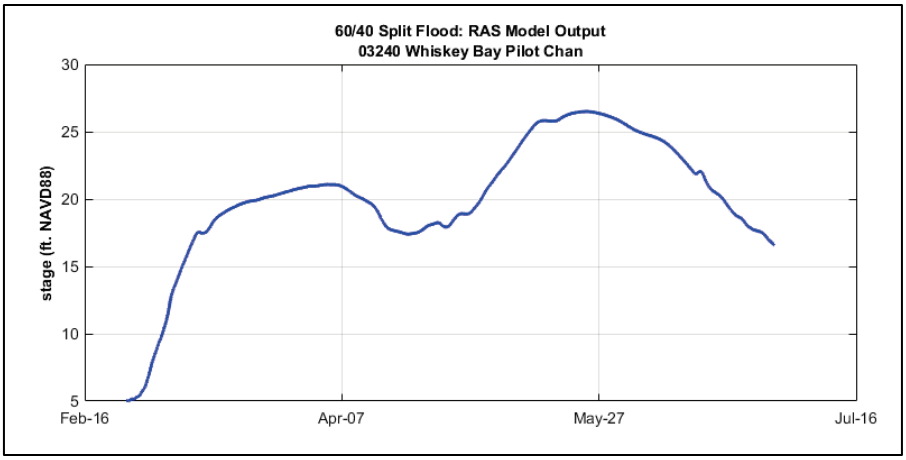

Figure A-22. Modeled stages in the Gulf Intracoastal Waterway (GIWW) south of Morgan City from the 60/40 simulation.

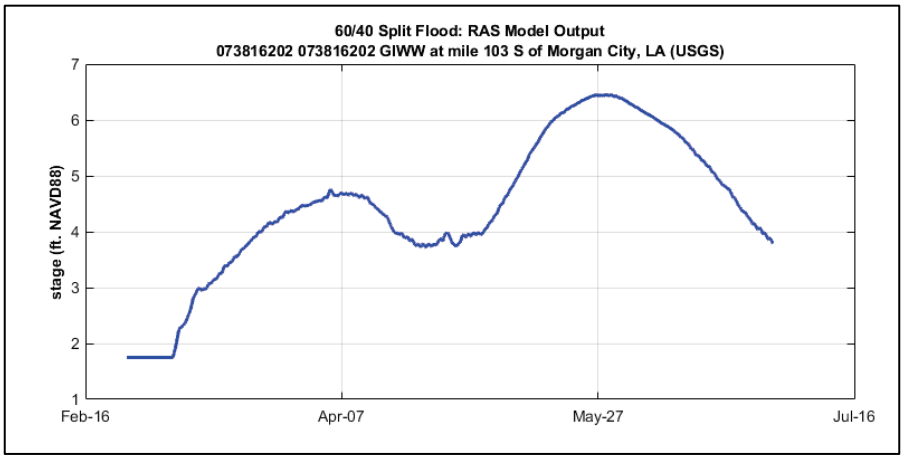

A.5 West bank of Red River—Bayou Natchitoches basin

Figure A-23. Time series of flow in cfs at Simmesport (*blue line*) overlaid with a time series of computed volume of water in the area on the west bank of the Red River (*red line*) for the 60/40 simulation.

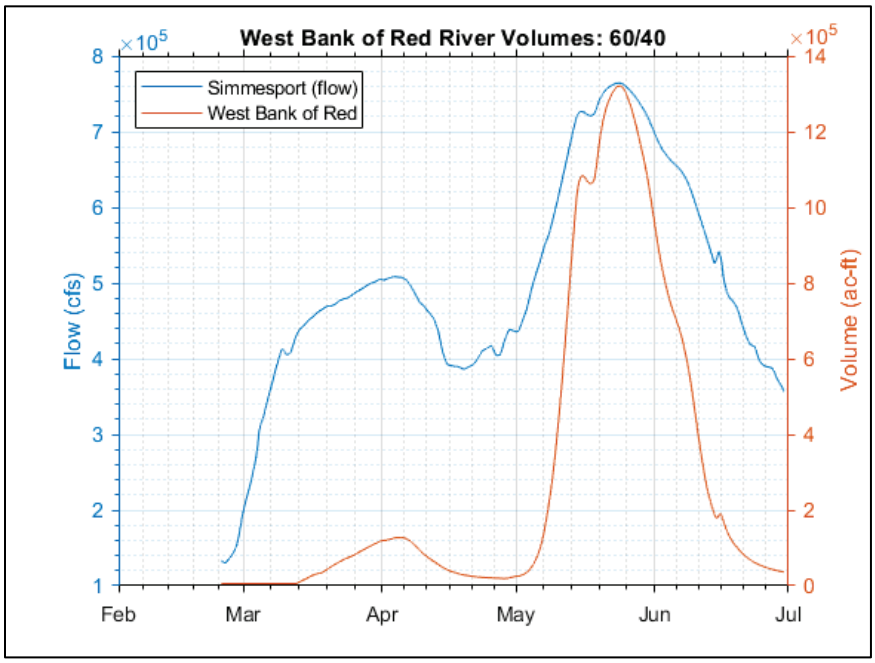

Figure A-24. Plot of flow in cfs at Simmesport versus computed volume of water in the area on the west bank of the Red River. *Line color* changes by simulation date for the 60/40 simulation.

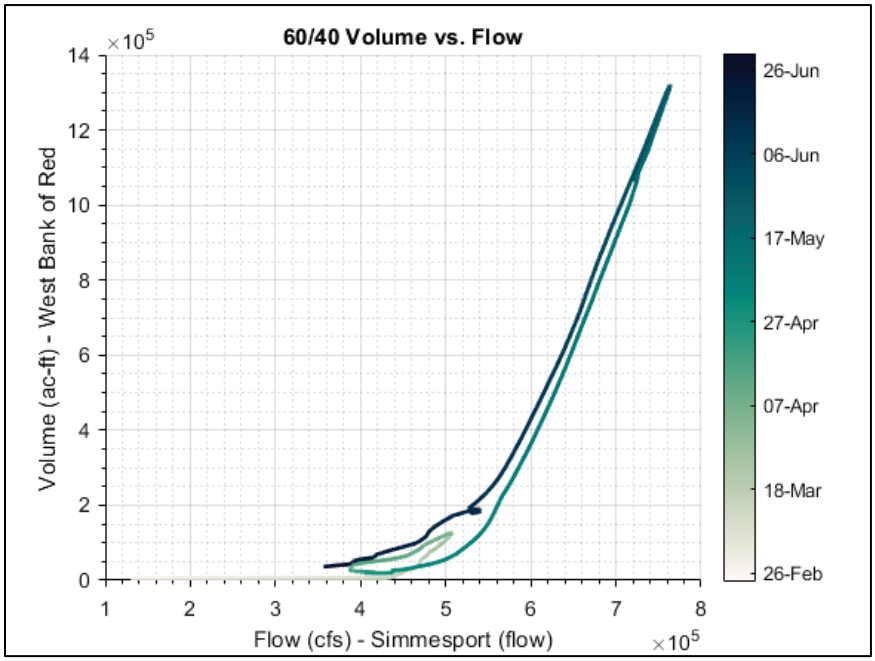

Figure A-25. Time series of stage at Simmesport (*blue line*) overlaid with a time series of computed volume of water in the area on the west bank of the Red River (*red line*) for the 60/40 simulation.

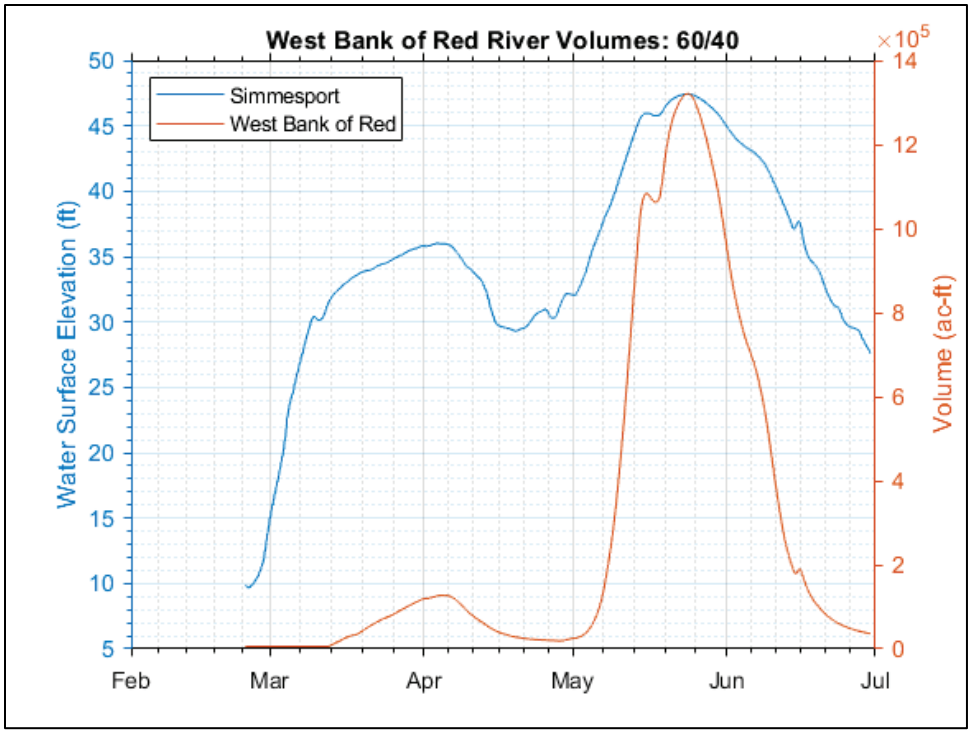

Figure A-26. Plot of stage at Simmesport versus computed volume of water in the area on the west bank of the Red River. *Line color* changes by simulation date for the 60/40 simulation.

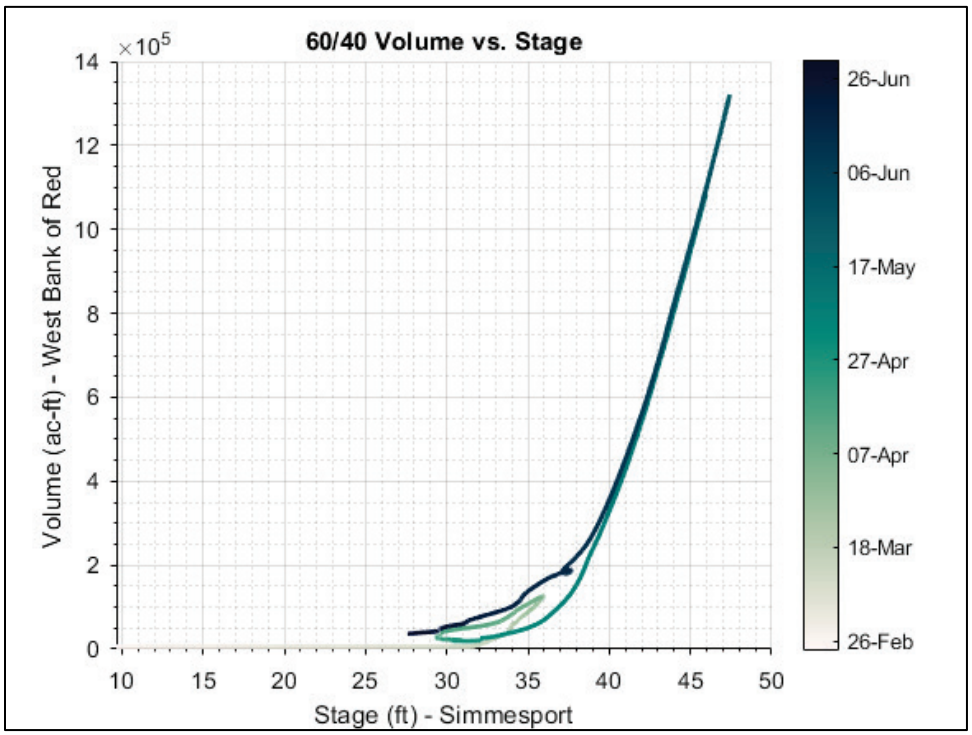

A.6 East bank of Red River—Alligator Bayou basin

Figure A-27. Time series of flow in cfs at Simmesport (*blue line*) overlaid with a time series of computed volume of water in the area on the east bank of the Red River (*red line*) for the 60/40 simulation.

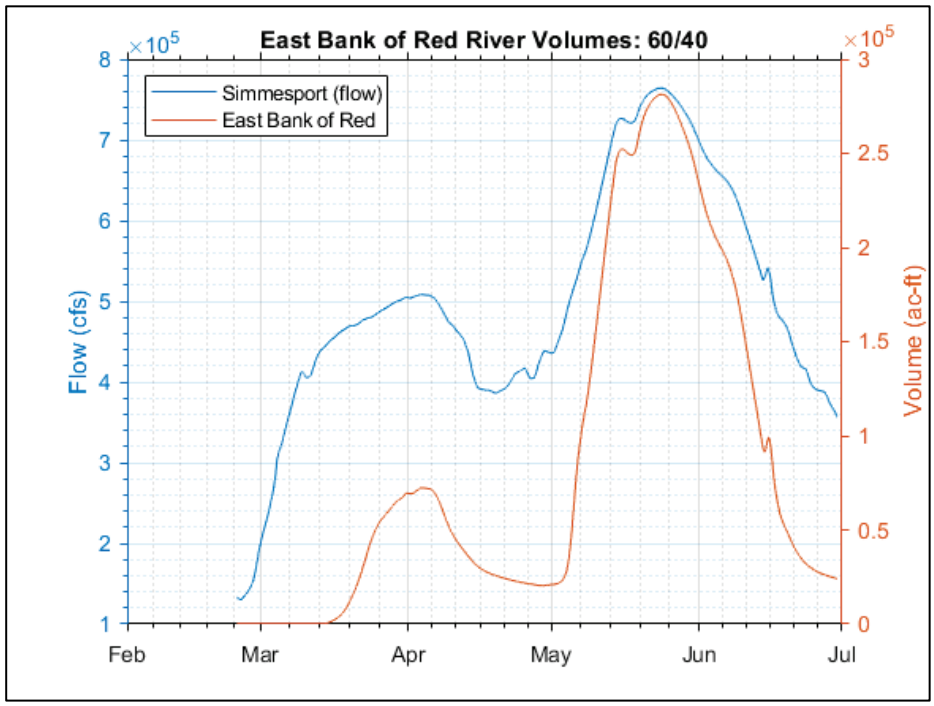

Figure A-28. Plot of flow in cfs at Simmesport versus computed volume of water in the area on the east bank of the Red River. *Line color* changes by simulation date for the 60/40 simulation.

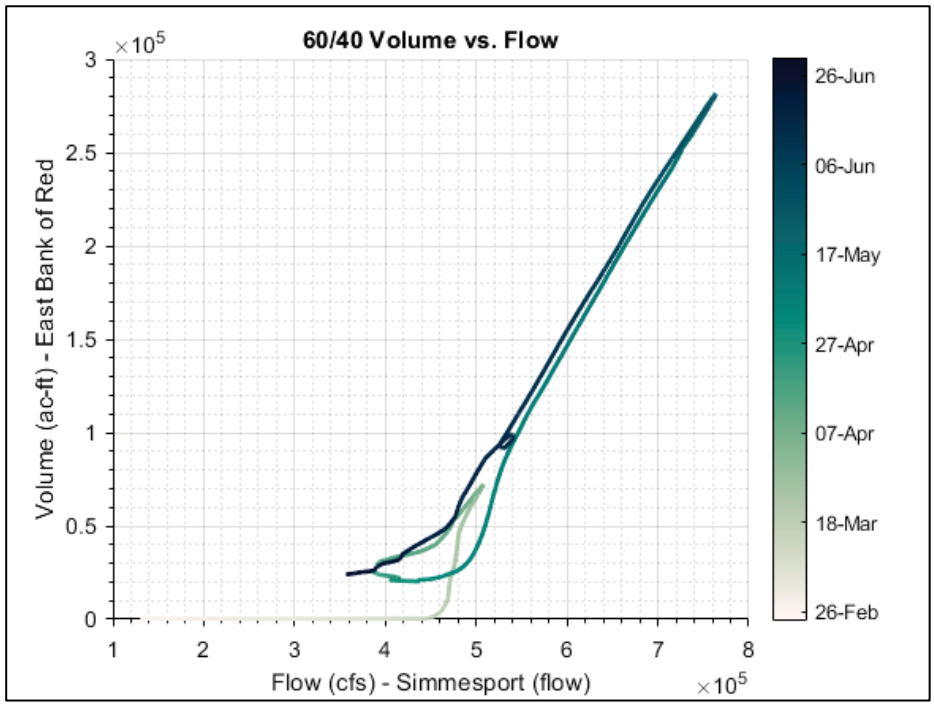

Figure A-29. Time series of stage at Simmesport (*blue line*) overlaid with a time series of computed volume of water in the area on the east bank of the Red River (*red line*) for the 60/40 simulation.

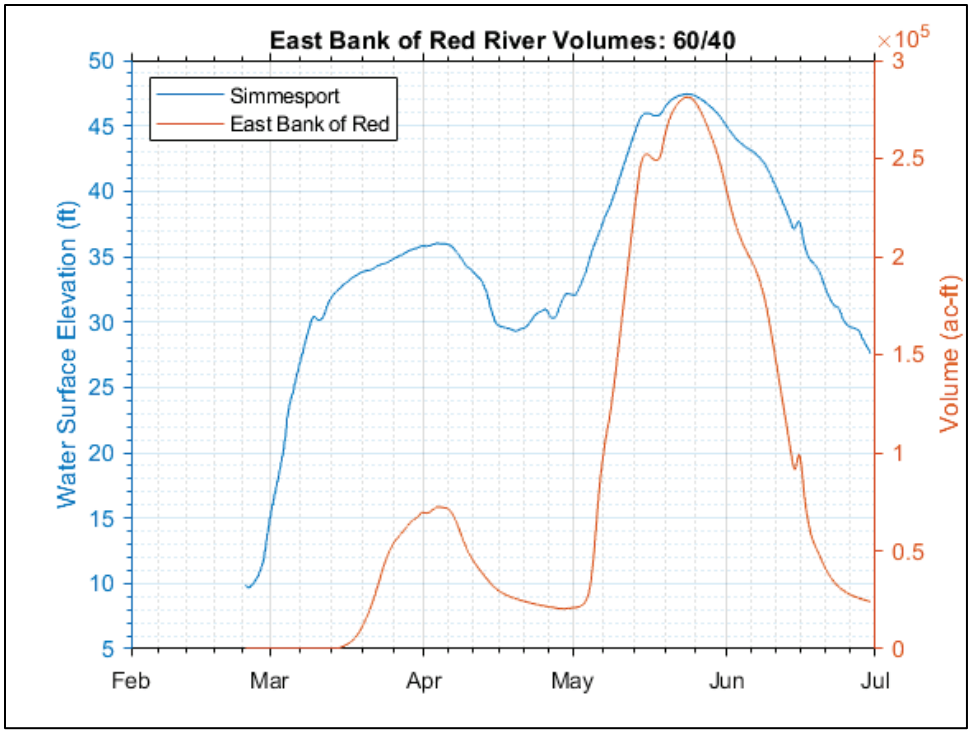

Figure A-30. Plot of stage at Simmesport versus computed volume of water in the area on the east bank of the Red River. *Line color* changes by simulation date for the 60/40 simulation.

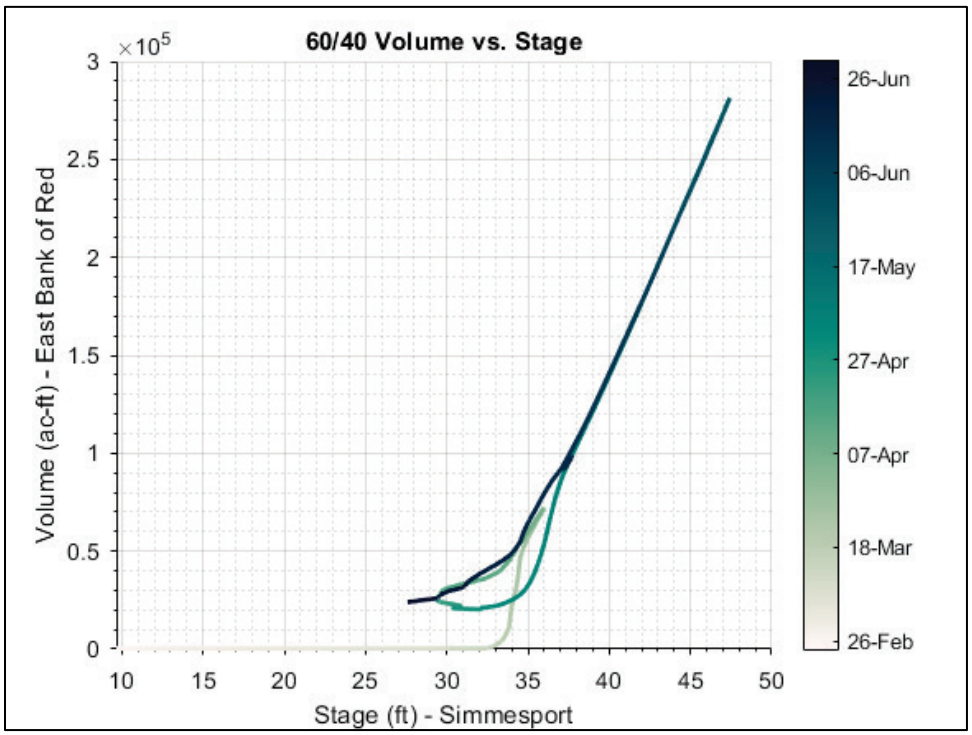

Figure A-31. Flow into storage (*blue* is western storage area, *orange* is eastern storage area) versus flow at Simmesport (cfs) for the 60/40 simulation.

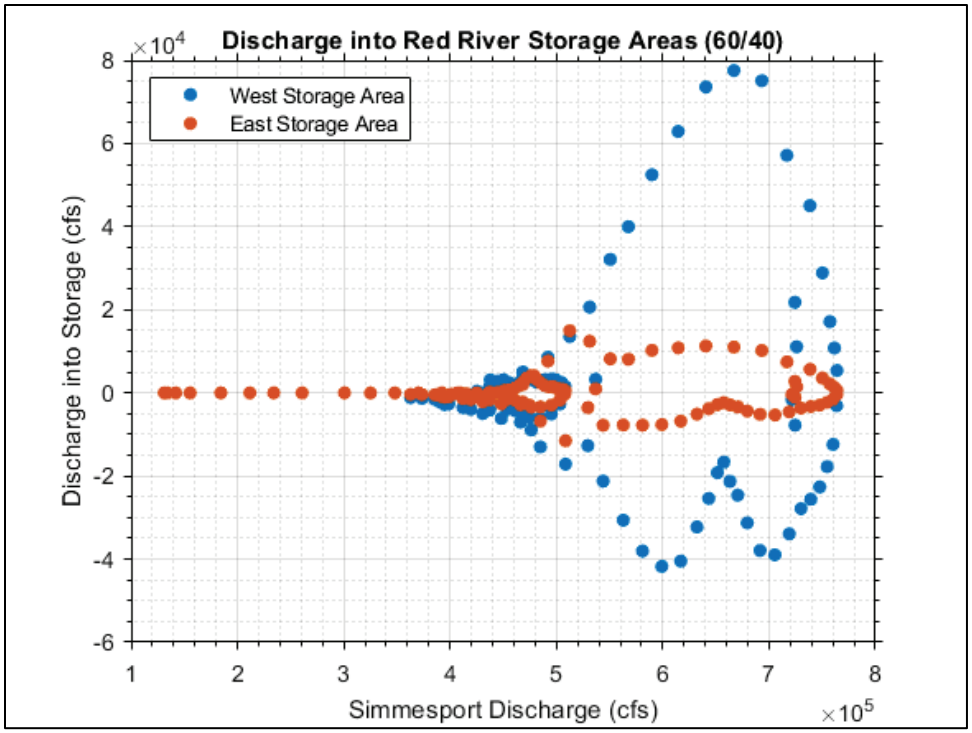

Figure A-32. Percentage of ORCC flows going into storage (*blue*, western area; *orange*, eastern area) versus flow at Simmesport (cfs) for the 60/40 simulation.

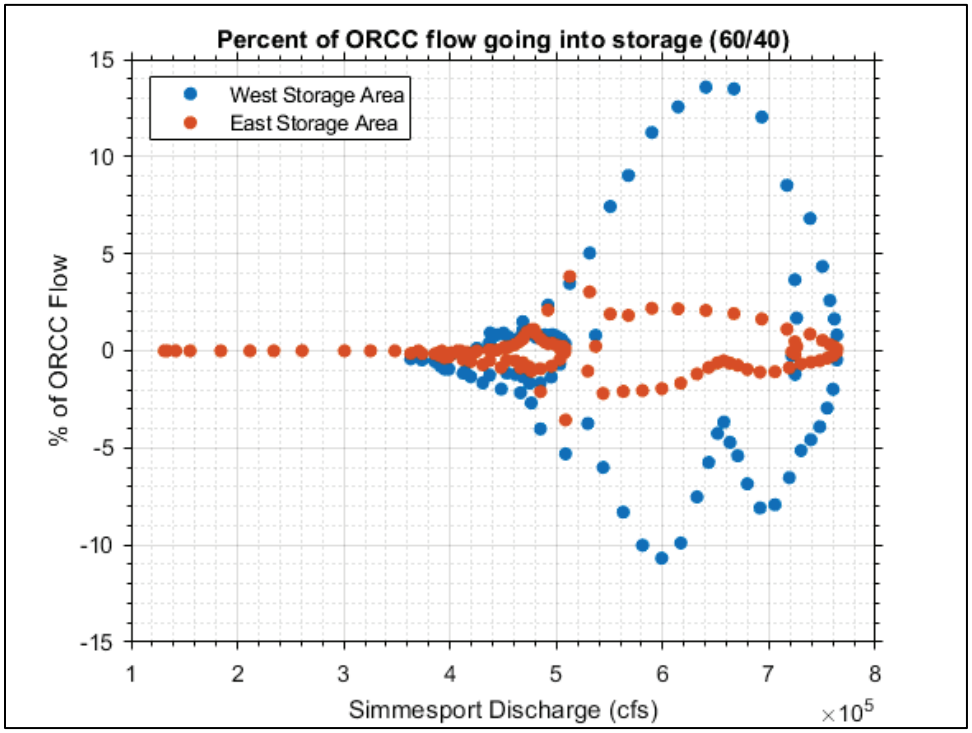

A.7 Old River 80/20 Split

Figure A-33. Modeled flow in the Red River upstream of the confluence with the Black River from the 80/20 simulation.

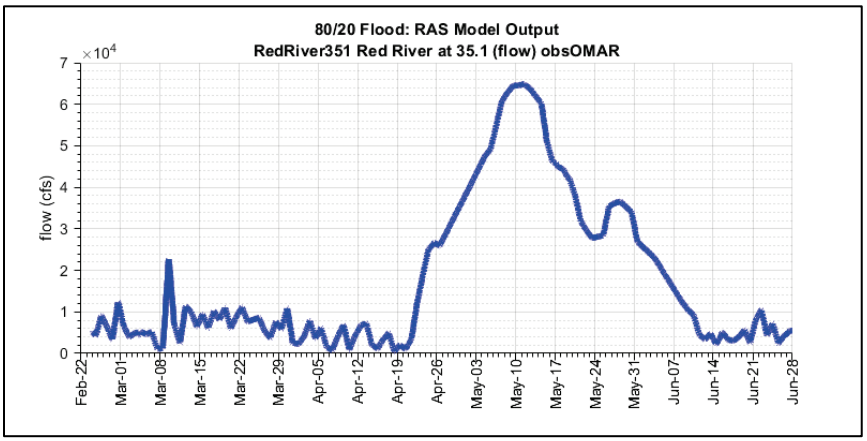

Figure A-34. Modeled flow at the site of the new stream gage at Madam Lee (downstream from the confluence with the Black River) from the 80/20 simulation.

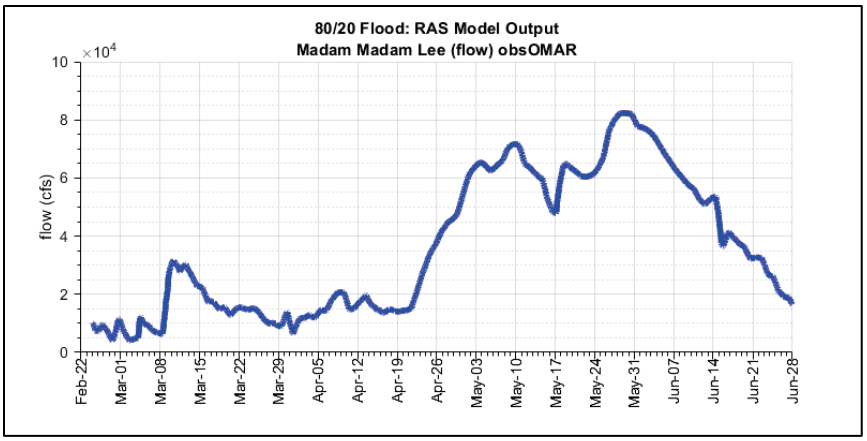

Figure A-35. Modeled flow for Wax Lake Outlet (outlet to the west of the main Atchafalaya River outlet) from the 80/20 simulation.

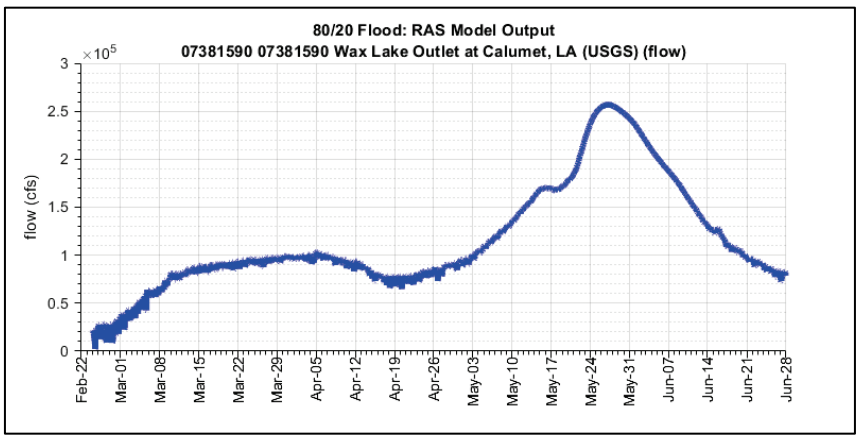

Figure A-36. Modeled flow at Simmesport along the Atchafalaya River south of the Old River Control Complex from the 80/20 simulation.

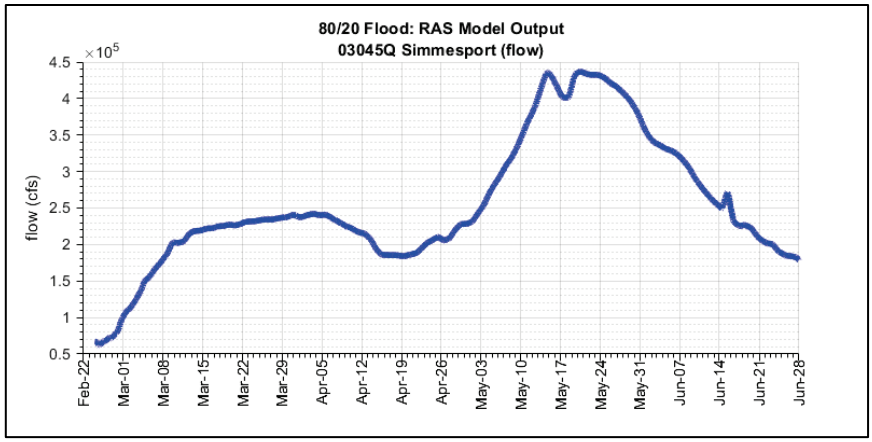

Figure A-37. Modeled stages in the Whiskey Bay Pilot Channel from the 80/20 simulation.

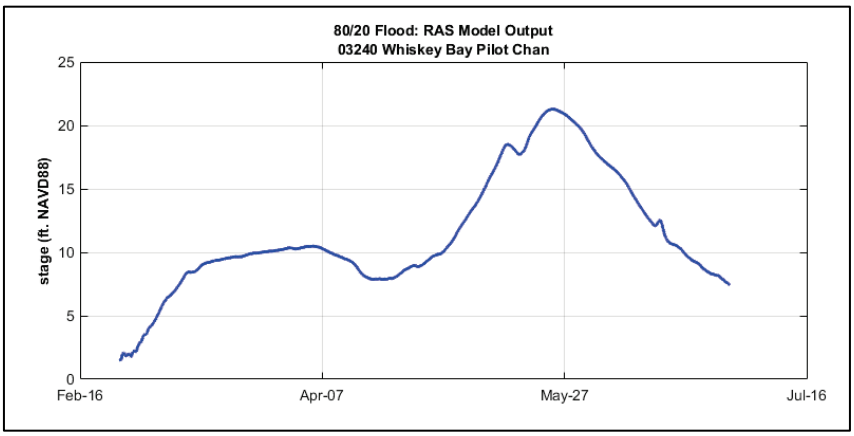

Figure A-38. Modeled stages in the GIWW south of Morgan City from the 80/20 simulation.

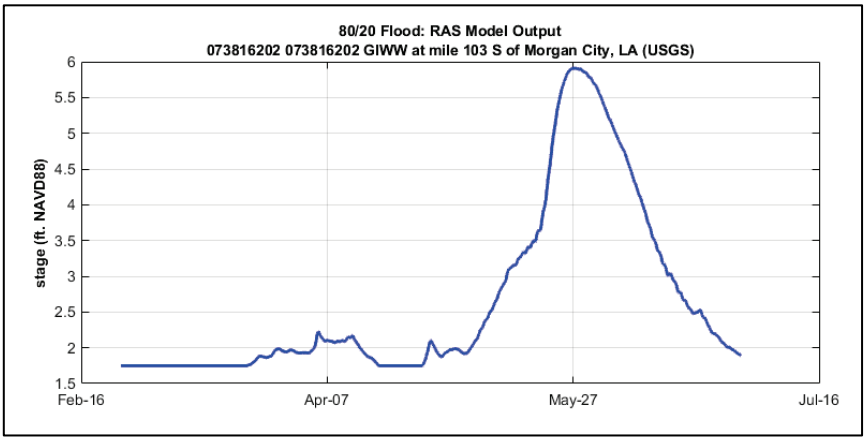

A.8 West bank of Red River—Bayou Natchitoches basin

Figure A-39. Time series of flow in cfs at Simmesport (*blue line*) overlaid with a time series of computed volume of water in the area on the west bank of the Red River (*red line*) for the 80/20 simulation.

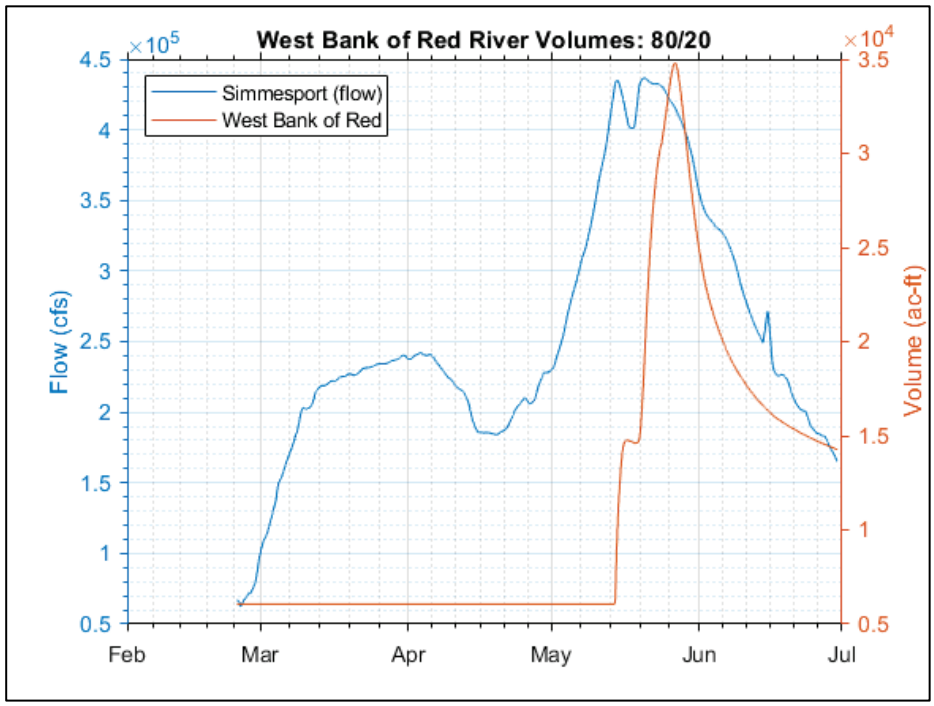

Figure A-40. Plot of flow in cfs at Simmesport versus computed volume of water in the area on the west bank of the Red River. *Line color* changes by simulation date for the 80/20 simulation.

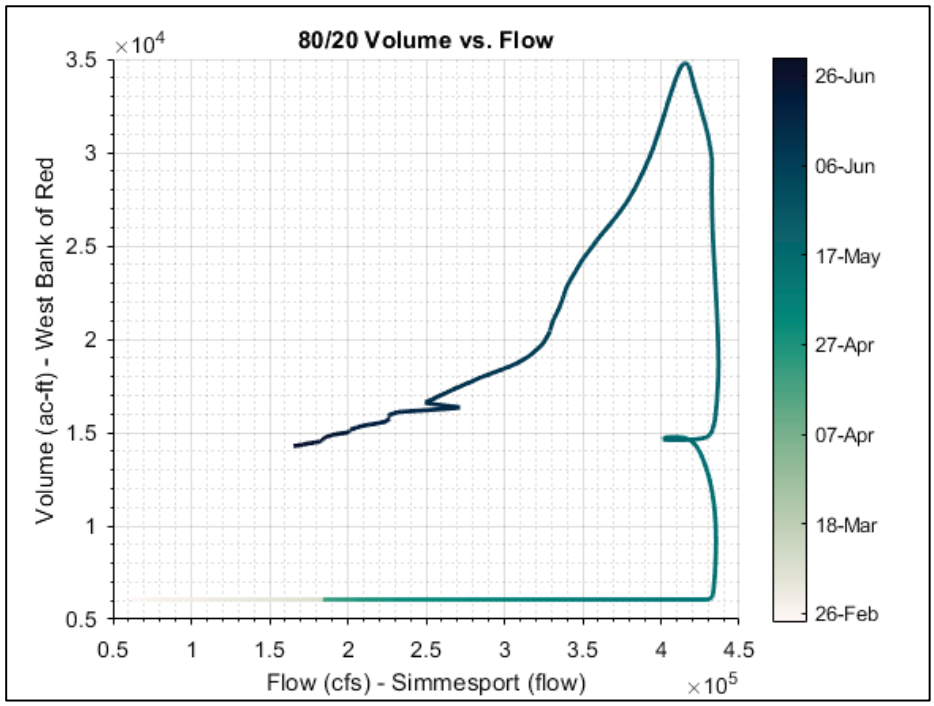

Figure A-41. Time series of stage at Simmesport (*blue line*) overlaid with a time series of computed volume of water in the area on the west bank of the Red River (*red line*) for the 80/20 simulation.

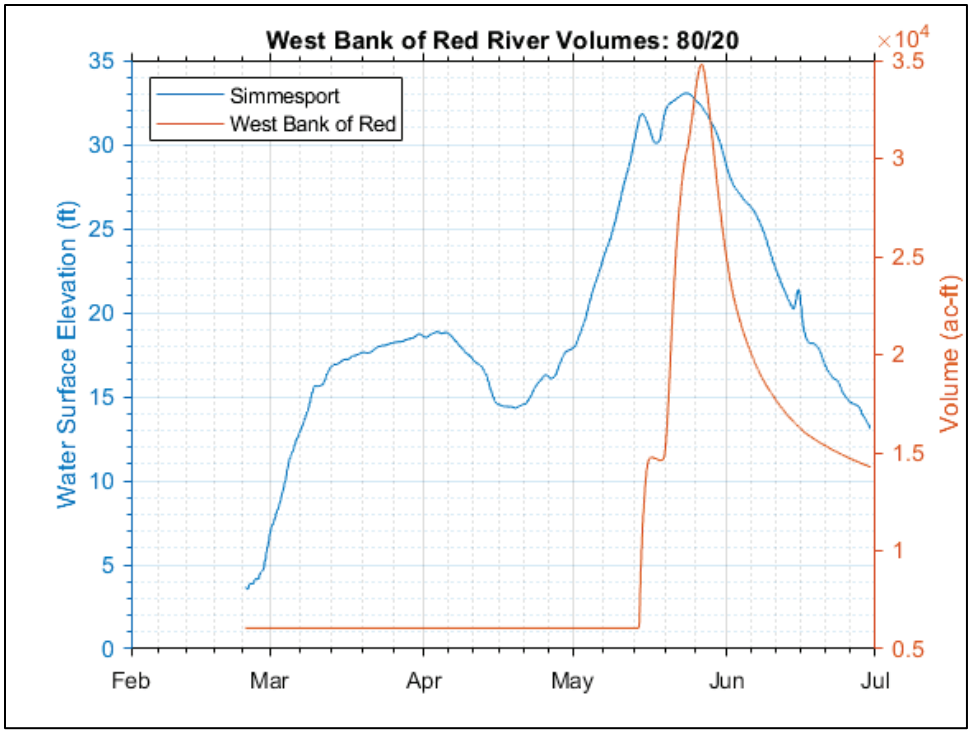

Figure A-42. Plot of stage at Simmesport versus computed volume of water in the area on the west bank of the Red River. *Line color* changes by simulation date for the 80/20 simulation.

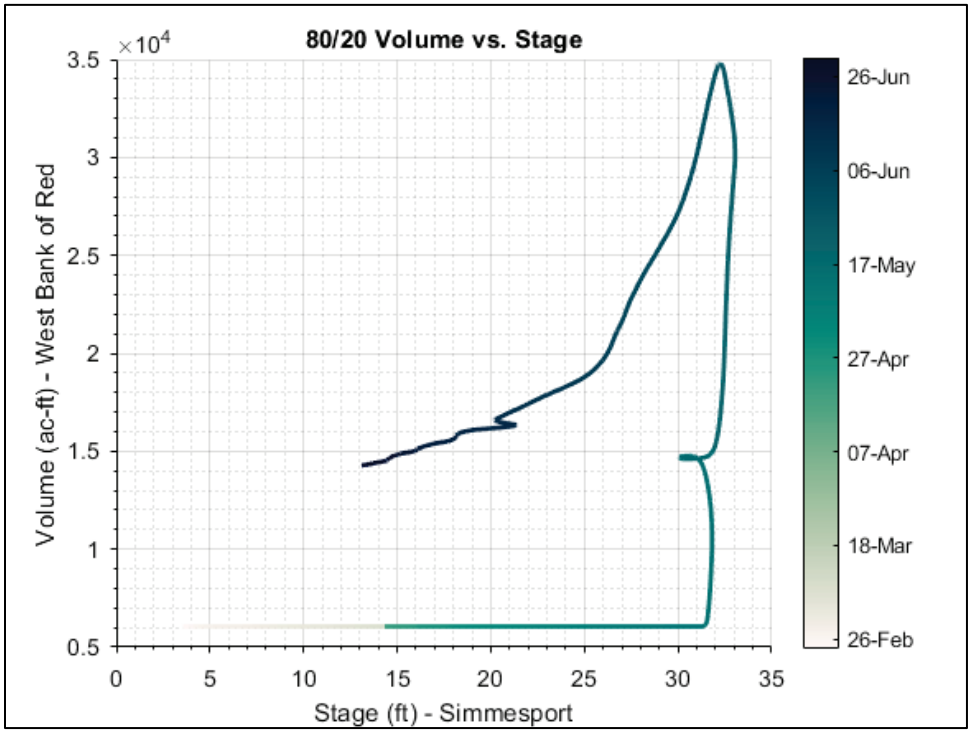

A.9 East bank of Red River—Alligator Bayou basin

Figure A-43. Time series of flow in cfs at Simmesport (*blue line*) overlaid with a time series of computed volume of water in the area on the east bank of the Red River (*red line*) for the 80/20 simulation.

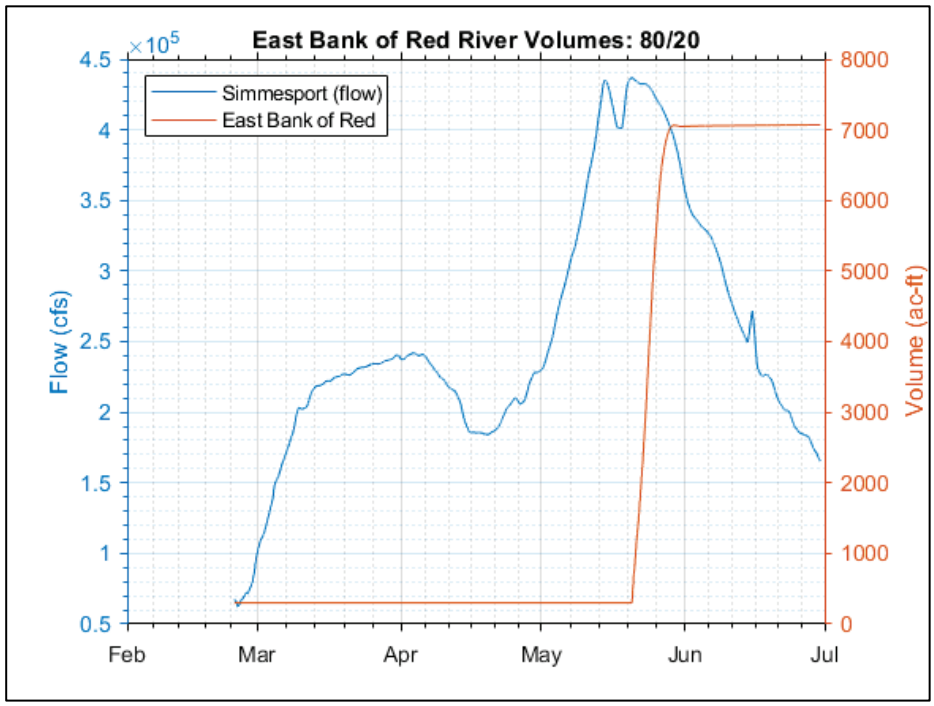

Figure A-44. Plot of flow in cfs at Simmesport versus computed volume of water in the area on the east bank of the Red River. *Line color* changes by simulation date for the 80/20 simulation.

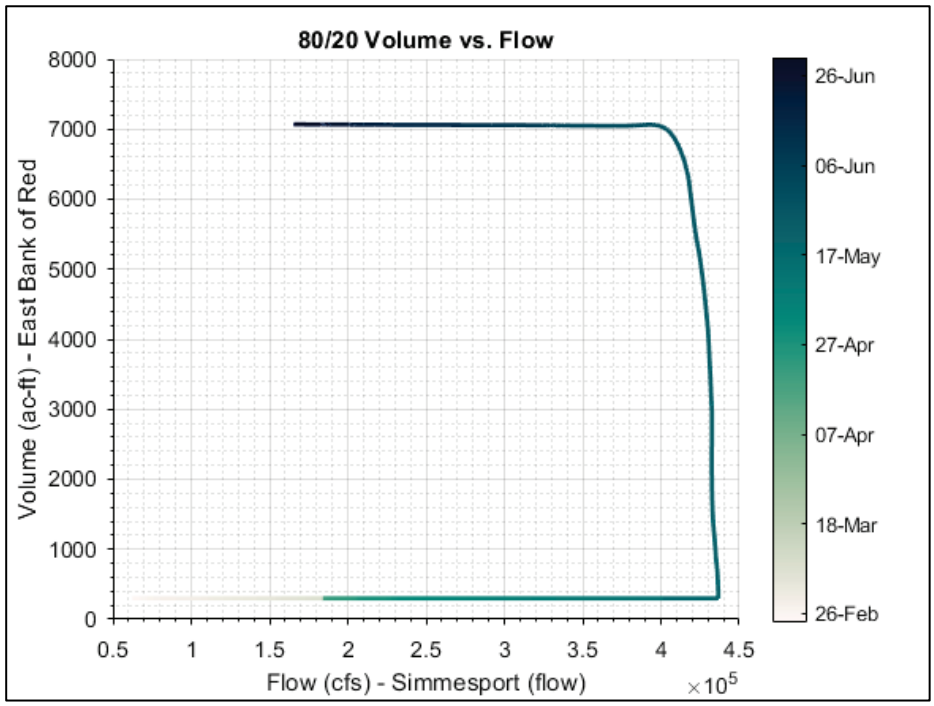

Figure A-45. Time series of stage at Simmesport (*blue line*) overlaid with a time series of computed volume of water in the area on the east bank of the Red River (*red line*) for the 80/20 simulation.

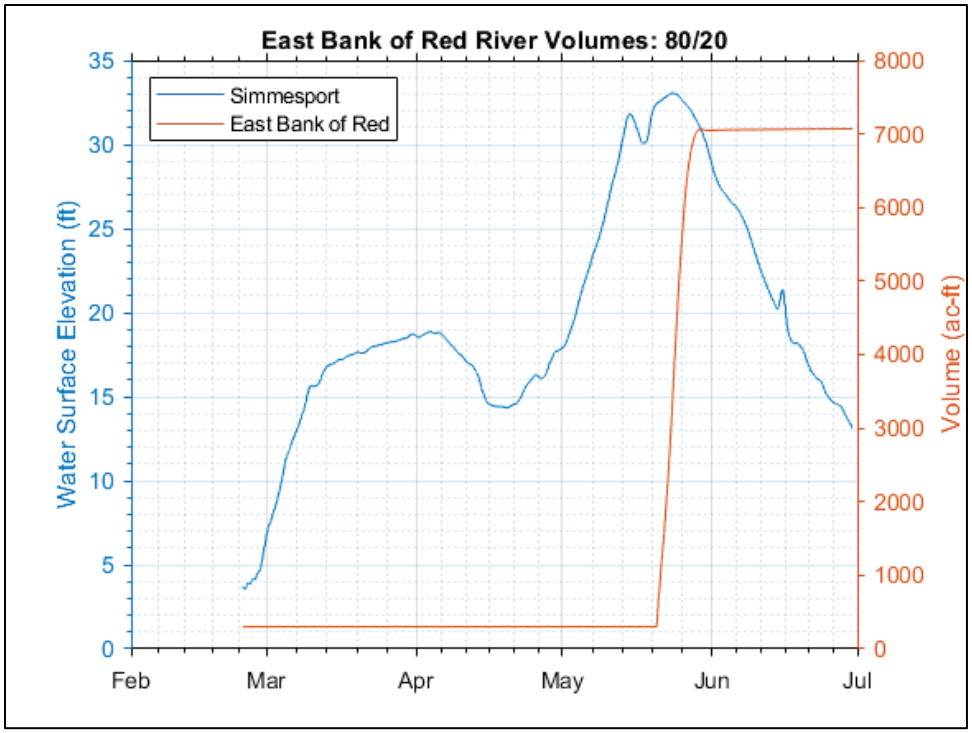

Figure A-46. Plot of stage at Simmesport versus computed volume of water in the area on the east bank of the Red River. *Line color* changes by simulation date for the 80/20 simulation.

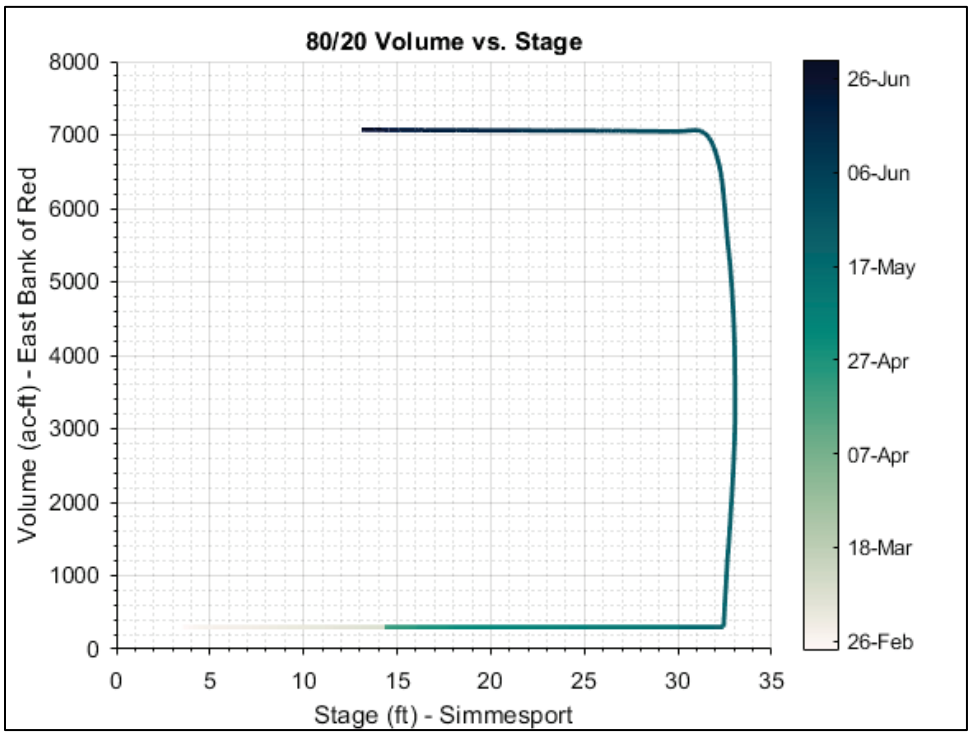

Figure A-47. Flow into storage (*blue* is western storage area, *orange* is eastern storage area) versus flow at Simmesport (cfs) for the 80/20 simulation.

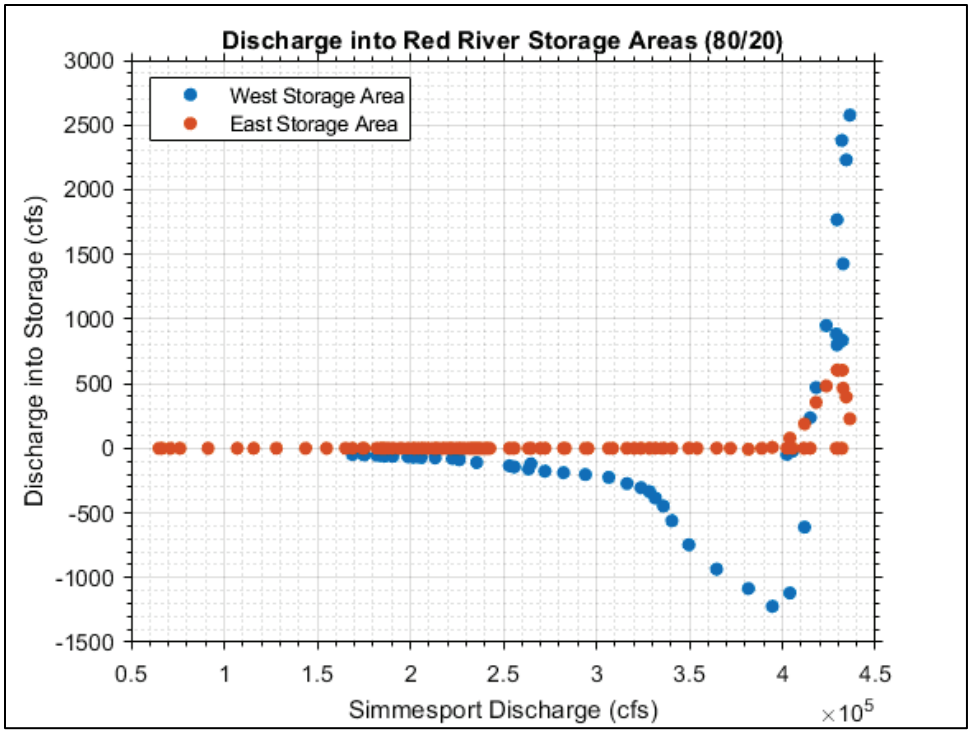

Figure A-48. Percentage of ORCC flows going into storage (*blue*, western area; *orange*, eastern area) versus flow at Simmesport (cfs) for the 80/20 simulation.

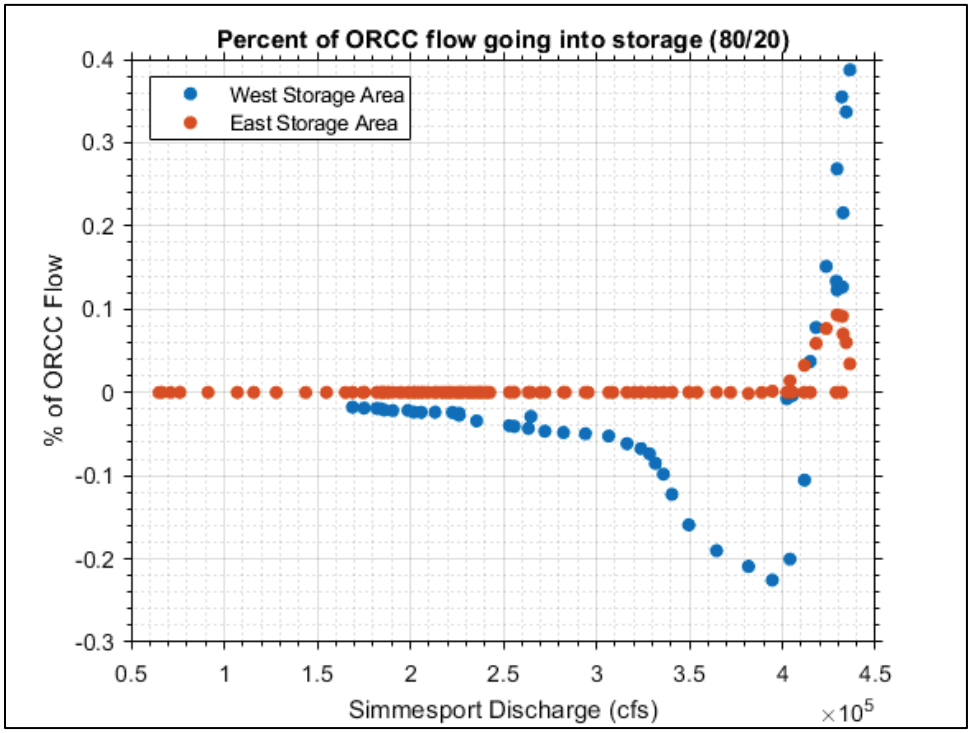

A.10 Extreme flows simulation

Figure A-49. Modeled flow in the Red River upstream of the confluence with the Black River from the extreme flows simulation.

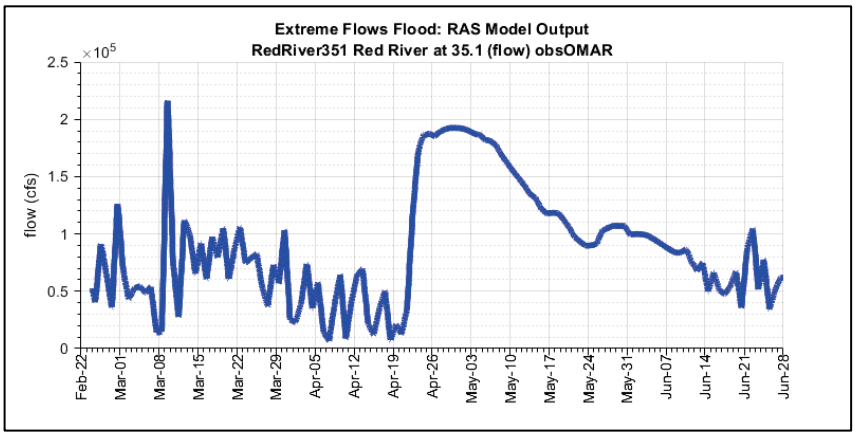

Figure A-50. Modeled flow at the site of the new stream gage at Madam Lee (downstream from the confluence with the Black River) from the extreme flows simulation.

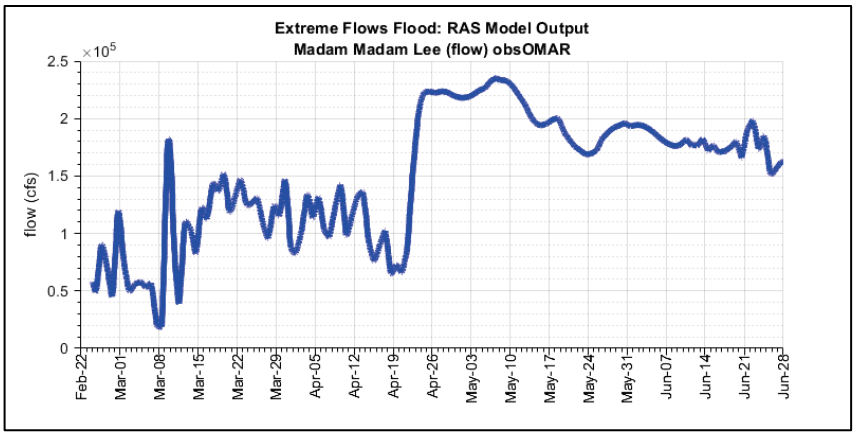

Figure A-51. Modeled flow for Wax Lake Outlet (outlet to the west of the main Atchafalaya River outlet) from the extreme flows simulation.

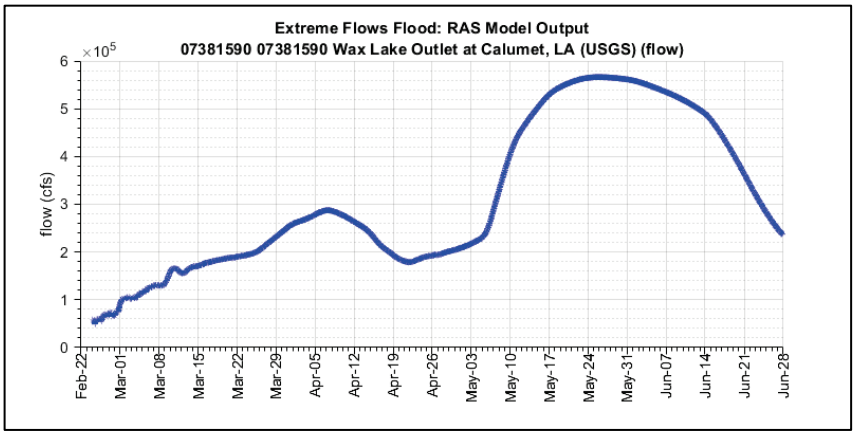

Figure A-52. Modeled flow at Simmesport along the Atchafalaya River south of the Old River Control Complex from the extreme flows simulation.

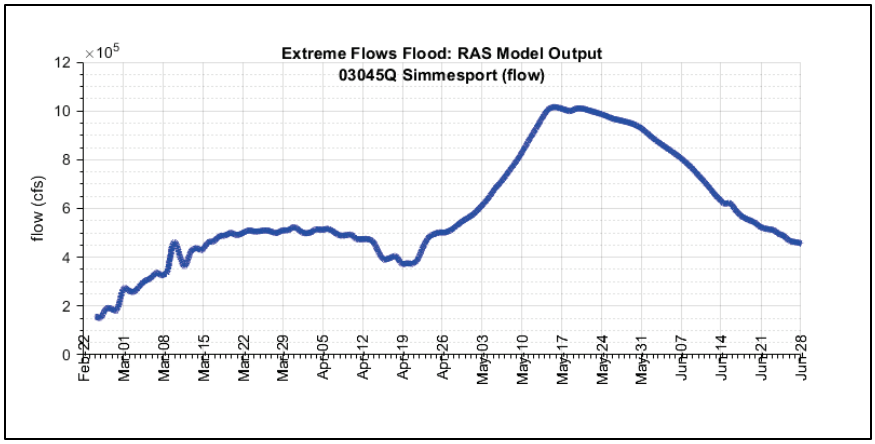

Figure A-53. Modeled stages in the Whiskey Bay Pilot Channel from the extreme flows simulation.

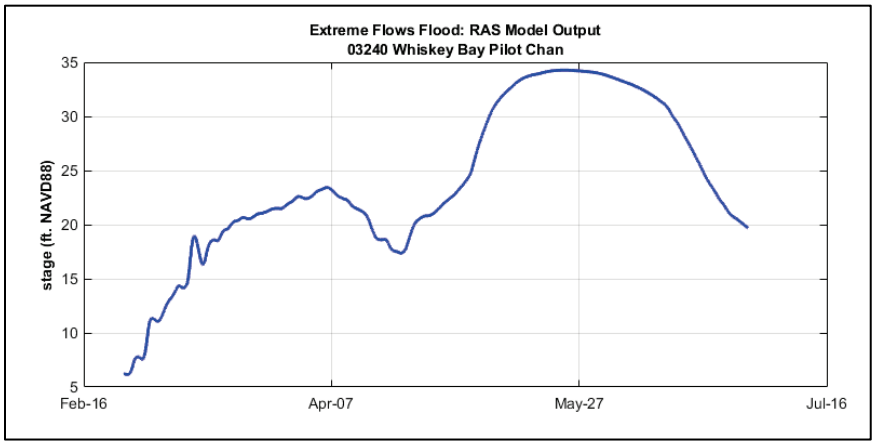

Figure A-54. Modeled stages in the GIWW south of Morgan City from the extreme flows simulation.

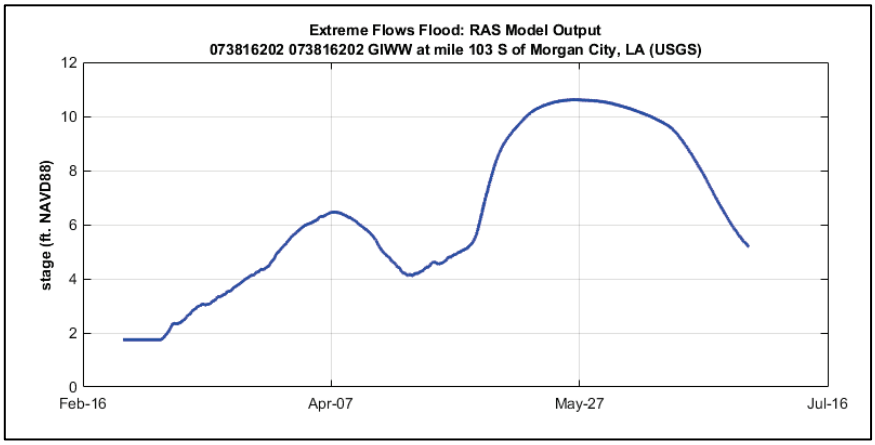

A.11 West bank of Red River—Bayou Natchitoches basin

Figure A-55. Time series of flow in cfs at Simmesport (*blue line*) overlaid with a time series of computed volume of water in the area on the west bank of the Red River (*red line*) for the extreme flows simulation.

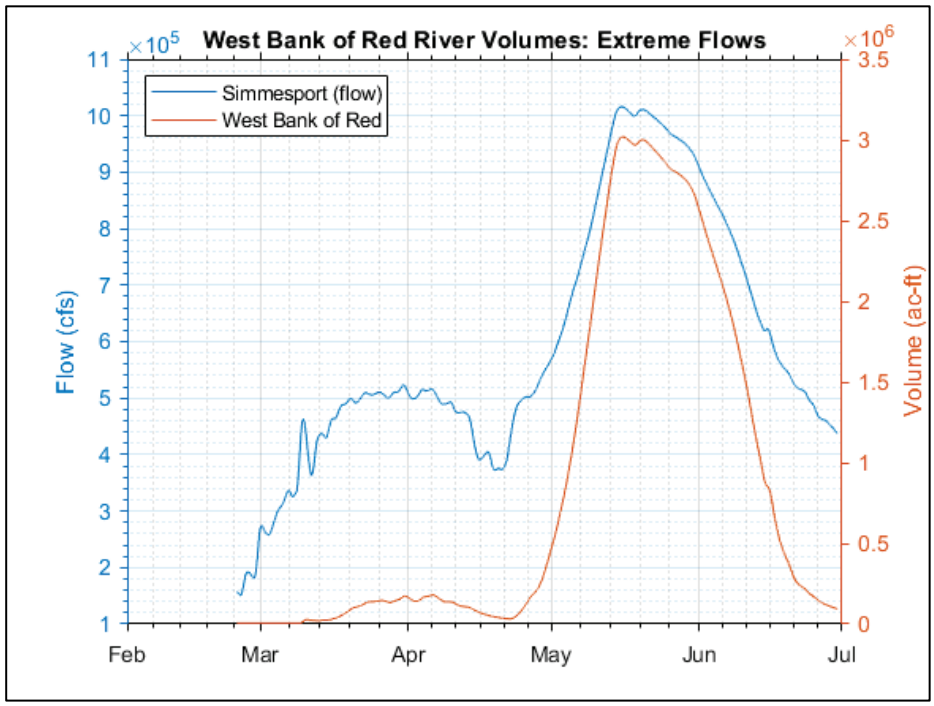

Figure A-56. Plot of flow in cfs at Simmesport versus computed volume of water in the area on the west bank of the Red River. *Line color* changes by simulation date for the extreme flows simulation.

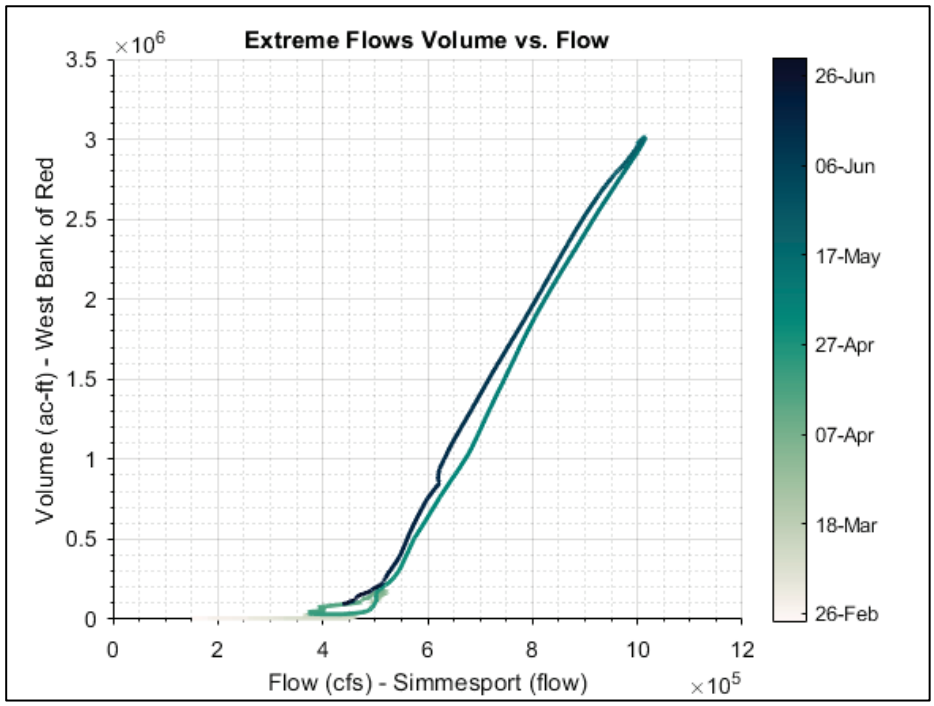

Figure A-57. Time series of stage at Simmesport (*blue line*) overlaid with a time series of computed volume of water in the area on the west bank of the Red River (*red line*) for the extreme flows simulation.

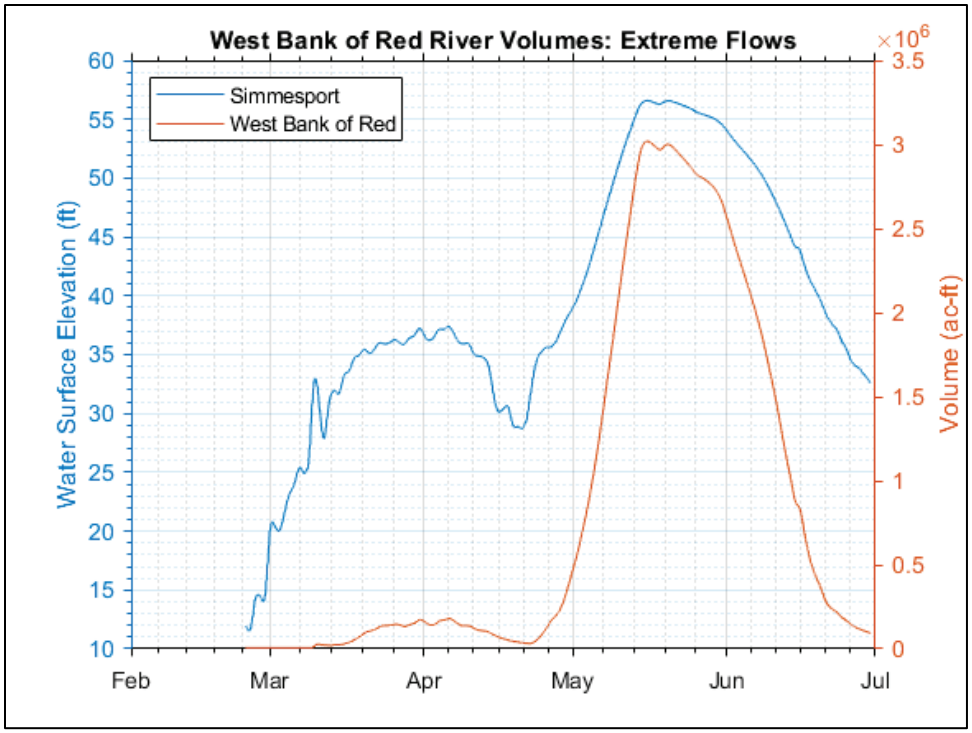

Figure A-58. Plot of stage at Simmesport versus computed volume of water in the area on the west bank of the Red River. *Line color* changes by simulation date for the extreme flows simulation.

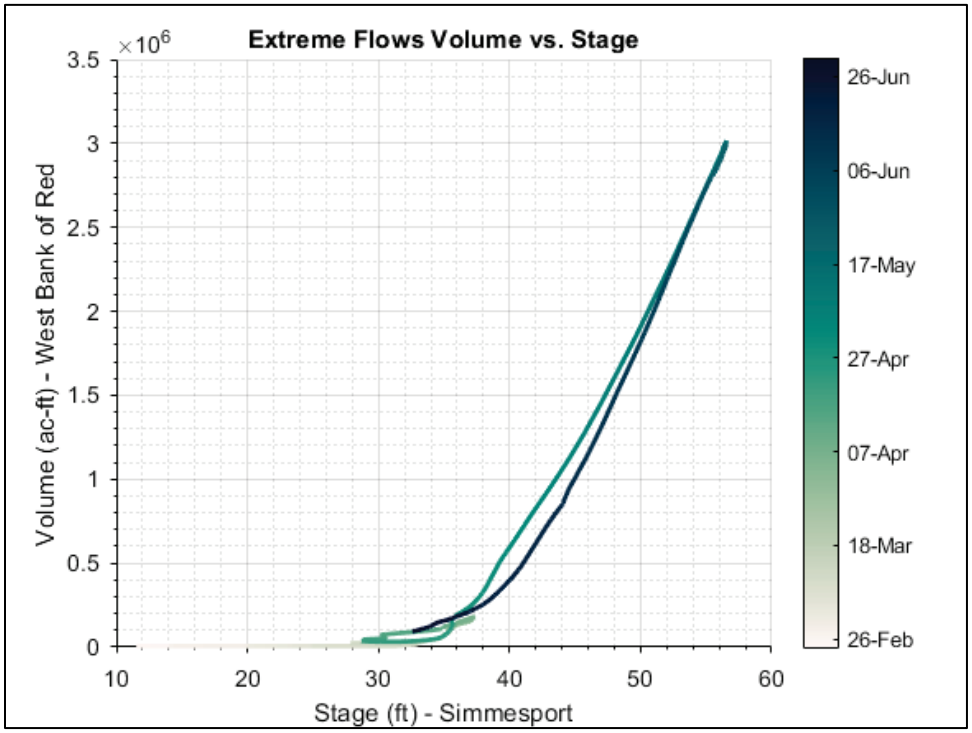

A.12 East bank of Red River—Alligator Bayou basin

Figure A-59. Time series of flow in cfs at Simmesport (*blue line*) overlaid with a time series of computed volume of water in the area on the east bank of the Red River (*red line*) for the extreme flows simulation.

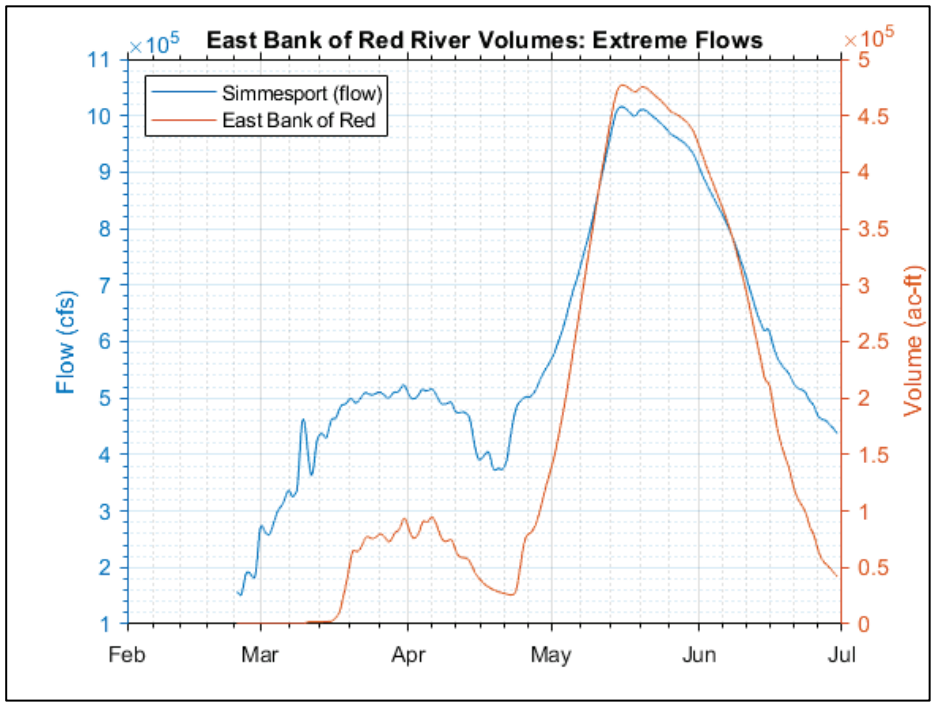

Figure A-60. Plot of flow in cfs at Simmesport versus computed volume of water in the area on the east bank of the Red River. *Line color* changes by simulation date for the extreme flows simulation.

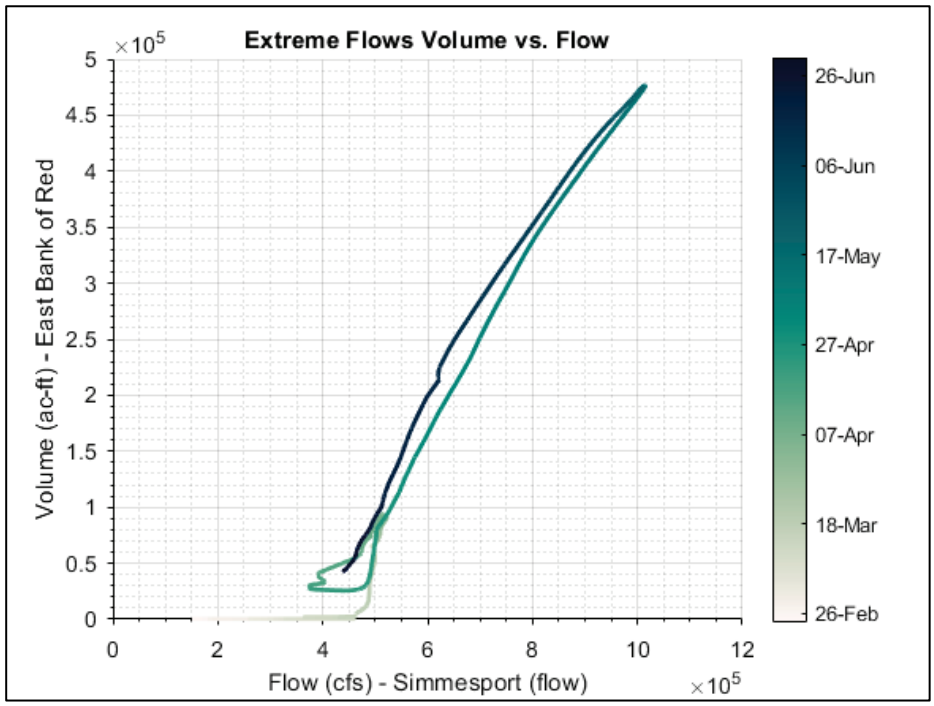

Figure A-61. Time series of stage at Simmesport (*blue line*) overlaid with a time series of computed volume of water in the area on the east bank of the Red River (*red line*) for the extreme flows simulation.

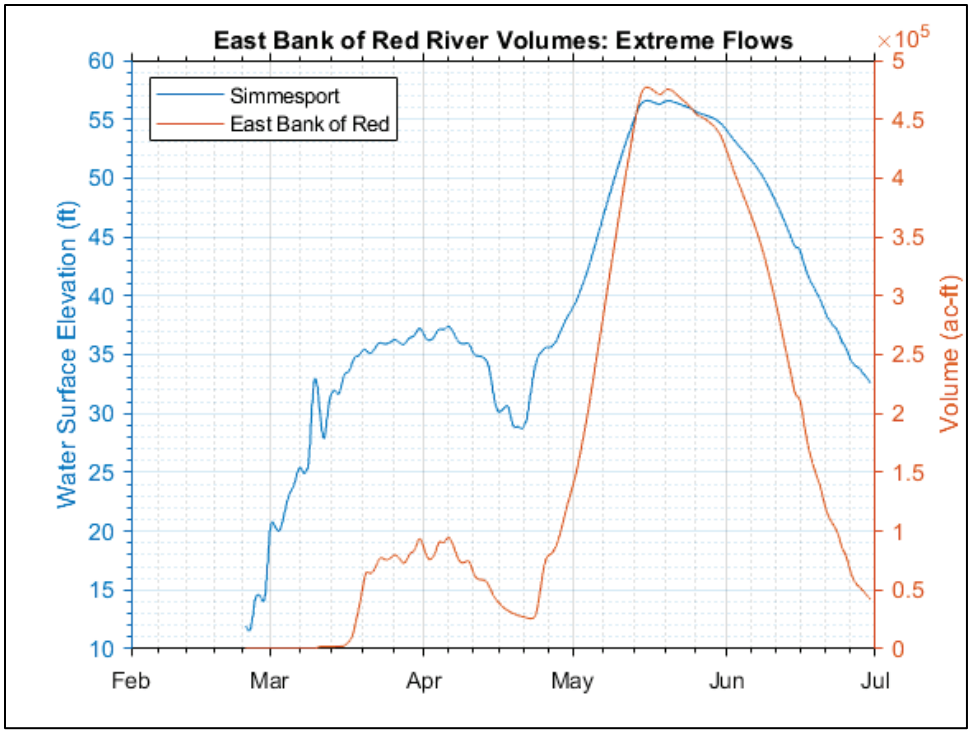

Figure A-62. Plot of stage at Simmesport versus computed volume of water in the area on the east bank of the Red River. *Line color* changes by simulation date for the extreme flows simulation.

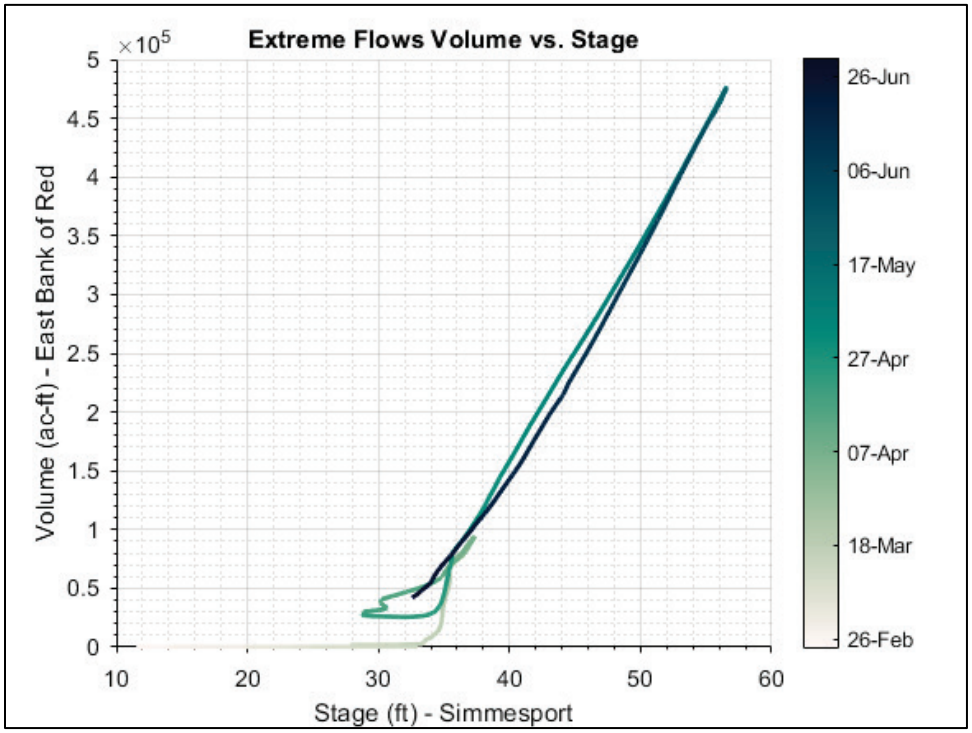

Figure A-63. Flow into storage (*blue* is western storage area, *orange* is eastern storage area) versus flow at Simmesport (cfs) for the extreme flows simulation.

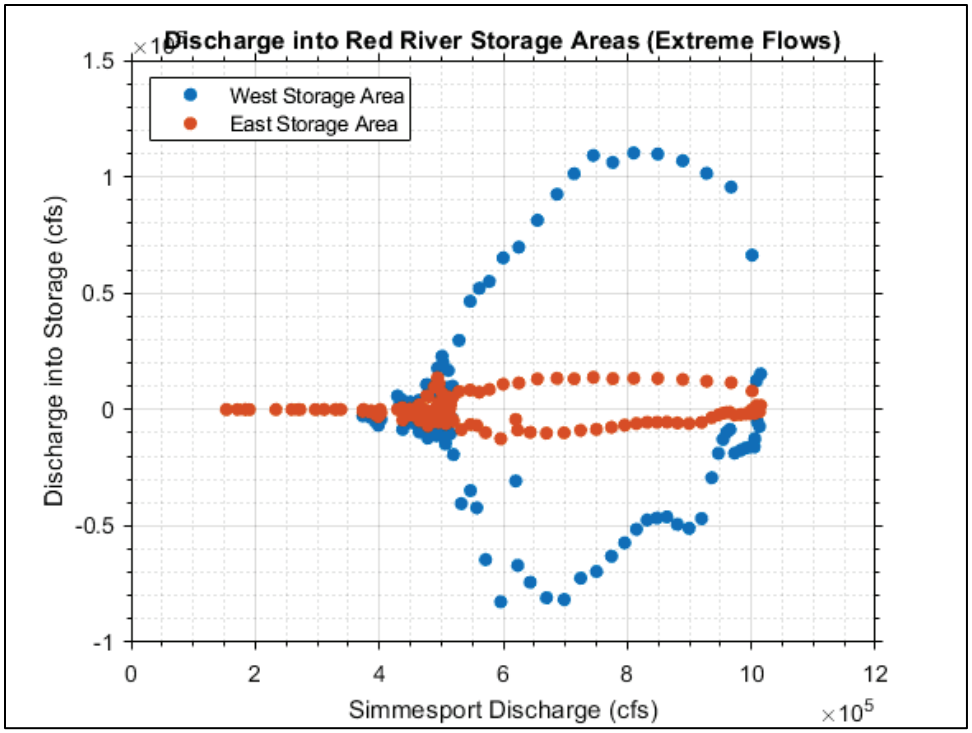

Figure A-64. Percentage of ORCC flows going into storage (*blue*, western area; *orange*, eastern area) versus flow at Simmesport (cfs) for the extreme flows simulation.

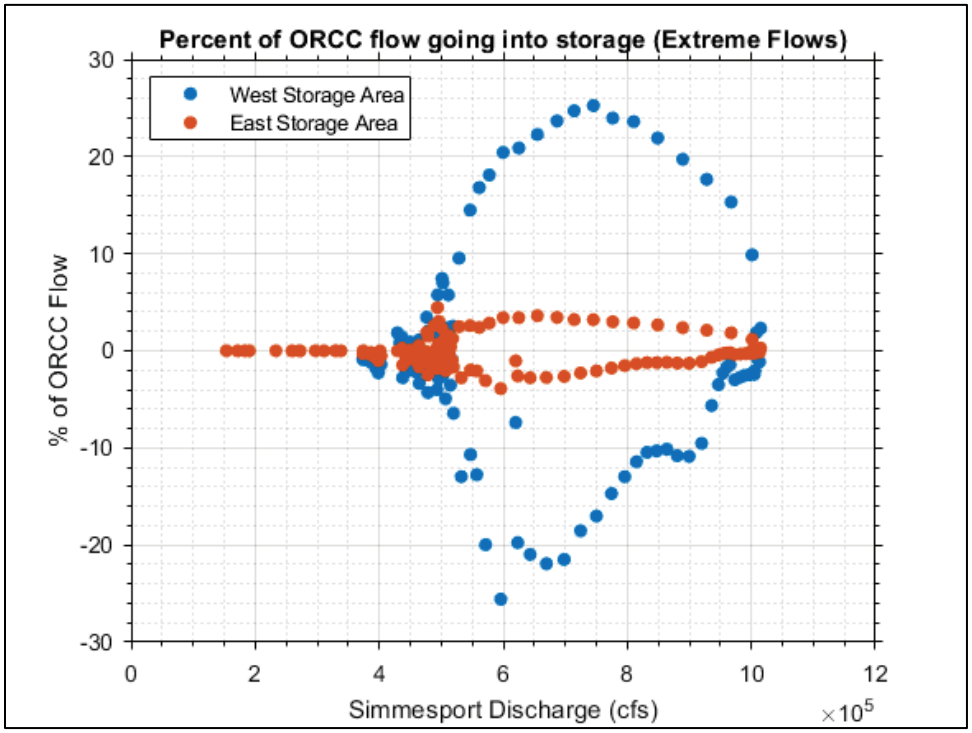

Appendix B: Supplemental Tables

This appendix contains tables detailing parameters used in the development of the model (Tables B-1 and B-2).

Table B-1. Outlet rating curve for how the Morganza spillway is operated as specified in RAS.

Mississippi Flow (cfs)	Release at Morganza (cfs)
0	0
100,000	0
1,500,000	0
1,600,000	100,000
1,700,000	200,000
1,800,000	300,000
1,900,000	400,000
2,000,000	500,000
2,100,000	600,000
2,200,000	600,000
2,300,000	600,000
2,400,000	600,000
2,500,000	600,000
2,600,000	600,000
2,700,000	600,000
2,800,000	600,000
2,900,000	600,000

Table B-2. Outlet rating curve for how the Bonnet Carré spillway is operated as specified in RAS.

Mississippi Flow (cfs)	Release at Bonnet Carré (cfs)
0	0
1,240,000	0
1,250,000	15,000
1,650,000	400,000

REPORT DOCUMENTATION PAGE

Form Approved

OMB No. 0704-0188

Public reporting burden for this collection of information is estimated to average 1 hour per response, including the time for reviewing instructions, searching existing data sources, gathering and maintaining the data needed, and completing and reviewing this collection of information. Send comments regarding this burden estimate or any other aspect of this collection of information, including suggestions for reducing this burden to Department of Defense, Washington Headquarters Services, Directorate for Information Operations and Reports (0704-0188), 1215 Jefferson Davis Highway, Suite 1204, Arlington, VA 22202-4302. Respondents should be aware that notwithstanding any other provision of law, no person shall be subject to any penalty for failing to comply with a collection of information if it does not display a currently valid OMB control number. PLEASE DO NOT RETURN YOUR FORM TO THE ABOVE ADDRESS.

1. REPORT DATE	2. REPORT TYPE	3. DATES COVERED (From–To)
August 2022	Final	FY21–FY22

4. TITLE AND SUBTITLE

Technical Assessment of the Old, Mississippi, Atchafalaya, and Red (OMAR) Rivers: HEC-RAS Model

5a. CONTRACT NUMBER

5b. GRANT NUMBER

5c. PROGRAM ELEMENT

6. AUTHOR(S)

David A. Fertitta, Maxwell E. Agnew, and David A. Ramirez

5d. PROJECT NUMBER

478534

5e. TASK NUMBER

5f. WORK UNIT NUMBER

7. PERFORMING ORGANIZATION NAME(S) AND ADDRESS(ES)

Hydrology, Hydraulics, and Coastal Branch
7400 Leake Ave
New Orleans, Louisiana 70118

River Engineering Branch
7400 Leake Ave
New Orleans, Louisiana 70118

8. PERFORMING ORGANIZATION REPORT NUMBER

MRG&P Report No. 41; Volume 8

9. SPONSORING / MONITORING AGENCY NAME(S) AND ADDRESS(ES)

US Army Corps of Engineers, Mississippi Valley Division
1400 Walnut Street
Vicksburg, MS 39180-6199

10. SPONSOR/MONITOR'S ACRONYM(S)

USACE MVD

11. SPONSOR/MONITOR'S REPORT NUMBER(S)

12. DISTRIBUTION / AVAILABILITY STATEMENT

Approved for public release; distribution is unlimited.

13. SUPPLEMENTARY NOTES

Funding provided by the New Orleans District through Project Number 478534.

14. ABSTRACT

Upstream of the confluence of the Red River, Atchafalaya River, and ORCC Outflow Channel are vast low-lying flat areas on both sides of the Lower Red River. During times of high water on the Lower Red—whether from upstream water on the Red itself or backwater from the ORCC Outflow Channel—enormous amounts of water flow over the natural riverbanks and flood this land. The loss of this water from the river into storage affects the operation of the ORCC, which in turn affects the stages and flows down the Atchafalaya and Mississippi Rivers. An improved understanding of the Red River backwater area and how water is stored during flood events is required to inform New Orleans District water management operations at the ORCC.

Hydraulic analyses provide a basis to assess the cause of the changes in water levels, current directions and velocities, and flow rates for the assessment area. The hydraulic model HEC-RAS is used during the study to expand on existing HEC-RAS models of the area and to help overcome gaps in data. Understanding the processes of how water leaves the Red River channel during both high Red River Flows and high flows from the ORCC, quantifying the volume and timing of the water moving into the Lower Red River, when the storage area fills up, and when the storage area begins to drain will greatly inform the water managers and operators of the ORCC and could help to optimize operation decisions.

15. SUBJECT TERMS

Atchafalaya River (La.), Dredging, Geomorphology, Hydraulic structures, Hydrodynamics, Mississippi River, Old River (La.), Red River (Tex.-La.), Sedimentation and deposition, Sediment transport

16. SECURITY CLASSIFICATION OF:			17. LIMITATION OF ABSTRACT	18. NUMBER OF PAGES	19a. NAME OF RESPONSIBLE PERSON
					David A. Fertitta
a. REPORT	b. ABSTRACT	c. THIS PAGE			19b. TELEPHONE NUMBER
Unclassified	Unclassified	Unclassified	SAR	76	501-862-1508